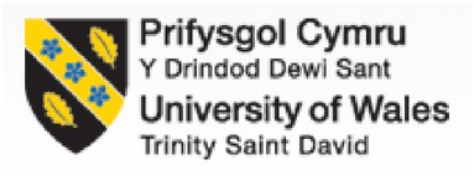
Aerodynamic Concept Testing of Sports 2000 MCR Using Driver In the Loop Simulation

by Jack Bridgeland

FILE	5368_JACK_BRIDGELAND_AERODYNAMIC_CONCEPT_TESTING_OF__SPORTS_2000_MCR_USING_DRIVER_IN_THE_LOOP_SIMULATION_128469_1046184846.DOCX (8.73M)		
TIME SUBMITTED	29-APR-2019 10:26AM (UTC+0100)	WORD COUNT	17784
SUBMISSION ID	105642118	CHARACTER COUNT	88374



Aerodynamic Concept Testing of a Sports 2000 MCR Using Driver in the Loop Simulation

Jack Bridgeland P145335

Date: 28/04/2019

BEng Motorsport Engineering

Major Project

M6X00417

Faculty of Architecture and Engineering

Abstract

An investigation into the aerodynamic characteristics of different design concepts of a Sports 2000 MCR is to be conducted utilizing a Base Performance Simulator, this simulator is a driver in the loop simulation tool which predicts how a vehicle should handle and can produce very accurate data. There have been some different design concepts that have been produced within the university and these are to be investigated.

The current MCR simulation model was compared to real 2018 race data from the UWTSD Team MCR race season. From this investigation practical and analytical testing was conducted to replicate the vehicle as accurately as possible. This includes Computational Fluid Dynamics and engine dynamometer testing which helped produce the MK1 Baseline model which would be the basis of the MK2 Iley, MK2 JHTT02 and the MK3 GJ02 concepts.

All concepts are programmed and dynamically compared using the simulation software utilising a software called MoTeC to analyse the data to investigate all the concepts.

The main aim of this project is to find out what concept will produce the biggest gains on track and help influence the Manufacturing of these designs.

Acknowledgments

I would like to thank Tim Tudor for all the support he has provided during this project and teaching me the relevant software and for all the time he has put into helping me.

I would also like to thank John Hughes and George Jones for supplying me with the CAD models of their design concepts and allowing me to use them for this report.

I would also like to thank Andrew Noble for being driver one in the simulator, for supplying me with the data from the MCR 2018 season and helping me through the entire project.

Declaration of Authenticity

This thesis is the result of the author's original research. It has been composed by the author and has not been previously submitted for examination which has led to the award of a degree.

Signed: Date: 28/04/2019

Table of Contents

1 Introduction 8

1.1 MCR 9

1.2 Simulation 10

1.3 Aerodynamics and CFD 14

2 Baseline Validation MK1 17

2.1 Original Simulation Model 17

2.1.1 Original Model: Map Testing 17

2.1.2 Original Model: Straight Line Testing 22

2.2 Aerodynamic Validation 25

2.2.1 MIRA Test Vehicle 25

2.2.2 Standard Bodywork MK1 28

2.2.3 Meshing Problems 28

2.2.4 Track Testing of New Aerodynamic Values 35

2.2.5 Engine Dynamometer Testing 36

2.2.6 Mass Distribution 38

2.2.7 Spring Rate 42

2.3 Increased Braking Force 44

3 Bodywork Concepts 48

3.1 MK2 Iley Splitter 48

3.1.1 Aerodynamic Forces 49

3.1.2 Simulator Testing: Aerodynamic Validation 53

3.2 MK3 JHTT02 (Concept) 53

3.2.1 Aerodynamic Forces 54

3.2.2 Simulator Testing: Aerodynamic Validation 56

3.3 MK4 GJ02 (Concept) 56

3.3.1 Aerodynamic Forces 57

3.3.2 Simulator Testing: Aerodynamic Validation 58

3.4 Aerodynamic Comparison of all Concepts 58

4 Simulation Comparison- Lap Testing MK1, MK2 & MK4 60
4.1 Lap Time Comparison 60
4.2 Speed Comparison 62
4.3 G-force Comparison 68
4.4 Dynamic Aerodynamic Performance Comparison 71
4.5 Understeer and Oversteer 74
4.6 Driver Feedback 78
4.7 Industry Standard Testing 80
4.7.1 Lane Change Manoeuvre 80
4.7.2 Steady State Corner Test 82
5 Conclusions 84
6 Evaluation & Further Works 86
7 References 89
8 Appendix 93

List of abbreviations

CFD – Computational Fluid Dynamics

CL – Co-efficient Of Lift

CD - co-efficient of drag

CoP – Centre of pressure

DIL – driver in the loop

DOL – driver out the loop

RPM – revolutions per minute

BPS – Base Performance Simulator

CAD – Computer Aided Design

List of Figures

Figure 1 Project Plan Flow Chart 8
Figure 2 MCR Example (Photgraphy, 2017) 9
Figure 3 BPS simulator 11
Figure 4 Simulator File Structure (Bridgeland & Noble, 2018) 12
Figure 5 Engine File Example 13
Figure 6 Suspension Layout 14
Figure 7 MoTec Screen Shot Displaying Aerodynamic forces 23
Figure 8 Coast Down Data Trace with Data Locations 24
Figure 9 MIRA Test Vehicle 25
Figure 10 Meshing Problem Example 29
Figure 11 Cause For Meshing Problems 29
Figure 12 Example of Bad Original Quality 30
Figure 13 Updated Part Mesh Sizes 31
Figure 14 Aerodynamic Programming Example 32
Figure 15 Separated MK1 Model 33
Figure 16 Engine Programming 38
Figure 17 MCR on Intercomp Scales 39
Figure 18 Mass On Each Wheel 39
Figure 19 New Mass Programming 40
Figure 20 Centre of Gravity programming 40
Figure 21 Spring Rate Tester 43
Figure 22 Original Spliter 48
Figure 23 MK2 Iley Splitter 49
Figure 24 Velocity Contour Case Comparison MK1 and MK2 51
Figure 25 Pressure Contour Lower Surface Case Comparison MK1 and MK2 52
Figure 26 Pressure Contour Upper Surface Case Comparison MK1 and MK2 52
Figure 27 MK3 JHTT02 Concept 54
Figure 28 Pressure Contour Comparison Upper Surface MK1 and MK3 55
Figure 29 Pressure Contour Comparison Lower Surface MK1 and MK3 55
Figure 30 MK4 GJ02 57
Figure 31 Oulton Park Track Position Turn one 64
Figure 32 Oulton Park Speed Comparison - Turn One 65
Figure 33 Oulton Park Turn 4 65
Figure 34 Oulton Park Speed Comparison - Turn Four 66
Figure 35 Oulton Park Wheel Load Comparison - Turn Four 66

Figure 36 Oulton Park Speed Comparison - Turn Five and Seven 67
Figure 37 Castle Combe G Force Comparison 68
Figure 38 Oulton Park G Force Comparison 69
Figure 39 Oulton Park G Force Comparison - Turn Three and Four 69
Figure 40 Oulton Park Lateral G Force Comparison - Turn Seven 70
Figure 41 Oulton Park Longitudinal G Force Comparison 70
Figure 42 Oulton Park Braking Force Required 71
Figure 43 Oulton Park Later Braking Example 71
Figure 44 Castle Combe Aerodynamic Load Comparison 72
Figure 45 Oulton Park Aerodynamic Load Comparison 72
Figure 46 Aerodynamic Load Comparison - Different Drivers 73
Figure 47 Slight Variation of CoP with Speed 73
Figure 48 Corner Radius and Theoretical Steer Maths Channels 74
Figure 49 Corrected Theoretical Steer Maths Channel 74
Figure 50 Understeer Channel 74
Figure 51 Understeer Comparison 75
Figure 52 Oulton Park Understeer Comparison - Turn Four 75
Figure 53 Oulton Par Understeer Comparison - Turn Fifteen 76
Figure 54 Understeer Comparison Both Drivers 77
Figure 55 Lane Change Manoeuvre Layout 81
Figure 56 Lane Change Within the Simulator (Bridgeland & Noble, 2018) 81
Figure 57 Moving Road and Rotating Wheels comparison MK4 87

List of Graphs

Graph 1 Castle Combe Original Simulation Model Comparison 18
Graph 2 Oulton Park Original Simulation Model Comparison 18
Graph 3 Castle Combe Original Simulation Model Speed Comparison 19
Graph 4 Oulton Park Original Simulation Model Speed Comparison 19
Graph 5 Castle Combe Lateral G Force Comparison 20
Graph 6 Oulton Park Lateral G Force Comparison 20
Graph 7 Castle Combe Longitudinal G Force Comparison 21
Graph 8 Oulton Park Longitudinal G Force Comparison 22
Graph 9 CFD Validation - Domain Position 26
Graph 10 CFD Validation - Domain Mesh Size 27
Graph 11 CFD Validation - Turbulence Model 27
Graph 12 Cl & Cd Comparison MK1 31

Graph 13 Simulation Aerodynamic Validation MK1 34
Graph 14 Oulton Park Updated Aerodynamism Speed Comparison 35
Graph 15 Simulator Updated Aerodynamics Lap Time Comparison 36
Graph 16 Power Curves from Practical Testing 37
Graph 17 Torque Comparison 38
Graph 18 Castle Combe Speed Comparison Updated Mass and Engine 40
Graph 19 Oulton Park Speed Comparison Updated Mass and Engine 41
Graph 20 Castle Combe Longitudinal G Force Comparison Updated Mass and Engine 42
Graph 21 Oulton Park Longitudinal G Force Comparison Updated Mass and Engine 42
Graph 22 Castle Combe Longitudinal G Force Comparison Increased Braking Force 44
Graph 23 Oulton Park Longitudinal G Force Comparison Increased Braking Force 45
Graph 24 Castle Combe Speed Comparison Updated Braking Force 46
Graph 25 Oulton Park Speed Comparison Updated Braking Force 46
Graph 26 Castle Combe Lap Time Comparison Updated Braking Force 47
Graph 27 Oulton Park Lap Time Comparison Updated Braking Force 47
Graph 28 Aerodynamic Comparison MK1 and MK2 50
Graph 29 MK2 Aerodynamic Validation Comparison 53
Graph 30 Aerodynamic Comparison Mk1 and MK3 54
Graph 31 Aerodynamic Validation MK3 56
Graph 32 Aerodynamic Comparison MK1 and MK4 57
Graph 33 MK4 Aerodynamic Validation 58
Graph 34 Aerodynamic Comparison MK1, MK2, MK3 and MK4 59
Graph 35 Castle Combe Lap Time Comparison 61
Graph 36 Oulton Park Lap Time Comparison 61
Graph 37 Castle Combe Speed Comparison 62
Graph 38 Oulton Park Speed Caomprison 63
Graph 39 Oulton Park Speed Comparison 64
Graph 40 Lane Change Manoeuvre Results 82
Graph 41 Steady State Corner Results 83
Graph 42 £/Second Comparison MK2 and MK4 84

List of Tables

Table 1 CFD Validation Parameter Sweeps 26
Table 2 CFD Validation - Chosen Settings 28
Table 3 Simulation Aerodynamic Calculator from Excel 33
Table 4 Spring Rate testing Results 43
Table 5 Setup Changes Required 60
Table 6 Driver One Feedback 79
Table 7 Driver Two Feedback 80
Table 8 Moving Road and Rotating Wheels Comparison MK4 86

List of Equations

Equation 1 Lift Force 23
Equation 2Lift Force Simulation 23
Equation 3 Aerodynamic Drag Force Simulation 24
Equation 4 Drag Force 24
Equation 5 Lift Force 32
Equation 6 Drag Force 32

1 Introduction

The aim of this report is to create an accurate simulation model of a Sports 2000 MCR race car using a Base Performance Simulator and evaluate a variety of different aerodynamic concepts which have been previously designed. There will be an evaluation of a slightly modified design with the only change being the front splitter and two other design concepts that are completely updated aerodynamic packages that conform to the Sports 2000 strict aerodynamic regulations. Below in figure one, shows a brief outline of the project and what works were planned.

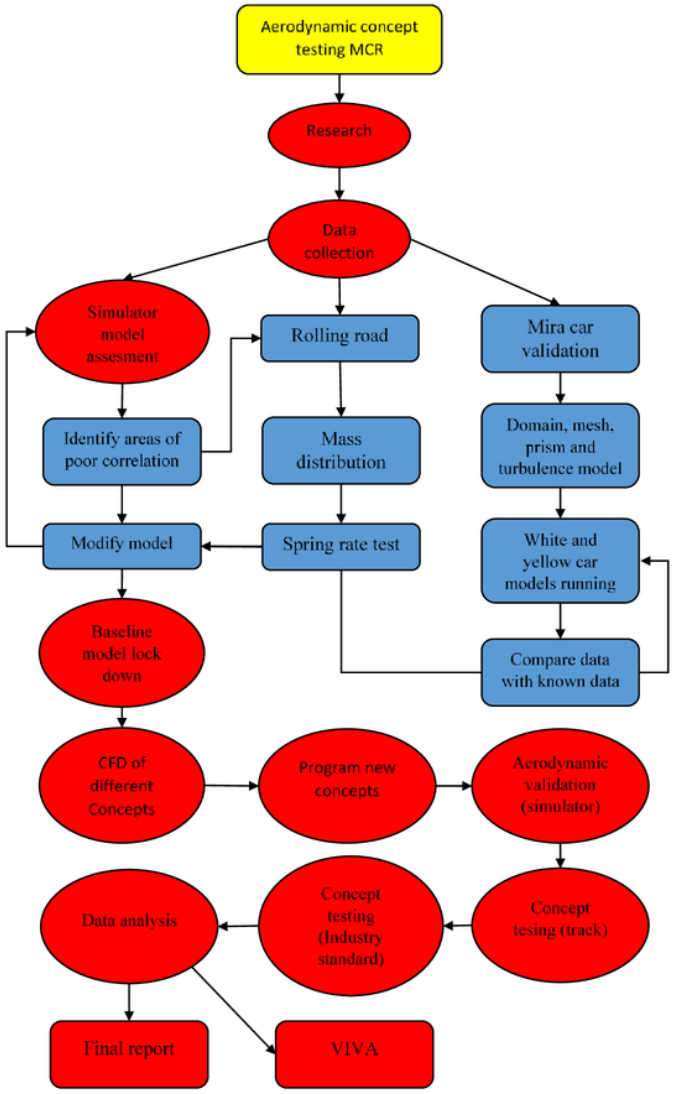


Figure 1 Project Plan Flow Chart

This type of project management was used because it is hard to time manage the testing of the concepts, due to this is hard to set a time frame for work that will change depending on the results from the previous sections. For example, finalising the baseline simulation model could have taken twice as long as planned which would have its impacts on the next section. Due to this it was decided to pan the rough outline of the project with no fixed time frames. There would be some project milestones for example baseline simulation model being locked down, since once that was completed continuation onto the next phase of the project could commence.

1.1 MCR

MCR race cars is a company that produces Sports prototype racing cars for circuit racing, track days, racing schools, sprints and hill-climb vehicles to compete in a variety of different race series, designed by Welshman Clive Hayes and Brazilian designer Luiz Fernando Cruz (MCR race cars, 2019). Within the Sports 2000 race series there are many MCR race cars on the grid, usually placing on the podium and winning the championship. In the past two years there has been a lack of development compared to others on the grid leading to them losing their dominance within the series. This has led to some aerodynamic concepts to be produced within the university to help regain the championship dominance. The vehicle that is going to be investigated is an MCR owned by the university that competes in the SRCC Sports 2000 Duratec class A championship, which has accumulated many podium finishes and a persistent 4th in the sprint championship for two years consecutively shown below in figure two.



Figure 2 MCR Example (Photography, 2017)

Figure two Above also clearly shows that the MCR is a very popular vehicle on the grid where the new concepts could provide Team MCR with extra performance over its competitors.

1.2 Simulation

Simulation has become a large part of vehicle testing within motorsport to predict the vehicles handling characteristics before it is even built and can suggest improvements to help aid the engineers and designers to produce a faster and more predictable race car (Morse, 2016). Driver in the loop simulation is becoming an accessible tool for motorsport, not just the high-end teams but for the lower end teams (ansible Motion, 2016). Driver in the loop simulation has a lower cost, more flexibility and fewer risks than other means of testing a vehicle (Kang, et al., 2013). There are two main types of simulation techniques which can characterise the vehicles handling. These are driver in the loop simulation (DiL) and driver out the loop simulation (DoL). As the name suggests one of them solely relies on having a driver and steering setup, the driver has full control over the route or track position of the vehicle. Driver out of the loop simulation is a multi-body point mass model which requires a lot of programming to mathematically calculate the response of the vehicle (Haaland, 2017). There are different software's which this can be achieved via, utilising complex mathematical programs like MATLAB or Adams (Colunga & Bradley, 2014). This type of simulation is not necessarily used for performance feedback so this would not be used for this investigation. Driver in the loop simulation is the method to be used in this report due to having access to a Base Performance Simulator on campus.

The simulator that will be used in this report is a Base Performance Simulator (BPS) 4.8 that runs on a software based on the Isi physics engine, shown below in figure three.



Figure 3 BPS simulator

Isi engine was primarily developed for the use of F1 teams but has been the basis of nearly every simulator or modern racing game. There are many different types of software, but they all run from the basics of the same type of programming and physics engine, which is good for simulating dynamic behaviour of a vehicle (Kang, et al., 2013). The version of the software that is available is not the most up to date as there is an Rfactor pro version which Is what most of the modern F1 teams would use, giving many more options and modification potential, while having a better quality of outputs. (rFpro, 2017) Even these days F1 teams are switching over to this more sophisticated software, which shows the relevance of the software itself (SAE International, 2014). Rfactor Pro uses a far more advanced graphics rendering and feedback system, giving a much greater level of realism and response to the driver, improving the accuracy of the results (Hoyle & Hurdwell, 2016). Another example of Rfactor Pro being more accurate, it has utilised modern technology and has had all the circuits LIDAR scanned to make the track model as accurate as possible. (rFpro, 2017)

Programming the vehicles characteristics is not just entering simple numbers, the structure of all the files needs to be understood before any coding or testing could be done. The BPS simulator works off the physics engine, ISImotor. This physics engine was first designed by a company called Image Space Inc and was released as an open source software in 1999 (Image Space Incorporated, 2016) which has been updated and re-released under the name ISImoter2 in 2005, which has been adopted and adapted by many different companies making computer games and accurate simulation models in high level racing with access to high level simulators (rFactor.net, 2013).

The Physics engine refers back to eight specific folders. Of these eight, five hold information to model the physics accurately and the other three hold coding about damage and other parts that are not relevant to this project. Figure four, below shows the file structure and how they will reference to each other during a test which was based on information from BPS (Base Performance Simulators, 2009)

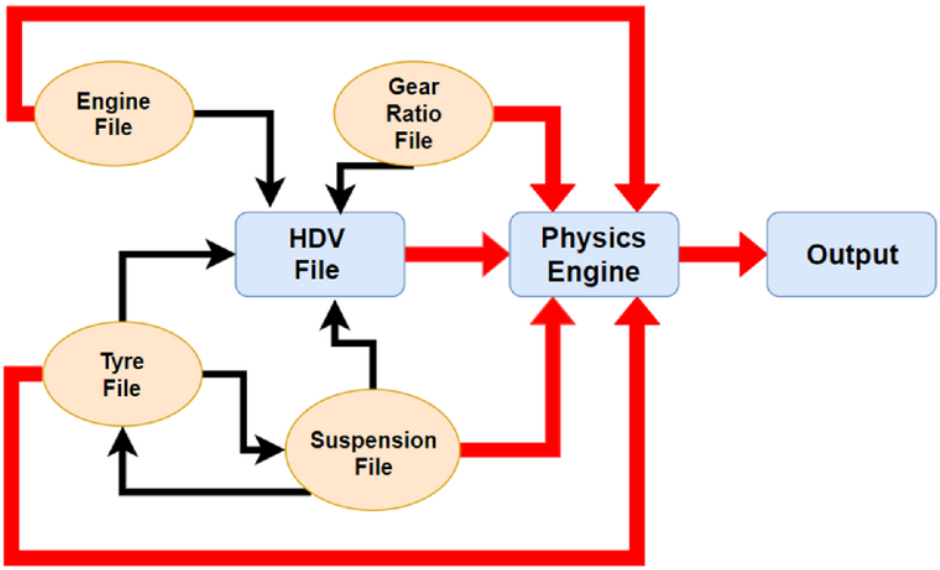


Figure 4 Simulator File Structure (Bridgeland & Noble, 2018)

The HDV file is the core of the coding which refers to all of the other files. The HDV file contains most of the parts of the coding which will be changed in this report, for example the aerodynamics and mass.

The engine file contains all relevant engine parameters. The main bulk of this is the torque curve which has been translated into a numerical form, which has the engine RPM and its corresponding torque values which is shown below in figure five.

```
RPMTorque=( 0.0, -10.0, -10.0)
RPMTorque=( 128.9, -10.5, -8.0)
RPMTorque=( 257.8, -11.1, -5.2)
RPMTorque=( 386.7, -11.6, -0.6)
RPMTorque=( 515.6, -12.1, 33.4)
RPMTorque=( 644.5, -12.7, 88.9)
RPMTorque=( 773.4, -13.2, 103.8)
RPMTorque=( 902.3, -13.7, 109.7)
RPMTorque=( 1031.2, -14.2, 114.4)
RPMTorque=( 1160.2, -14.8, 118.1)
RPMTorque=( 1289.1, -15.3, 121.2)
RPMTorque=( 1418.0, -15.8, 124.1)
RPMTorque=( 1546.9, -16.4, 127.0)
RPMTorque=( 1675.8, -16.9, 129.5)
RPMTorque=( 1804.7, -17.4, 131.8)
RPMTorque=( 1933.6, -18.0, 133.9)
RPMTorque=( 2062.5, -18.5, 135.9)
RPMTorque=( 2191.4, -19.0, 138.1)
RPMTorque=( 2320.3, -19.6, 140.5)
RPMTorque=( 2449.2, -20.1, 143.2)
RPMTorque=( 2578.1, -20.6, 145.9)
RPMTorque=( 2707.0, -21.2, 148.7)
RPMTorque=( 2835.9, -21.7, 151.4)
RPMTorque=( 2964.8, -22.2, 153.9)
RPMTorque=( 3093.8, -22.8, 156.2)
RPMTorque=( 3222.7, -23.3, 158.2)
RPMTorque=( 3351.6, -23.8, 160.1)
RPMTorque=( 3480.5, -24.3, 162.0)
RPMTorque=( 3609.4, -24.9, 163.8)
```

Figure 5 Engine File Example

The engine file also contains specific engine characteristics, for example the heat dissipation and launch control properties. Most of these are not applicable to the model that will be created as these values will be unknown or the vehicle does not have these options.

The gear ratio file holds all the information about gear ratios and final drives. In this section all the available ratios can be programmed, and these can be changed within the software in the menu. This allows the user to change ratios without having to learn the coding structure of the model and easily change the ratios without having to exit the software.

The suspension file contains the location of all the suspension pickup points which is implemented in the standard X, Y and Z axis coordinate system. Using these co-ordinates, the physics engine can accurately predict how the suspension geometry would change under a dynamic load condition. These co-ordinates were previously checked for accuracy previously in another project, as such there was no need to modify the suspension

geometry, but they were checked within a free software called suspension editor which displays the geometry programmed which is shown below in figure six.

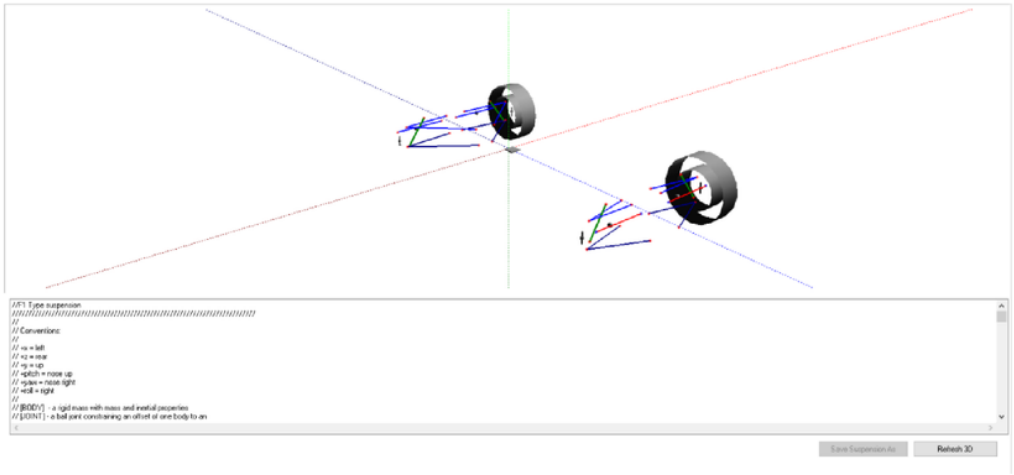


Figure 6 Suspension Layout

The tire file contains nearly all the data about how the tyre will act and how much grip it will provide. The main section of interest is the slip curves that are programmed. These are separated into different sections which are Front longitudinal acceleration, front lateral acceleration and the same for the rear. This section also contains parameters like the rolling radius of the tire, wear levels, and many more which will not be altered within this report.

As stated by J.E Bernard and C.L Clover, there are three things to consider before any simulation should take place, outlined below (Bernard & Clover, 1994)

- Is the model appropriate for the vehicle?
- Is the simulation based on equations that replicate the model?
- Are the input parameters correct?

These questions will influence how this model is created and evolved throughout this report to make sure it is as accurate as possible, and the relevant things will be changed.

1.3 Aerodynamics and CFD

Aerodynamics is the study of airflow around an object and what effects the object has on the airflow (NASA, 2017). In recent years, especially in formula one, aerodynamics has become a vital part of building a fast and controllable race vehicle (Mariani, et al., 2015). In the past the only real way to predict how the air would flow around an object is to use a wind tunnel. Wind tunnels were original designed for use in aviation. The first wind tunnel was designed and built by a man called Frank H. Wenham in the year 1871 in England (Rumerman, 2019).

He designed a wind tunnel to try and see the flow structures behind wing elements. In modern times using a wind tunnel has been implemented for vehicle manufacturing and analysis to drive the design of a vehicle. These days' wind tunnels are primarily used to validate computational fluid dynamics (CFD) work carried out on the geometry. CFD is a tool to predict how a fluid flows over or through and object (CFD, 2019). External flow is what is used to help predict the aerodynamic effects within the automotive industry (Lanfrit, 2005). CFD is just a prediction (Katz, 1995), thus the need for actual wind tunnel data to be collected to make sure that the predictions produced are accurate (Mariani, et al., 2015). Due to the mathematics that are used within CFD which is based off the Navier-Stokes equations (Blais & Bertland, 2015). Due to this CFD can't be taken as an absolute value but if the results are validated arcuately they can be regarded as representative. CFD is one of the main reasons that F1 has become faster and the vehicles are creating higher G-forces (Toyota Motorsport, 2011). There are many different settings that can influence the results obtained from CFD these are briefly outlined below.

- Domain setting – the size and position of the domain can influence the results. This is due to an effect called blockage where the fluid that is flowing around an object encounters the extremities of the domain. That fluid needs to go somewhere which leads to it all shifting and creating pressure on the boundary of the domain which could influence the results. Many companies have investigated this effect within wind tunnels (SAHIN, 2004) the position of the test piece in the domain is also important due to the fact that, if there is not enough test area behind the model all of the turbulence might not be picked up, thus changing the results.
- Mesh sizing – the size of the mesh can have an impact on the results, for example if the geometry is complicated and a large mash size is placed on it the detail might not be captured and the surface will not be representative. The same can be said for the quality of the results with a large mesh compared to a small mesh (Katz & Venkateswaran, 2011).
- Mesh quality – highly skewed elements and elements with bad quality can decrease the accuracy of the CFD results (sas Ip, n.d.) according to the Ansys handbook minimum skewness should be no less than 0.001 (Ansys, 2016)
- Turbulence model – within the software there are many different turbulence models that could be used. Each model will predict how the turbulence forms, and this will affect the overall results. According to Landfrits book the best model for external ground vehicle aerodynamics is K-Epsilon Realisable non equilibrium wall functions. (Lanfrit, 2005).

Cl and CD are dimensionless coefficients and they are not dependant on speed or external condition whereas drag and lift forces are calculated using the CL and CD with air density and speed within the equations. (Segers, 2008). The simulator has a form of the CL and CD within the coding to calculate the aerodynamic forces that would be applied to the model. This is explained in more depth further into this report.

The Centre of pressure (CoP) is the point where the aerodynamic force acts upon through a specific point the same way that the mass of the vehicle works about the centre of gravity (Nasa, 2012).

2 Baseline Validation MK1

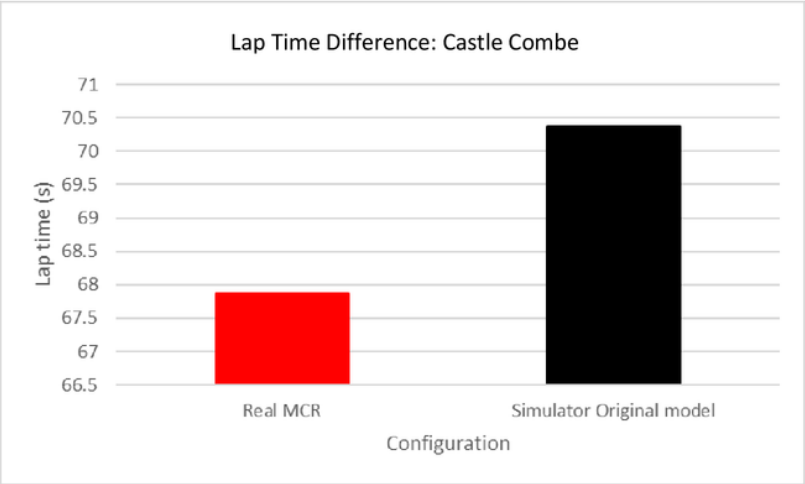
An existing model of the Sports 200 vehicle had already been programmed into the simulator. The model in question had not been validated against the most recent race data from the 2018 race season of the MCR. Due to this an investigation was needed to determine the deviation in the data from the real vehicle to the simulation model.

2.1 Original Simulation Model

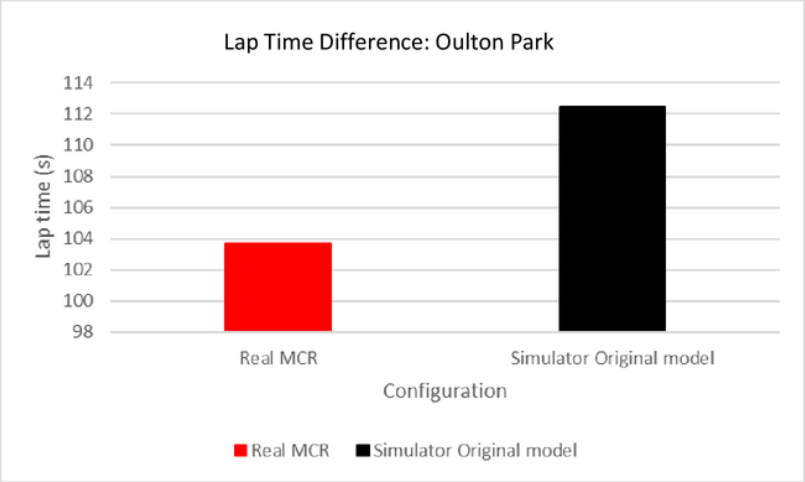
Circuit lap testing and straight-line validation was conducted to generate data for comparison of the simulation model to the real vehicle data. The main areas of investigation were lap time, speed and the G-forces produced under acceleration and cornering which are known as longitudinal and lateral G-forces from the lap testing. The CL and CD of the vehicle will be calculated from some straight-line testing which is a commonly employed practice, as per (SAE Interantional, 2012).

2.1.1 Original Model: Map Testing

Within the simulator there are many different tracks that have been modelled within the original software. Looking through the calendar from the 2018 season of the MCR and the models that were programmed into the simulator two tracks were selected. The choice of tracks was limited due to there being different variations of the track layout from the race, compared to what was programmed into the simulator. The two tracks chosen were Oulton Park and Castle Combe which will be used throughout the rest of this investigation. These two tracks were chosen due to their mixture of high and low speed corners and both tracks have a varied amount of gradient changes which could influence the aerodynamic characteristics of the vehicle under dynamic load conditions. Oulton Park has quite a large gradient change compared to Castle Combe. The driver was instructed to do ten laps while trying to be as consistent as possible while still pushing the limits of the vehicle, just like how the driver of the real vehicle drives. Once the data was collected it was analysed using Motec i2 Analysis software. These analysis results would drive the evolving iterations of the baseline model to see where the model deviates from the real vehicle. Below in graphs one and two, Shows the lap time differences from the real vehicle to the original model at the two chosen circuits.

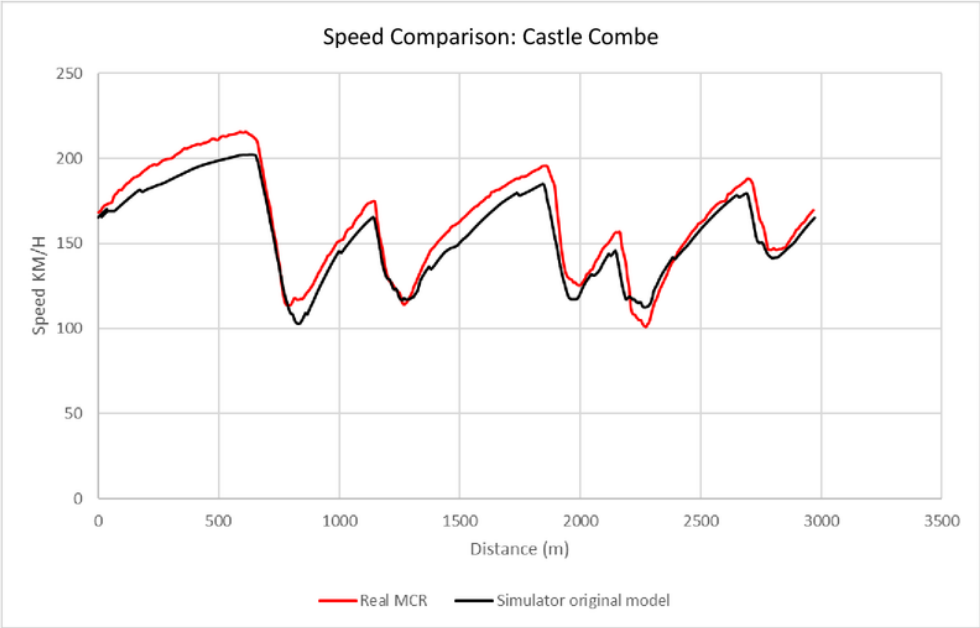


Graph 1 Castle Combe Original Simulation Model Comparison

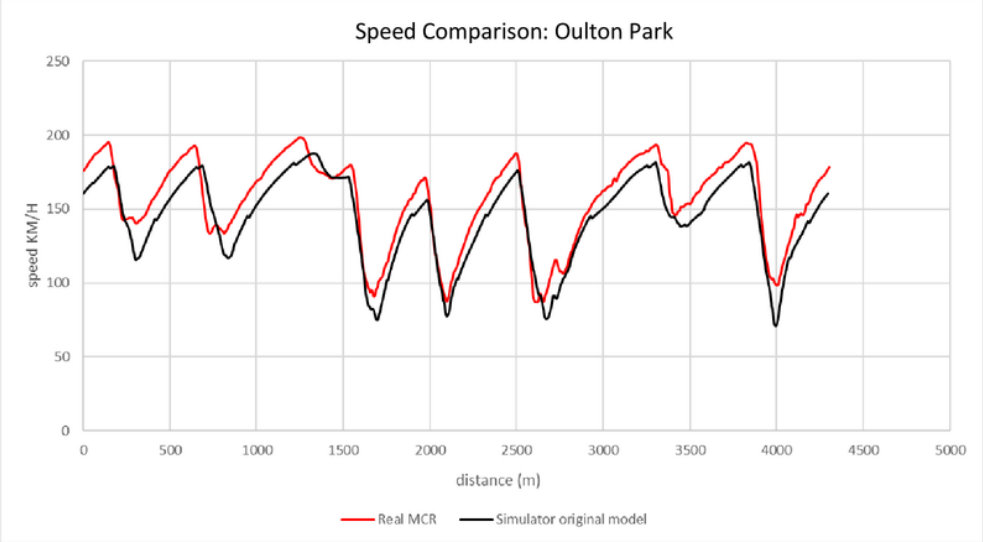


Graph 2 Oulton Park Original Simulation Model Comparison

From the graphs above the simulator model is slower over a total lap at both tracks that have been chosen. The exact cause of this difference, be it cornering speeds or straight-line speeds, cannot be determined without further analysis. More in depth analysis of the lap data was required, shown below in graphs four and five.



Graph 3 Castle Combe Original Simulation Model Speed Comparison

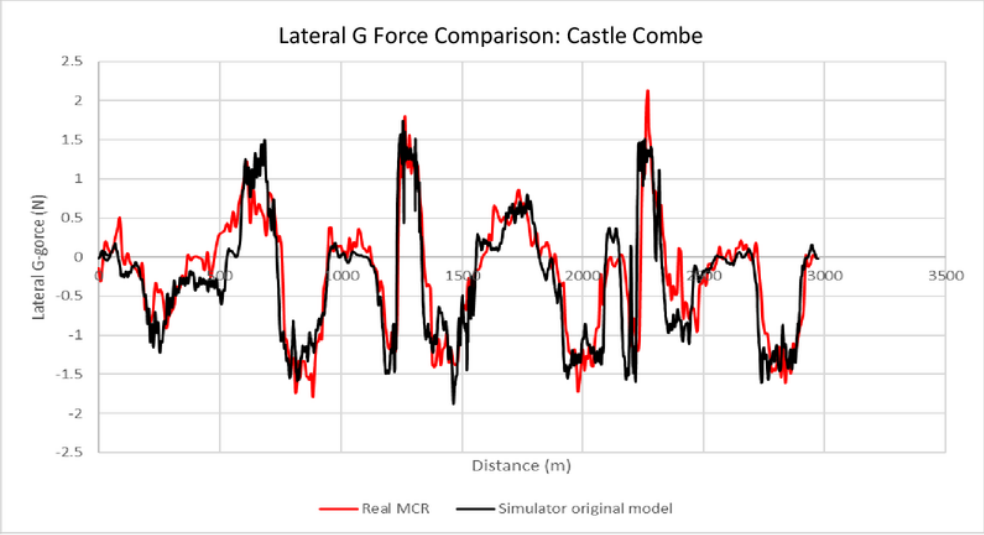


Graph 4 Oulton Park Original Simulation Model Speed Comparison

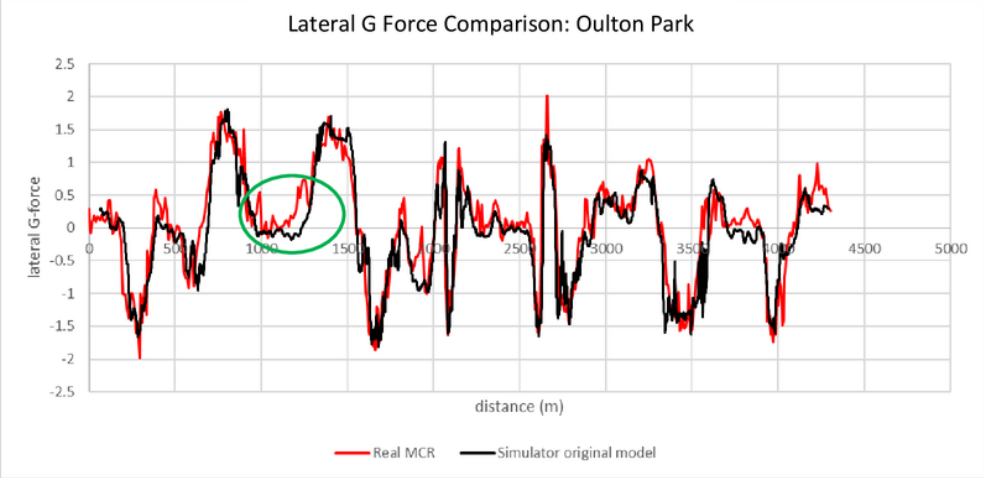
Over the entire course of the laps at both tracks, the speed of the simulator model is noticeably lower than the real vehicle. This could be due to three main factors. The largest contributing factor could be the overall power of the model being inaccurate, which would be highlighted in the reduced accelerations seen in the comparison data. The second could be the mass of the vehicle being too high, potentially accounting for the slower accelerations, as

well as the lower cornering speeds, due to the impact on the handling characteristics of the model with the increased mass. Excessive aerodynamic drag could also influence this, however due to there being a deficit in the slow and high-speed corners this could be influencing the results less, due to the fact the aerodynamic drag of the vehicle is highly dependent on the velocity. Due to this, given there are discrepancies seen across all velocities, whilst drag force could still be a contributing factor, it is unlikely the route cause.

The longitudinal and lateral G-forces were then also compared from the same laps, the results can be seen below in graphs five and six.



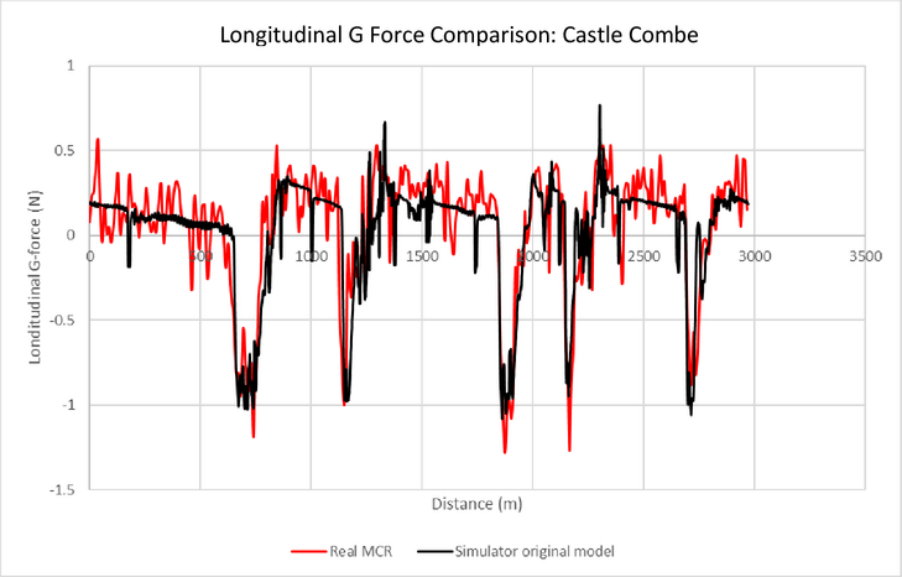
Graph 5 Castle Combe Lateral G Force Comparison



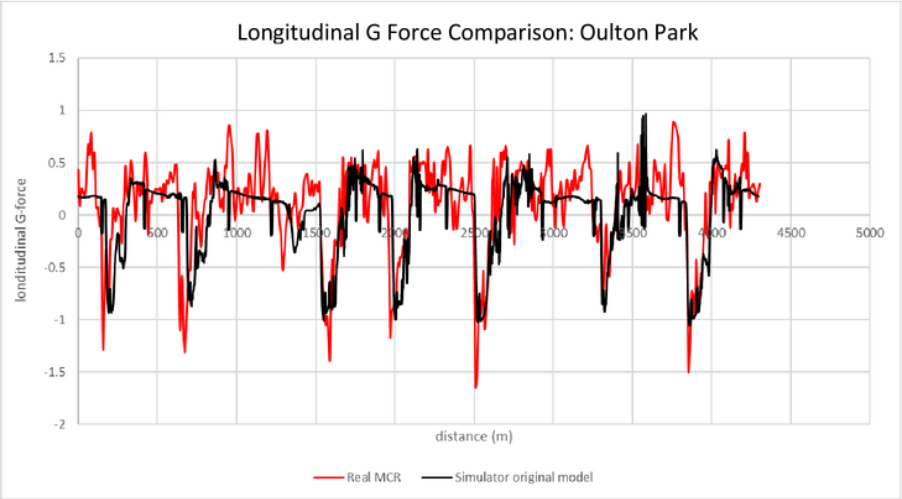
Graph 6 Oulton Park Lateral G Force Comparison

From the lateral G-force comparisons it shows that there is some quite close correlation between the simulation model and the real vehicle. There are some areas of the track where the data does not seem to correlate that well. For example, the area highlighted in graph six, which is around a corner and does not correlate, where the simulation model is producing lower lateral G-forces. It was decided that this could be due to driver differences given that the MCR racing driver was not available to do the simulation testing thus, direct comparison is difficult. Additionally, there is potential that the track model is not correct within the programming, which could account for some of the variance seen. This area will be monitored to see if any of the changes to the model make this area of correlation closer.

The longitudinal G-force was then compared shown below in graphs seven and eight.



Graph 7 Castle Combe Longitudinal G Force Comparison



Graph 8 Oulton Park Longitudinal G Force Comparison

From the longitudinal G-force comparison, where positive shows when the vehicle is accelerating and negative shows when the vehicle is de-accelerating. They show that both follow roughly the same trend. When the vehicle is braking, in the real vehicle data, there are higher peaks, in some cases up to 50% higher than the simulated data. This could be caused by two main factors which are the longitudinal tyre grip or the braking torque within the coding. Due to the accelerations being quite representative it was decided that the tyre grip factor within the model is quite accurate, but it was the braking force of the model which might be too low, so this will be investigated. The acceleration trend of the simulation model also seems to be slightly low. This could be due to the same areas which are affecting the overall speed of the vehicle over the laps.

2.1.2 Original Model: Straight Line Testing

Straight line testing can be done to work out the Cl and Cd of the vehicle quite easily. This method has been used for many years in the car industry before CFD became a mainstream tool for the average car designer (Bernard & Clover, 1994). Using the skidpan track on the simulator which has a large long and flat drag strip these tests could be done two tests were done which are explained below.

2.1.2.1 Constant Speed Test

A constant speed test was done to find the Cl of the vehicle at a certain speed. It was decided to use the speed of 35m/s which will be used in the CFD modelling. This speed has been derived from the average speed of the vehicle over the course of a lap. It was found that driving the current model to the soft limiter of second gear gave the desired speed. From

this the data was analysed and the appropriate maths channels were created in the output software called MoTec.

To create the maths channels the equation to calculate Cl was used which is shown below in equation one Which was re-arranged to find Cl.

$$lift\ force\ = Cl \times A \times 0.5 \times \rho \times V^2$$

Equation 1 Lift Force

To find the lift force of the vehicle the equation below was used.

$$lift\ force = Total\ Tire\ Load - Total\ Static\ Tire\ Load$$

Equation 2Lift Force Simulation

The static load was calculated from all four of the wheels loads, with the vehicle static, which equates to the mass of the vehicle including fuel and the driver when there are no external forces acting upon it. Using these equations, the Cl would be clearly displayed in MoTec and was recorded. Below in figure seven, shows a screen shot from MoTec of the Cl when at the speed of 35m/s.

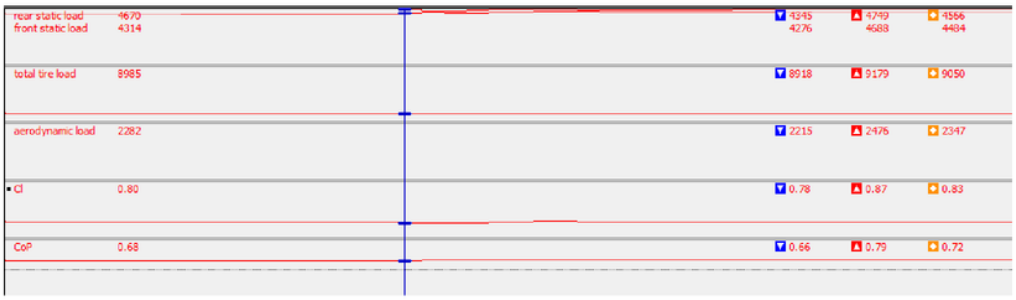


Figure 7 MoTec Screen Shot Displaying Aerodynamic forces

The screen shot from MoTec shown above in figure seven Shows the area of steady state where the vehicle was traveling at 35m/s. from this the Cl does change slightly over this time period, so the average number was used which was 0.83. This value would be a minus number due to it being downforce and not lift, but the way the maths channels were programmed it is a positive in this case. From this test the Cl value is too high compared to the Mira data of the old specification vehicle which had a Cl of -0.58. the CoP was also tested while doing this which was found to be on average 72% forward, considerably forward biased, and this will be compared in the CFD section further into this report.

2.1.2.2 Coast Down Test

A coast down test was done to calculate the drag of the vehicle, this can be done in a wind tunnel (Segers, 2008) on a real vehicle but due to this being impractical within this project it was done computationally. A coast down test is when a vehicle it taken up to a high speed and then put into neutral, allowing the vehicle coast until it is stationary, with the aerodynamic drag force and mechanical resistances causing the deceleration. This was also conducted on the skidpad track runway as it has no gradient to influence the results, nor is the track programmed with any wind conditions that would normally need to be accounted for. The drag force can then be calculated from the data using equation three, shown below. This test will work out the total drag force of the vehicle which is not what needs to be investigated. To rectify this the mechanical resistive force from the moving parts of the vehicle was calculated in the low speed section below 10m/s where aerodynamics is minimal and then this is taken away from the total drag force to give the aerodynamic drag force.

$$Aerodynamic\ Drag\ Force = Total\ Drag\ Force - Mechanical\ Drag\ Force$$

Equation 3 Aerodynamic Drag Force Simulation

Below in figure eight shows a graph of velocity against time of the data that was collected during the coast down and roughly where the measurements were taken for the calculations where red indicated the high-speed section and black indicated the low speed section.

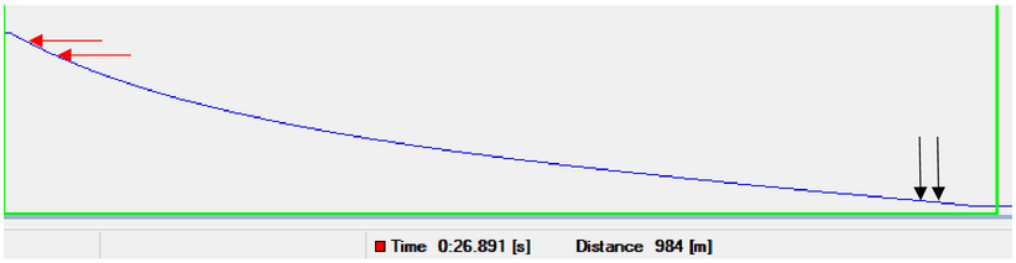


Figure 8 Coast Down Data Trace with Data Locations

Once the aerodynamic drag forces were calculated, using equation four, shown below the Cd could be calculated after rearranging it for CD.

$$Drag\ force\ = Cd \times A \times 0.5 \times \rho \times V^2$$

Equation 4 Drag Force

The value for the drag that was obtained from this was 0.53 which is close to the value from the MIRA wind tunnel which was 0.52. This was within an acceptable variance, so it was decided that the drag values were being predicted correctly for the baseline model.

2.2 Aerodynamic Validation

To be able to accurately model the aerodynamic performance of the MCR, the aerodynamic drag, lift and centre of pressure need to be found for the current bodywork. Team MCR from the university has previously taken the old specification MCR to the MIRA wind tunnel and collected some data which would satisfy the CL and CD of the vehicle in question, but each geometry would need to be tested in the CFD software. This MIRA data would be used to validate the results from CFD. There are slight variances expected due to CFD being a prediction of the airflow and due to geometry differences between the model and the actual vehicle (Gartman, et al., 2011).

2.2.1 MIRA Test Vehicle

Before the MCR could be tested in CFD a validation study was performed to find the optimum settings within the CFD software of ANSYS. MIRA have a test vehicle called the test notch back which is widely used for validation and real wind tunnel data is available for this geometry, a CAD model of which is shown below in figure nine.

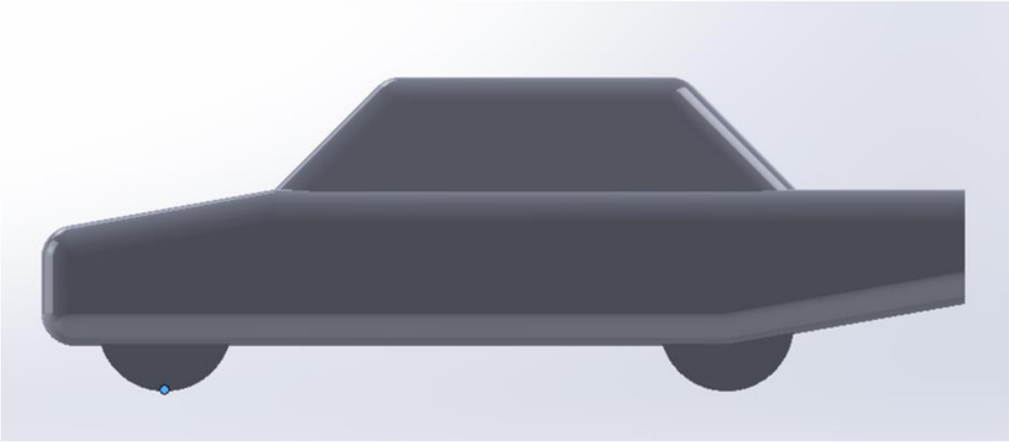
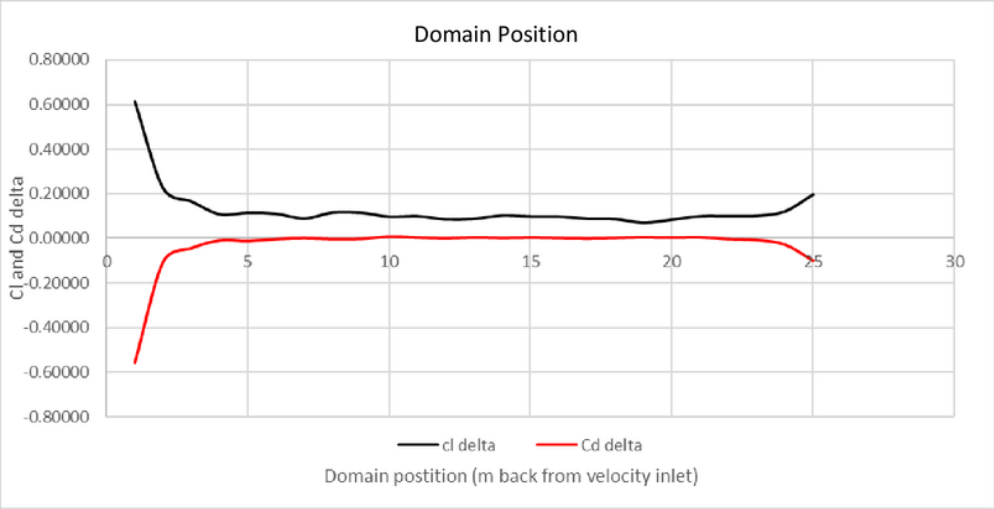


Figure 9 MIRA Test Vehicle

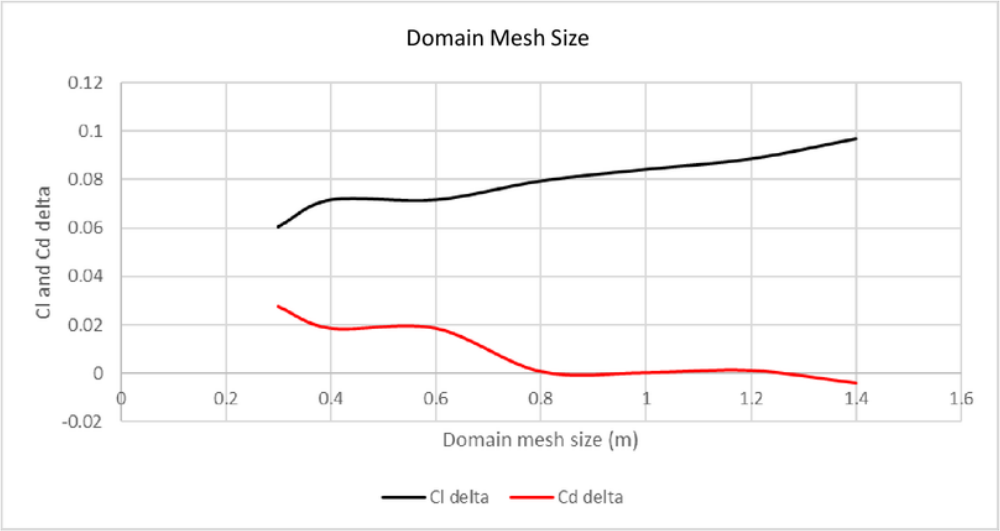
The parameter sweeps that were conducted are shown below in Table one. And graphs nine ten and eleven show the results from three of the sweeps.

Parameter	Sweep Range
Domain Size	2X – 10X
Domain Position	1m – 25m
Domain mesh	0.3m – 1.5m
Density Box Size	0X – 3X
Density Box Position (from front of vehicle)	0% - 100%
Density Box Mesh Size	0.07m – 0.5m
Prism Layers on The Road	1 - 10
Prism Layers on The Vehicle	1 - 10
Turbulence Model	Sweep of different types that were representative

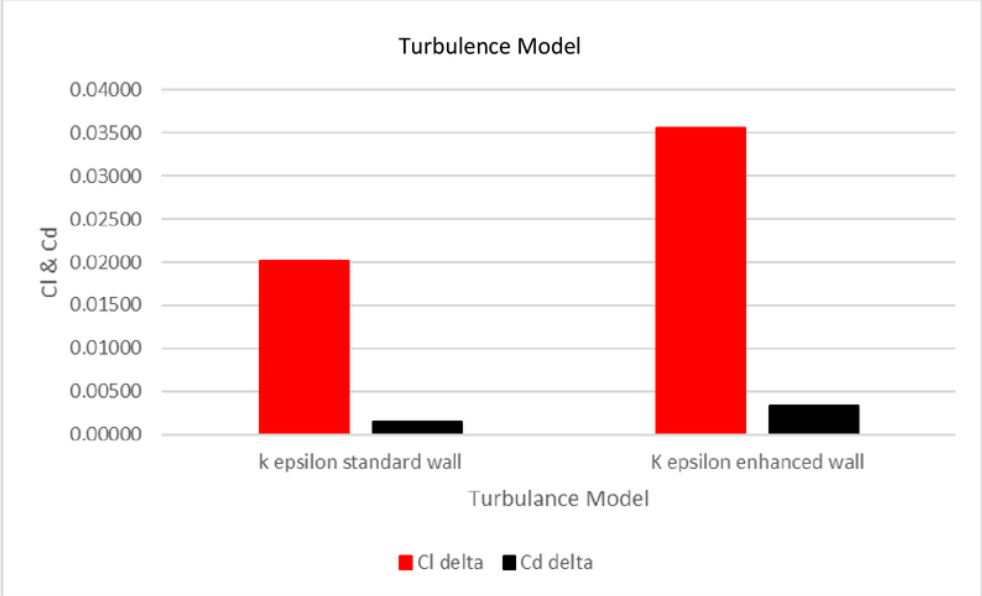
Table 1 CFD Validation Parameter Sweeps



Graph 9 CFD Validation - Domain Position



Graph 10 CFD Validation - Domain Mesh Size



Graph 11 CFD Validation - Turbulence Model

Parameter sweeps were done to find which settings produced the results that were as close to the data that is provided MIRA. The parameter sweeps conducted yielded the following optimal settings, detailed below in table two.

Permeter	Setting Chosen
Domain size	7x Test piece length
Domain position	13m From the front of domain
Domain mesh size	0.8m
Density box size	1.5x size of test piece
density box position	middle
Density box mesh size	0.3m
Test piece mesh size	0.01m
Prism layers on test piece	5
Prism layers on road	3
Turbulance model	K-Epsilon Realisable non equilibrium wall functions

Table 2 CFD Validation - Chosen Settings

These results will be a starting point of meshing the actual MCR, but they might need adapting to represent the geometry and to get a good mesh quality, while the same settings will be used within Fluent

2.2.2 Standard Bodywork MK1

A pre-existing CAD model of the MCR was provided which accurately represents the vehicle and will be used to test in CFD to find the CL, CD and CoP of the vehicle. Using the settings found in the Mira test car validation it was attempted to put a volume mesh onto the vehicle which uncovered some problems with the geometry and the mesh settings themselves not capturing the detail that was on the model. These problems needed to be corrected before CFD could be completed on this model for accurate and repeatable results (CFD, 2019).

2.2.3 Meshing Problems

The first problem that occurred while meshing the MK1 geometry was on the rear end of the bodywork where, even though there was a surface, when the mesh was applied to it, there would be a hole in the geometry. This could lead to the results from the CFD to be inaccurate. Figure ten shows the area of concern. Resolving the issue in this area increased the time period that was planned for this validation, which postponed all the other testing that needed to occur after this.

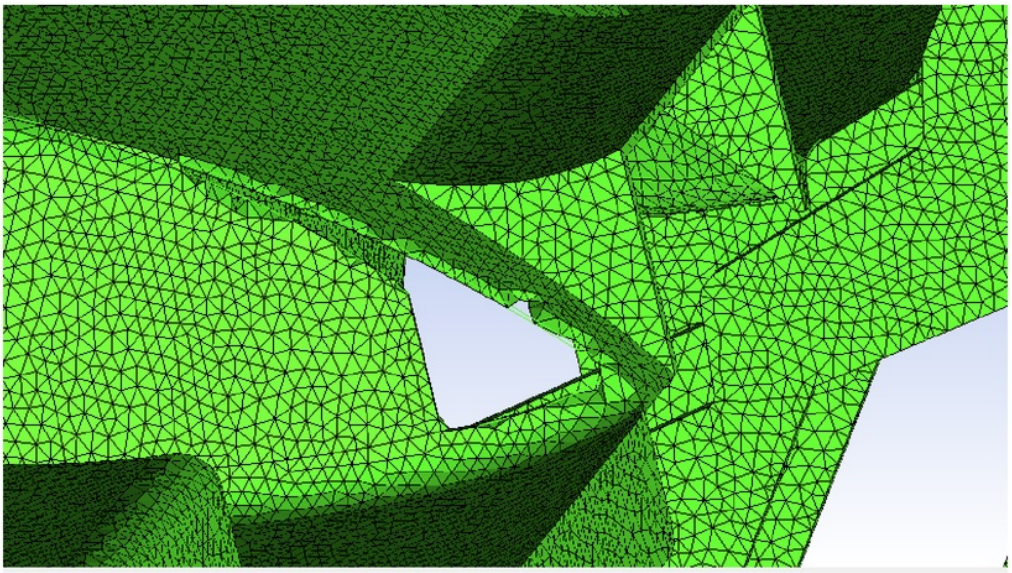


Figure 10 Meshing Problem Example

This problem reiterates the importance of working with a clean and well created model which is stated in the Ansys instruction manual (Ansys, 2016).To rectify this the rear end of the model was recreated without the sliver which was protruding from the roll hoop section of the geometry which is what was causing the geometry issues further rearward. This can be seen below in figure eleven

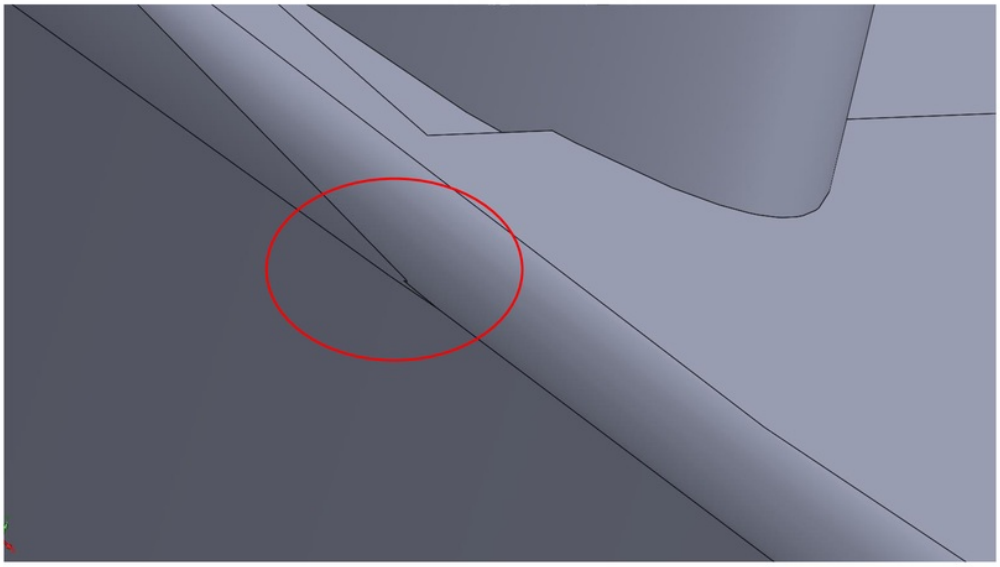


Figure 11 Cause of the Meshing Problems

Now the vehicle geometry would mesh fully with the settings found from the MIRA car validation study, however the orthogonal quality and the skew had a very high count, and, in some cases, the orthogonal quality would be negative which means that the cell itself would turn or fold into itself. Due to this some of the mesh settings would need to be changed accordingly on certain components. The main area of bad orthogonal quality was around the wheels, between the engine and the rear clamshell and between the road and the floor of the vehicle. There were other areas of concern in the complex sections of geometry, for example, the rear wing and the splitter where the mesh did not accurately represent the geometry. These areas of bad orthogonal quality were increased once the prism layers where extruded from the surfaces shown below in figure twelve, Where it is clearly shown that the bad orthogonal quality is where the prism layers have been extruded as you can see the expansion the further away from the MCR it gets, which led to reducing the amount of prism layers on these components compared to the MIRA study to achieve a useable mesh.

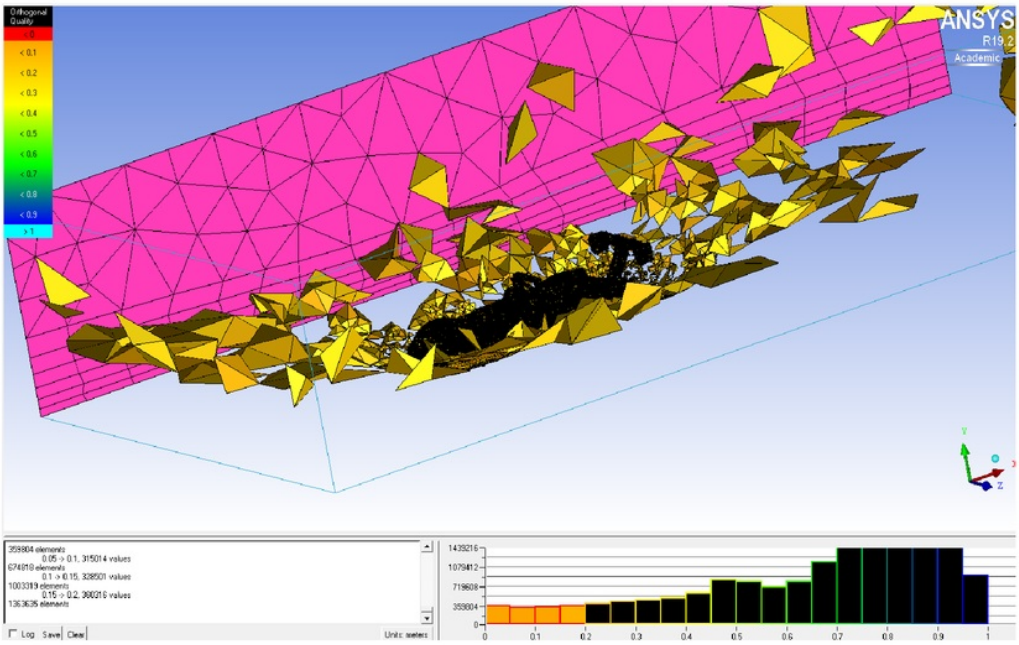


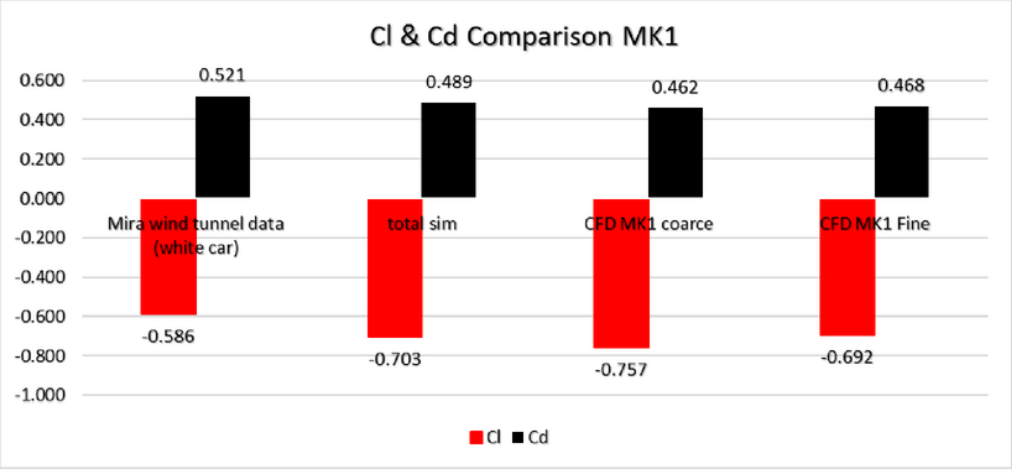
Figure 12 Example of Bad Original Quality

In some cases, the mesh needed to be refined in certain areas, so the mesh size was reduced. Reducing the mesh size can seriously increase the computing time and a balance was needed to be made between the mesh refinement and the computing time (sas Ip, n.d.). Below in figure thirteen, shows the new mesh sizes on the geometry which created an acceptable level of orthogonal quality and skewness.

Part	Prism	Hexa-core	Maximum size	Height	Height ratio	Num layers
BODY	☐	☐				
LOUVRES	☐		0.004	0	0	0
MCR	☑		0.01	0	0	4
PRESSURE_OUTLET	☐		0	0	0	0
ROAD	☑		0	0	0	3
SOLID_1_1	☐		0			
SPLITTER	☑		0.015	0	0	4
SPLITTER_ENDPLATES	☑		0.005	0	0	4
SYMMETRY_1	☐		0	0	0	0
SYMMETRY_2	☐		0	0	0	0
SYMMETRY_TOP	☐		0	0	0	0
VELOCITY_INLET	☐		0	0	0	0
WHEELS	☐		0.02	0	0	0
WING	☑		0.005	0	0	4

Figure 13 Updated Part Mesh Sizes

Now the model would mesh with as little orthogonal quality issues and skew of the elements, CFD runs could be conducted. The results were compared to MIRA data of the old specification car. Below in graph twelve, Shows the difference in the MIRA data, Total Sim CFD results and the MK1 CFD run. There are two CFD runs shown on the graph which shows the difference between a coarser mesh and a finer mesh. The finer mesh correlates to the given data much closer which stresses the point that the finer the mesh the more accurate the results will be.



Graph 12 Cl & Cd Comparison MK1

It is worth noting that the CD from the CFD is lower than the actual vehicle in the wind tunnel. This could be due to other external influences. For example, the CAD model does not have any radiators in the side pods which would create more drag.

2.2.3.1 Programming Aerodynamics into the Simulator

Within the HDV file of the model there is a section that controls the aerodynamics of the vehicle. The aerodynamic section is split into different subsections which influence different parts of the vehicle shown below

- Body
- Front wing (splitter)
- Rear wing
- Diffuser

The front and rear wings have a drag and lift base values which require not just the CL and CD of that component but instead it needs each value multiplied by other variables which is then multiplied by the velocity squared. This is based off the lift and drag force equations,

$$lift\ force\ = Cl \times A \times 0.5 \times \rho \times V^2$$

Equation 5 Lift Force

$$Drag\ force\ = Cd \times A \times 0.5 \times \rho \times V^2$$

Equation 6 Drag Force

The Cl of the vehicle needs to be multiplied by the frontal area, the density of air and 0.5 and then the simulator will multiply by the velocity squared to work out the forces. The body and diffuser have a difference within the coding compared to the wings. The body only has a drag base value and the diffuser only has a lift base value. Due to this the lift of the whole body was used in the diffuser and the drag from the main body was programmed into the body drag base value. Shown below in figure fourteen.

```
[DIFFUSER]
DiffuserBase=(-0.24,-6.5,50)

[BODYAERO]
BodyDragBase=(0.432)
```

Figure 14 Aerodynamic Programming Example

To be able to get the Cl and CD values for each component separately the model needed to be split before it is meshed. Below in figure fifteen shows the model separated within ICEM. Note the wheels, splitter endplates and louvres are also separated this is due to having to put a different size mesh on them or without prism layers to make them representative to the model while keeping the orthogonal quality as low as possible.

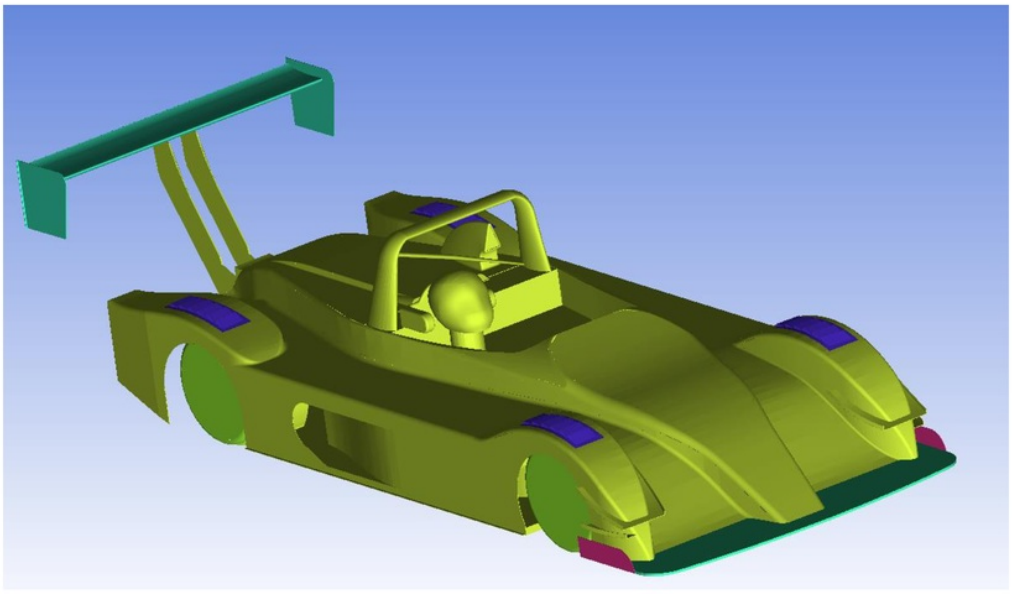


Figure 15 Separated MK1 Model

Once the model is separated, separate force reports within Fluent can be created which will give the CL and CD for those components. An excel spreadsheet was created to convert these to what needs to be programmed into the simulator. Shown below in table three.

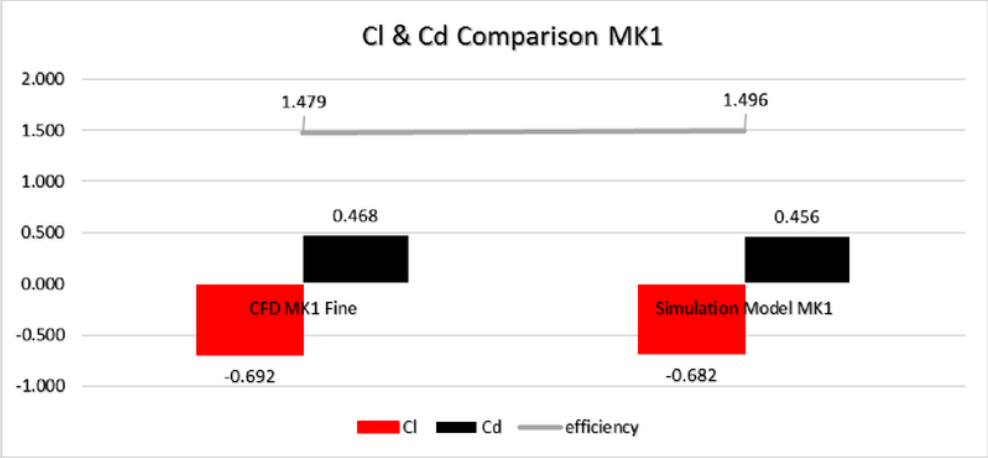
	simulator converter							
	Splitter		Rear Wing		Body	Diffuser used for body cl	total	
	Cl	Cd	Cl	Cd	Cd	Cl	Cl	Cd
Cfd results	-0.96345	0.05189	-0.49727	0.03574	0.40195	-0.38577	-1.8465	0.48959
input into sim	-0.77313	0.04164	-0.39904	0.02868	0.32255	-0.30957	-1.48174	0.39288

Table 3 Simulation Aerodynamic Calculator from Excel

The straight-line tests were then repeated with the new aerodynamic values to see if the aerodynamic forces were being predicted correctly within the simulator. From these results it was found the CL was being over predicted and increasing with speed which came out at 0.86 at 35m/s which is the same air speed that was used in CFD. The centre of pressure was moving forward the faster the vehicle went. Further investigation was done to find one of the reasons this was happening. Within the aerodynamic coding in the HDV file there are what's called degradation factors applied to the different aerodynamic devices. The degradation factors are a number between zero and one with the latter being the highest amount of change. The degradation factors will change the aerodynamic force of that component with a change in height. The higher the number the more sensitive the vehicle will become with attitude changes. The faster the vehicle moves the more force it produces lowering the vehicles ride height, thus increasing the force produced, resulting a compounding increase in aerodynamic force that is unrealistic. This was only happening with

the splitter and diffuser values and not the rear wing, hence the centre of pressure moving forward. While testing the model the rear end was going very light, with little grip and was not driveable at high speeds, as a result of the significant shift in centre of pressure forward. To stop this happening the degradation factors were all set to zero and the straight-line testing was repeated. This in turn reduced the amount the centre of pressure was moving; however, it did not completely fix this problem as the Cl was found to still be increasing and the CoP still moving forward.

It was decided at this point to change how the aerodynamic forces were programmed to eliminate the influence of these unwanted characteristics. The diffuser was deleted, and the Cl was only programmed on the front and rear wing of the vehicle. This made it easy to get the centre of pressure exactly where it was from the CFD. From the CFD of this model the CoP was 60% forward. The total Cl of the vehicle was divided by 0.6 and this was programmed into the front wing and the rest was on the rear wing. This change eliminated the Cl and the Cop from changing while the vehicle was increasing its velocity down the runway. The results from this can be seen below in graph thirteen, Compared to the CFD results. This is not an ideal way to program these figures but after many hours of testing this seemed to be the only way to make the simulation model accurate and driveable. This programming approach will make the model less accurate but as stated in a paper called, The influence of slipstreaming on Sports prototype race car performance, “the effect of many variables are impossible to quantify and adoptions and simplifications do not reduce the accuracy of the performance predictions” (Dominy, et al., 2000), thus supporting the decision to simplify the programming procedure.

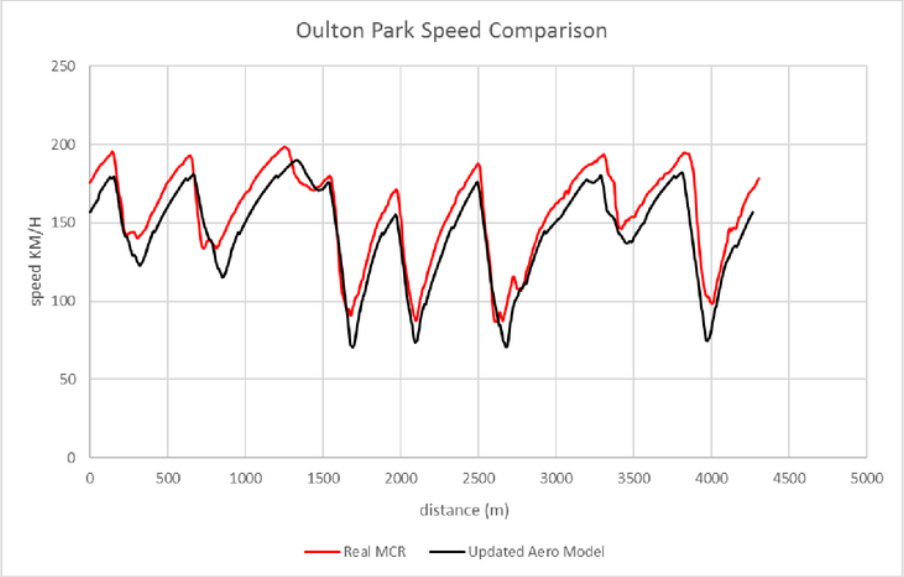


Graph 13 Simulation Aerodynamic Validation MK1

From these tests it was concluded to program every concept in the same way, to keep the tests constant and comparable with the degradation factors set to zero. This would not be entirely representative to the real vehicle but without doing an entire investigation into the aerodynamic sensitivity of the MCR to pitch, yaw and roll the degradation factors could not be calculated within the time frame due to the amount of computational time needed to investigate this for all concepts.

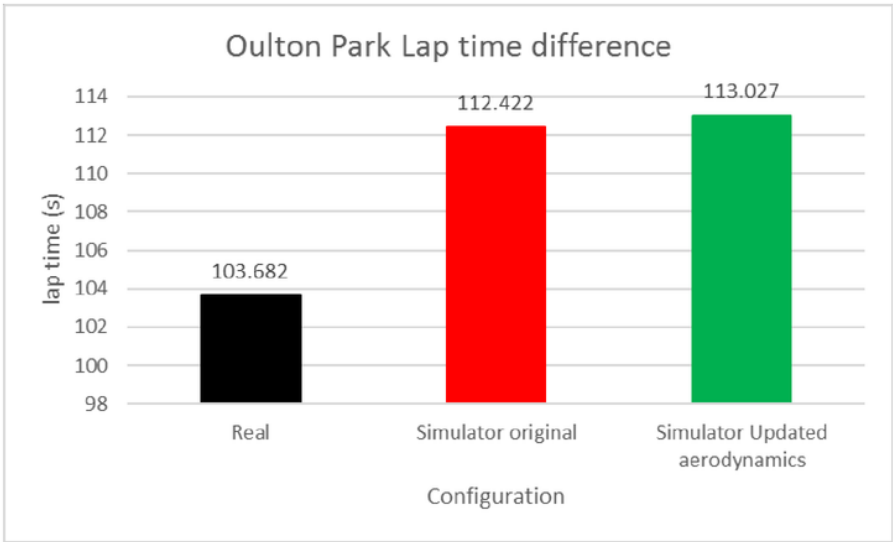
2.2.4 Track Testing of New Aerodynamic Values

The new aerodynamic forces were then used to test to see if they have made the data correlate more to the real vehicle. Graph fourteen, below shows the new speed trace against distance of the real MCR data at Oulton Park.



Graph 14 Oulton Park Updated Aerodynamism Speed Comparison

These updated aero figures did not make much difference on the speed of the vehicle over the course of the lap. There was a similar amount of change in the lateral and longitudinal G-force graphs which can be found in Appendix one and two. These changes had a negative effect on the lap times as the new lap time increased from the baseline shown below in graph fifteen



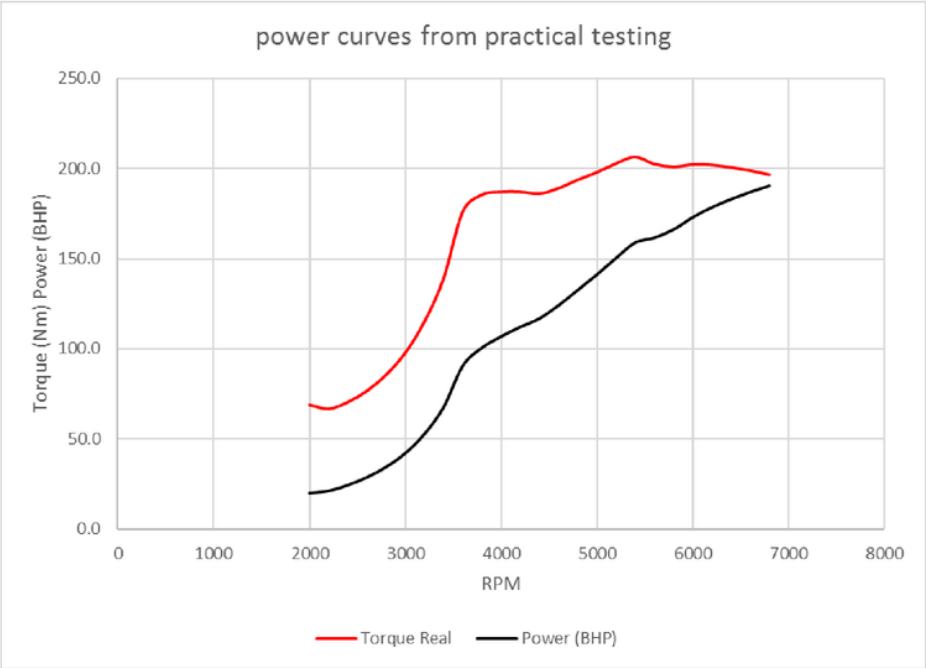
Graph 15 Simulator Updated Aerodynamics Lap Time Comparison

This decrease in lap time is due to the reduction in the lift values programmed compared to the original model which was being over predicted.

These results prove that the model is still inaccurate. Due to this some practical testing was planned to find where the error in speed was originating.

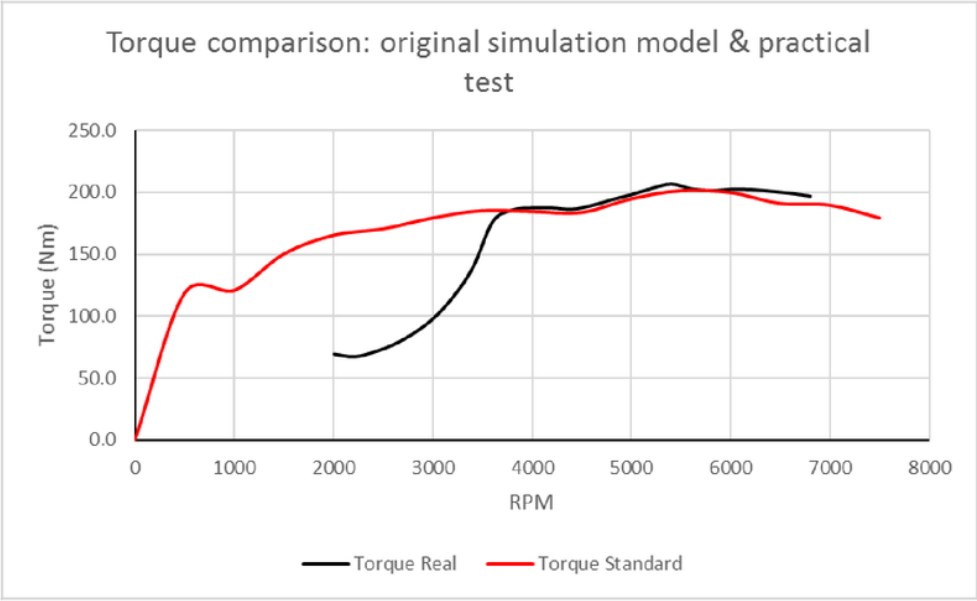
2.2.5 Engine Dynamometer Testing

Due to, when the original simulation model was tested, and the speed over the entire course of the lap was lower than the real vehicle, it was decided to test the power of the real vehicle with the use of the Maha chassis dynamometer, available on the university campus. The MCR was tested, to produce the power curves for torque, back torque and power that the vehicle was producing at the wheels and crank. The Maha Company has been a well-established company for many years with top quality equipment and calibrated machinery. Maha is one of the world's leading manufacturers of workshop and vehicle inspection equipment (Maha, 2018) and the dynamometer used was installed only 4 months prior and thus should have valid calibration. Graph sixteen below shows the power and torque values collected from the dynamometer testing.



Graph 16 Power Curves from Practical Testing

Due to the simulator working just off the torque values of the engine, the BHP was neglected. The torque of the engine was overlaid against what was already programmed into the software which can be seen below in graph seventeen.



Graph 17 Torque Comparison

From graph seventeen the low-end torque has a clear difference compared to the dyno results. Above 4000RPM the torque curves are very similar but there is slightly more torque at the higher rev range between 4000RPM and 7000RPM. This could be the reason for the deficit over an entire lap. The lower rev range would not make much difference to the results due to when the vehicle is on track it is rare that the engine will go below 4000 RPM (Gilani, 2012).

The location of the torque settings is within the engine.ini file which has a section about the power, which is organised as follows: RPMTorque=(RPM, Back torque, Forward Torque). Below figure sixteen shows an example of how the engine torque is programmed through the entire RPM range, thus accurately representing the dynamometer data collected.

RPMTorque=(0.0, -5, 0.0)
RPMTorque=(500.0, -11, 30)
RPMTorque=(1000.0, -19, 50)
RPMTorque=(1500.0, -29, 70)
RPMTorque=(2000.0, -41, 80)
RPMTorque=(2500.0, -48, 100)
RPMTorque=(3000.0, -55, 125.6)
RPMTorque=(3500.0, -62, 170.5)
RPMTorque=(4000.0, -67, 187.3)
RPMTorque=(4500.0, -73, 189.3)
RPMTorque=(5000.0, -76, 198.1)
RPMTorque=(5500.0, -82, 206.6)
RPMTorque=(6000.0, -85, 202.4)
RPMTorque=(6500.0, -90, 199.1)
RPMTorque=(7000.0, -89, 196.8)
RPMTorque=(7500.0, -80, 189.6)

Figure 16 Engine Programming

2.2.6 Mass Distribution

The mass distribution is a highly important part of simulating the real vehicles handling characteristics (Brayshaw & Harrison, 2005).The mass of the vehicle is programmed into the HDV file of the vehicle and a percentage of that mass is put into the rear wheels while it is static to give an accurate distribution. To find these values, the MCR was placed on Intercomp corner weight scales and the values recorded. This was done with the driver in the seat, with their mass included, to make the results as accurate as possible to the real vehicle when it is on track. Below in figure seventeen shows the MCR on the scales and in figure eighteen the values for the mass sitting on each wheel of the vehicle.



Figure 17 MCR on the Intercomp Scales



Figure 18 Mass on Each Wheel

From these measurements 60% of the mass is over the rear axle and the total mass of the vehicle and driver was 596.5Kg this was programmed into the simulator through the HDV file shown below in figure nineteen.

```
Mass=596.5
```

Figure 19 New Mass Programming

These numbers were significantly different to those in the original model. The mass was previously programmed to 620kg and the mass distribution was around the wrong way were 60% of the mass was over the front wheels. This can be seen below in figure twenty, where the first number is the percentage of the mass over the rear wheels.

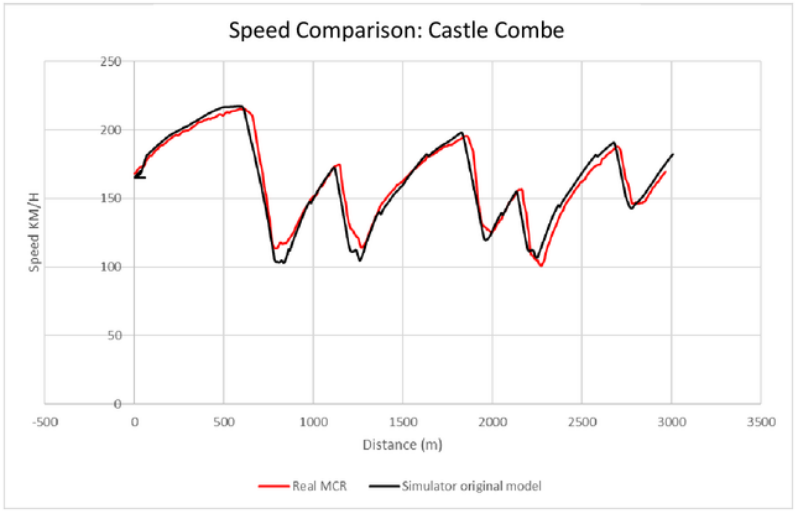
```
CGRearRange=(0.4, 0.010, 40)  // fraction of weight on rear tires
```

Figure 20 Centre of Gravity programming

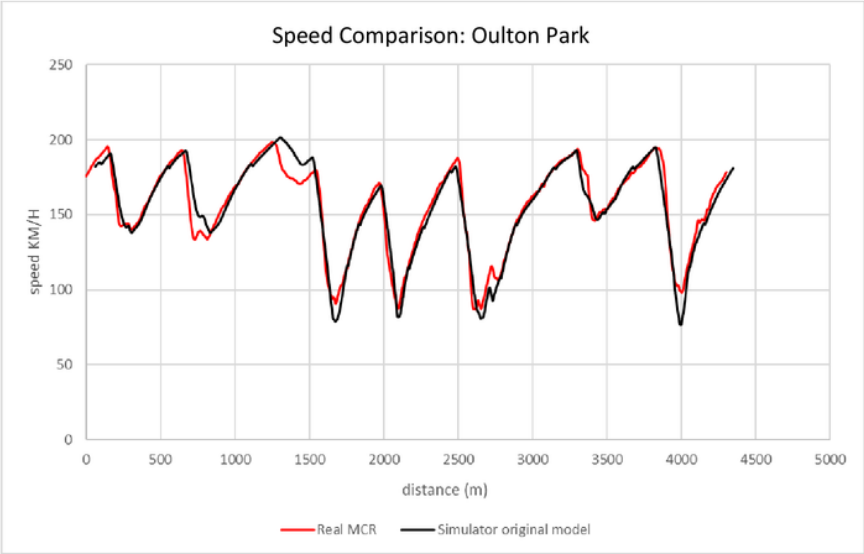
The next step was to validate that the simulator was predicting the mass distribution correctly. This was done by loading into the Skidpad track moving to the flat surface at the start of the runway and staying stationary for a period. The data was collected from this and analysed. Using the wheel loads, a maths channel was produced to display the total front and rear loads of the vehicle going through the tires, by adding the two front tire loads together and the rear tyre loads together. This confirmed that the mass was now correct, and the mass was properly distributed. This was then saved as a constant value within MoTeC to use for the new static weight while doing a straight-line test.

2.2.6.1 Simulator Lap Testing

The new configuration was tested on the same tracks and driver as previously used. Graphs eighteen and nineteen below, show the speed trace over the course of a lap around both the chosen tracks.

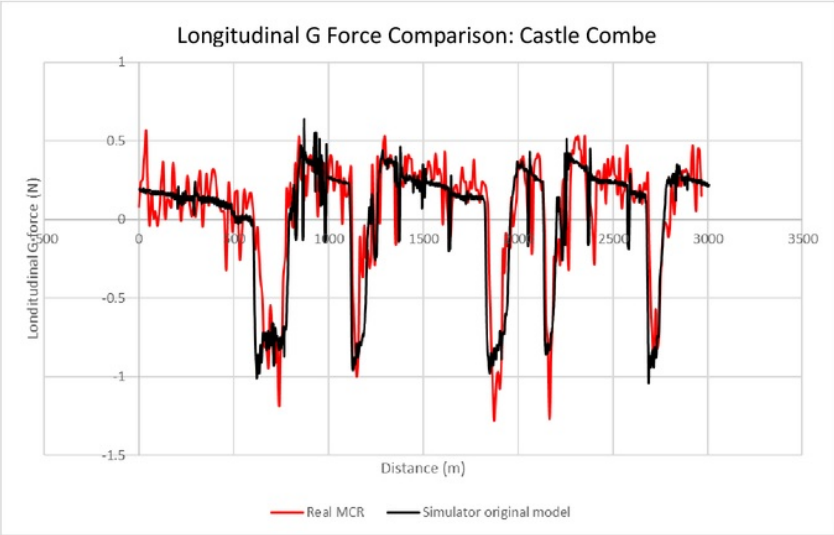


Graph 18 Castle Combe Speed Comparison Updated Mass and Engine

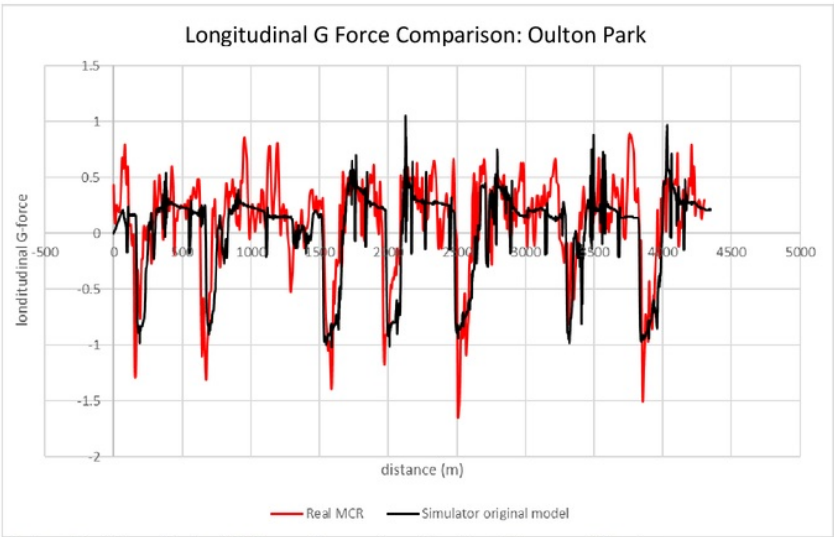


Graph 19 Oulton Park Speed Comparison Updated Mass and Engine

These changes have brought the speed traces much closer to those of the real vehicle. The main differences between the two sets of data now are under braking. The gradient of these sections is less on the simulator model in the majority of the corners. This could be due to the braking force being too low, which influenced the decision to test a higher braking force, once all the practical testing was completed (Castillo, et al., 2016). This is also shown in the longitudinal G-force graphs, shown below, where under braking the simulation model is not reaching the same amount of G-force in the braking zones. With the speed trace graphs there is a section of the data which does not correlate at Oulton Park on the third corner. This corner is a long and very fast left-hand corner. With further investigation into why, in the simulator, the corner could be taken at a much higher speed, it was concluded that the driver in the MCR was braking slightly around that specific corner and the simulation driver was only lifting off the throttle pedal. This highlights a difference between driving styles and also that fear factor could be having an effect on the confidence of the driver on this fast corner.



Graph 20 Castle Combe Longitudinal G Force Comparison Updated Mass and Engine



Graph 21 Oulton Park Longitudinal G Force Comparison Updated Mass and Engine

2.2.7 Spring Rate

Spring rates are one of the factors that effects the weight transfer experienced while the vehicle is undergoing a dynamic situation. The springs are the resistive force that pushes back between the suspension and chassis elements. Making sure these are programmed correctly is a vital part of a simulation model (Chang & Lu, 2008). Using a spring rate tester within the university, the springs were compressed by an inch and the force they put onto the scales is what needs to be programmed into the simulator. All four of the springs were

tested. The setup that is used to measure the spring rate is shown below in figure twenty-one



Figure 21 Spring Rate Tester

Table four, below shows the spring rate for the front and rear springs of the vehicle

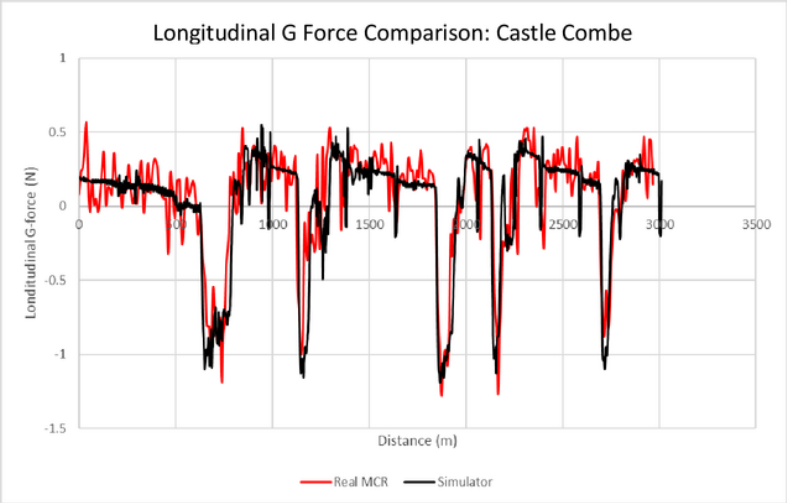
Position	Spring rate Lb/inch
Front	275
Rear	400

Table 4 Spring Rate testing Results

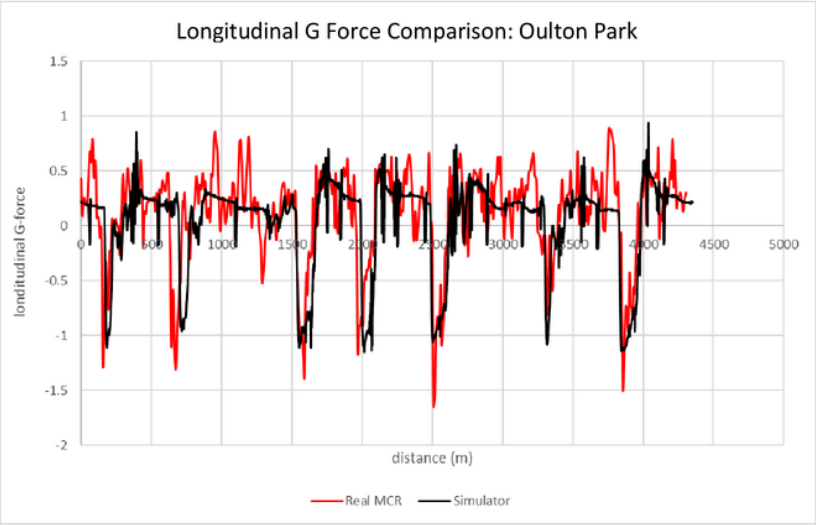
Within the coding for the spring rate, they are programmed as a range of rates so they can be changed within the software menu structure. On further investigation the measured spring rates were within this range and already set to the correct base rate so these did not need additional testing.

2.3 Increased Braking Force

Looking at the data collected after all the practical testing had been programmed it was decided that the longitudinal G-force under braking in the simulator was not reaching the same high values as the vehicle would see in the real world. Due to the difference only being in the braking zones and not while the vehicle was accelerating it was decided to increase the braking force applied, to try and get these to correlate more and not change the tyre grip factors as these appear correct. The braking force on the original model was set to 700, it was decided to increase this to 900 and was re-tested on the same tracks with the same driver. Below graphs twenty-two and twenty-three shows how much closer this made the baseline to the real vehicle.



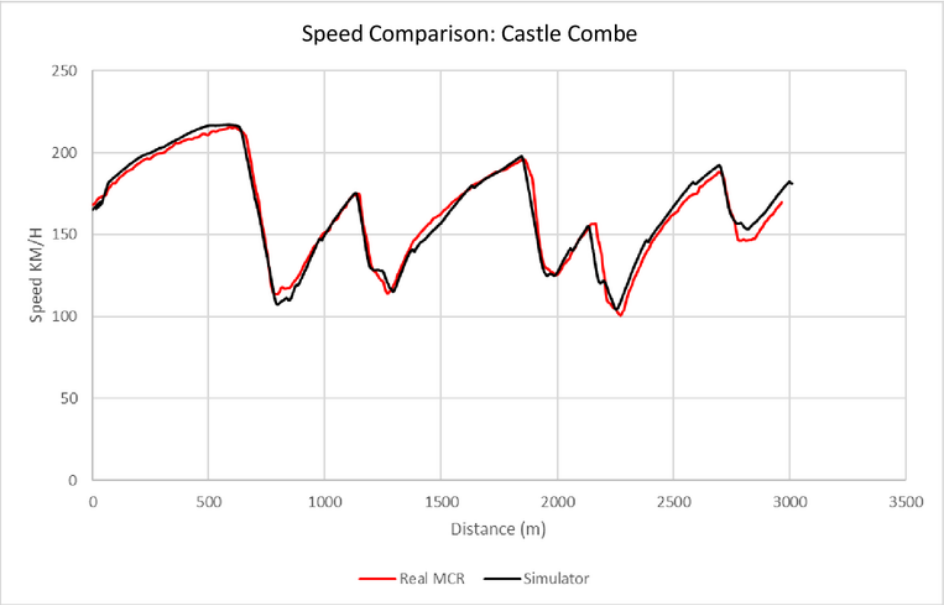
Graph 22 Castle Combe Longitudinal G Force Comparison Increased Braking Force



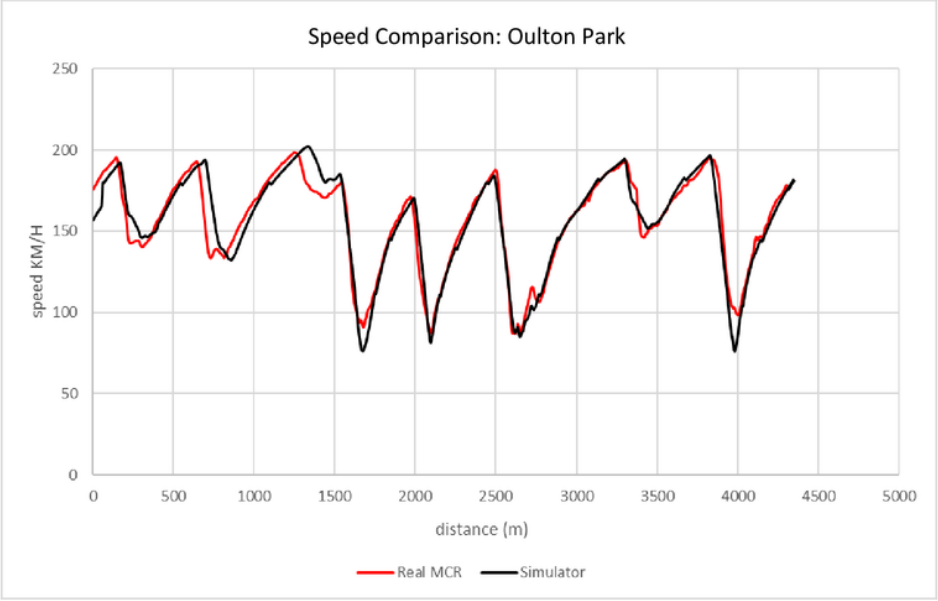
Graph 23 Oulton Park Longitudinal G Force Comparison Increased Braking Force

From the increase in the braking force the peaks of the longitudinal G-force have correlated better to the original vehicle. There is a slight difference with how much they correlate at the different track, for example at Oulton Park the spikes are still quite a bit higher than at Castle Combe. It was decided to not change the braking force anymore due to the gradients of the speed traces shown below in graphs twenty-four and twenty-five Being very similar. It is also worth noting that the data from the real vehicle is a lot more sensitive and the data traces are a lot peakier than the simulator data. This could be due to vibrations going through the chassis, or even just that the sensor moves slightly with where it is mounted to the vehicle.

The speed comparison from this change is negligible but there are signs of driver differences in the braking zones as shown below in graphs twenty-four and twenty-five

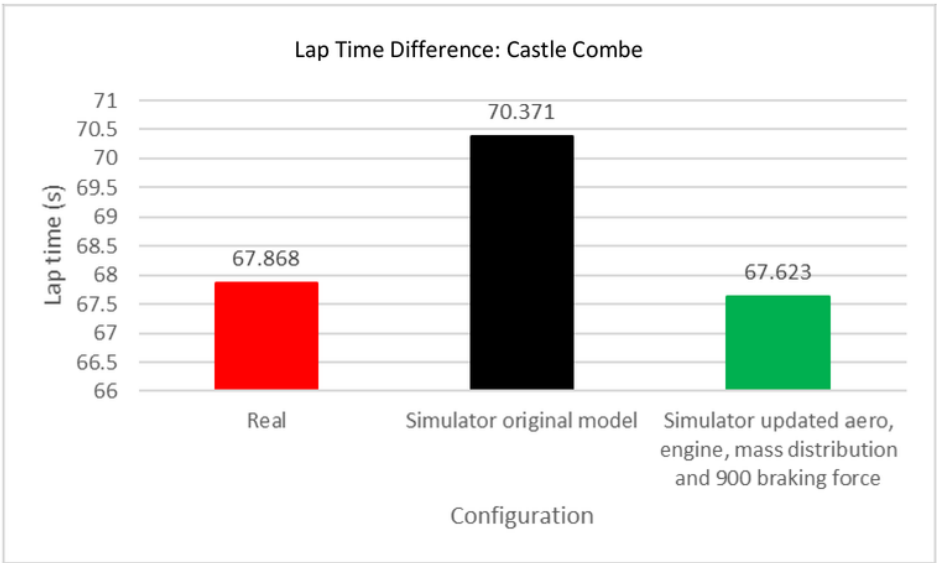


Graph 24 Castle Combe Speed Comparison Updated Braking Force

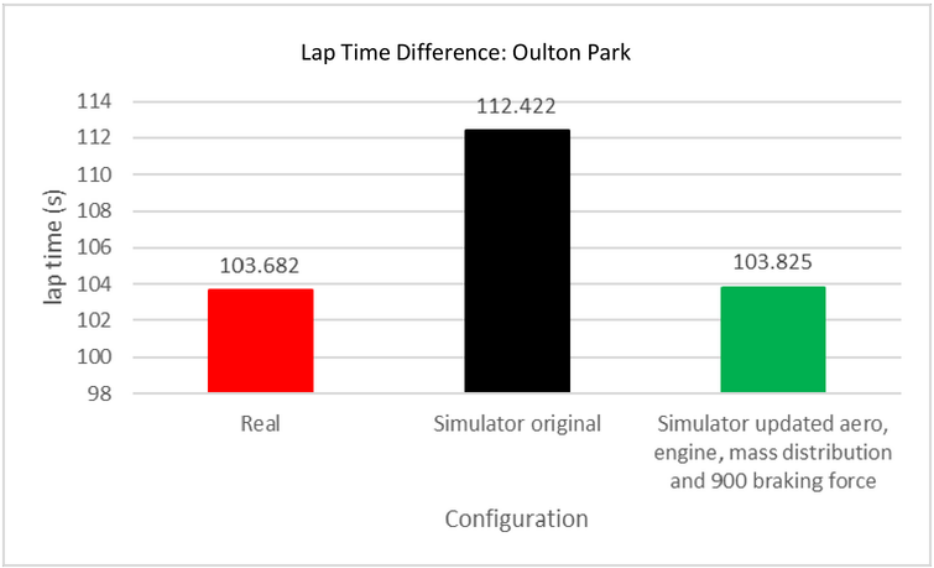


Graph 25 Oulton Park Speed Comparison Updated Braking Force

The last set of data to compare was the lap times of the baseline compared to the real MCR which can be seen below in graphs twenty-six and twenty-seven.



Graph 26 Castle Combe Lap Time Comparison Updated Braking Force



Graph 27 Oulton Park Lap Time Comparison Updated Braking Force

The new baseline model is much faster over the course of a lap than the original model. The baseline model is also within 0.3 seconds per lap of the real data, which is an acceptable allowance (Kang, et al., 2013). Due to this it was decided that the baseline model correlates well enough for it to represent the real vehicle and the baseline for the MK1 was locked down ready to be modified with the aerodynamic values from the other concepts.

3 Bodywork Concepts

Three different design concepts have been created within the university. The MK2 is an updated splitter design, the MK3 is a whole-body work package and the MK4 is built from the Mk3 with some tweaks and improvements to allow for clearance to the chassis for manufacturing.

3.1 MK2 Iley Splitter

As stated previously the MK2 is an updated splitter design by John Iley of Iley designs (Iley, 2019). This concept has a larger and smoother expansion zone, with a raised leading edge to encourage more air to flow under the vehicle and raise the high pressure that builds up on the front of the leading edge upwards, thus reducing the blockage effect of the air flow that goes under the splitter. Below in figure twenty-two and twenty-three, shows the original splitter design compared to the MK2 Iley design.

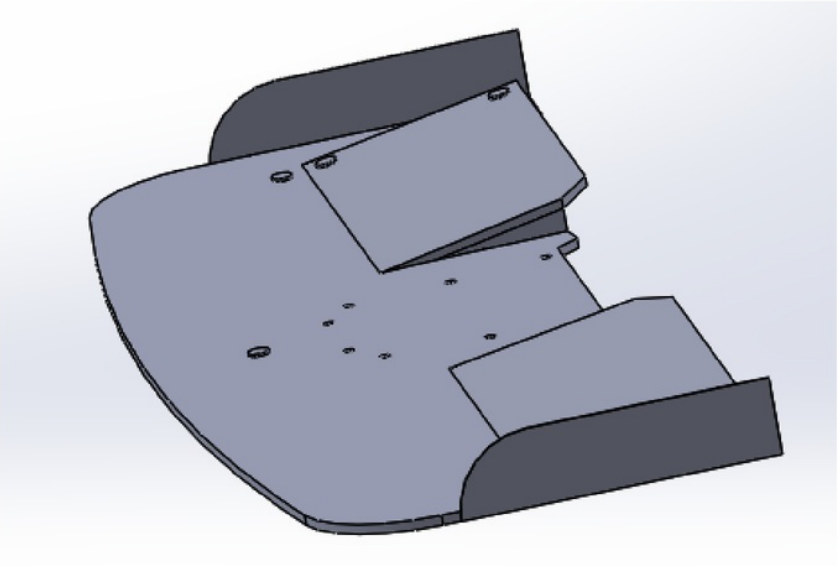


Figure 22 Original Splitter

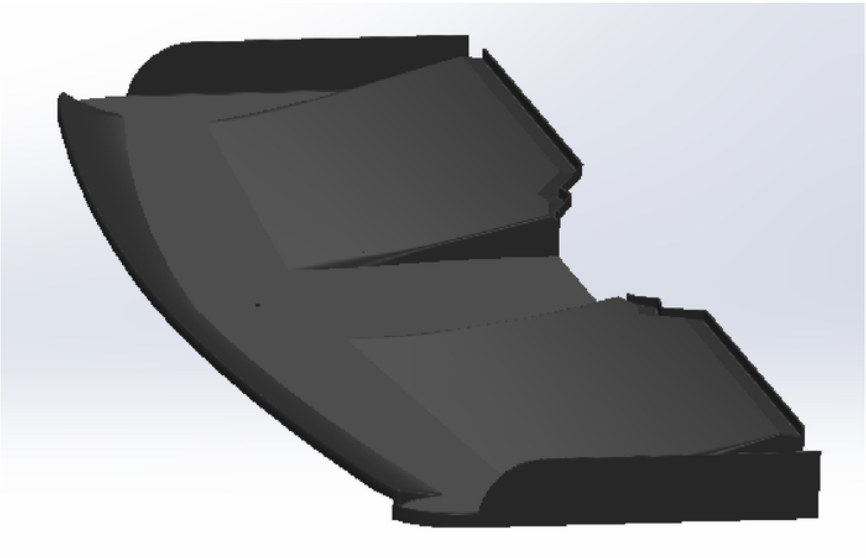
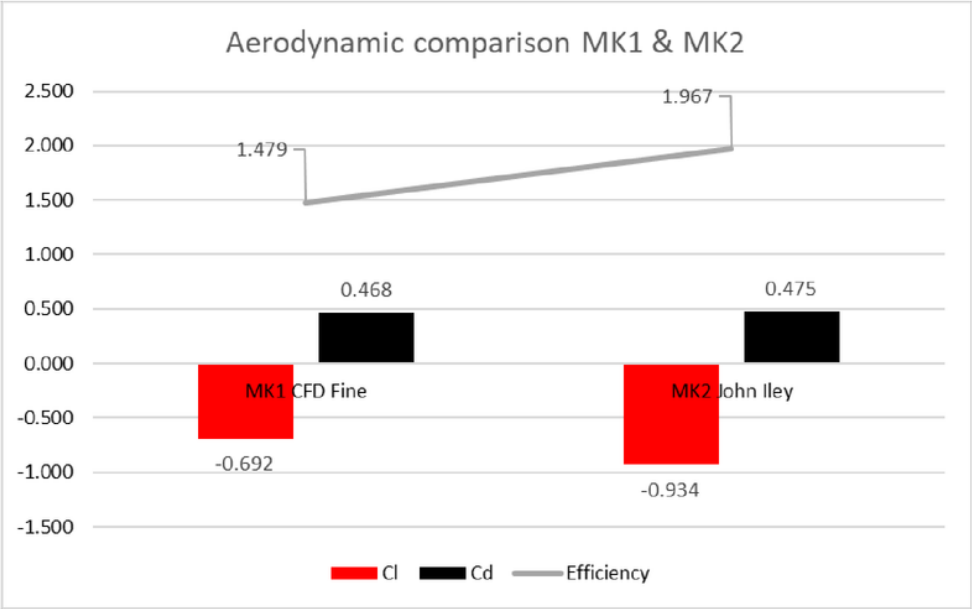


Figure 23 MK2 Iley Splitter

This new splitter is designed to increase the frontal downforce of the vehicle so that it will reduce the understeering characteristics that every MCR has. Even though this component has been manufactured, it is yet to be tested on the vehicle, so no track data was available to validate against.

3.1.1 Aerodynamic Forces

The original bodywork with the new MK2 Iley splitter was processed and run through the CFD software. All the same mesh settings and fluent settings were used from the baseline model to make sure that the results are comparable. The model was also set to the same ride height used previously of 40mm and with no rake. Graph twenty-eight below shows the comparison between the MK1 and the MK2



Graph 28 Aerodynamic Comparison MK1 and MK2

From these results the new splitter design produces more downforce with the drag marginally increasing. This has increased the aerodynamic efficiency of the vehicle, which in theory should make the vehicle handle better and yield faster lap times, without sacrificing the top speed of the vehicle.

The centre of pressure has migrated 4% further forward than the MK1, bringing it to 64% forward. This was expected, as the rear geometry of the vehicle has stayed the same.

When investigating this new geometry there is a clear difference in the velocity of the air that is traveling under the splitter within the expansion zones and the raised leading edge shown below in figure twenty-four Which is from a case comparison within Ansys, which displays the difference with two different investigations. There is no significant difference seen in the velocity on the upper side of the splitter.

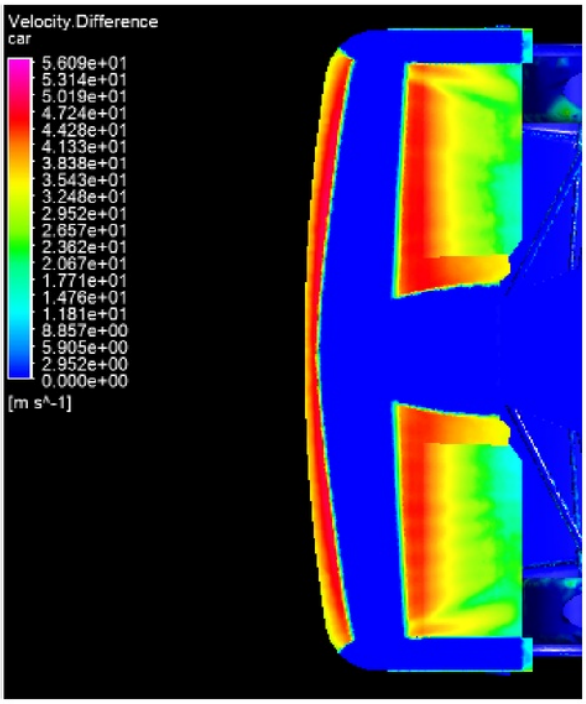


Figure 24 Velocity Contour Case Comparison MK1 and MK2

With the increase in velocity there is also a decrease in the pressure on the underside of the splitter. This is due to the relationship between pressure and velocity. Which is as velocity increases the pressure will decrease due to the conservation of energy, energy can't be created or destroyed. As the kinetic energy increases another form of energy must decrease which is why the pressure will decrease. This can be seen below in figure twenty-five, the top left is the MK1, top right is the MK2 and the bottom displays the differences between the two pressure contours.

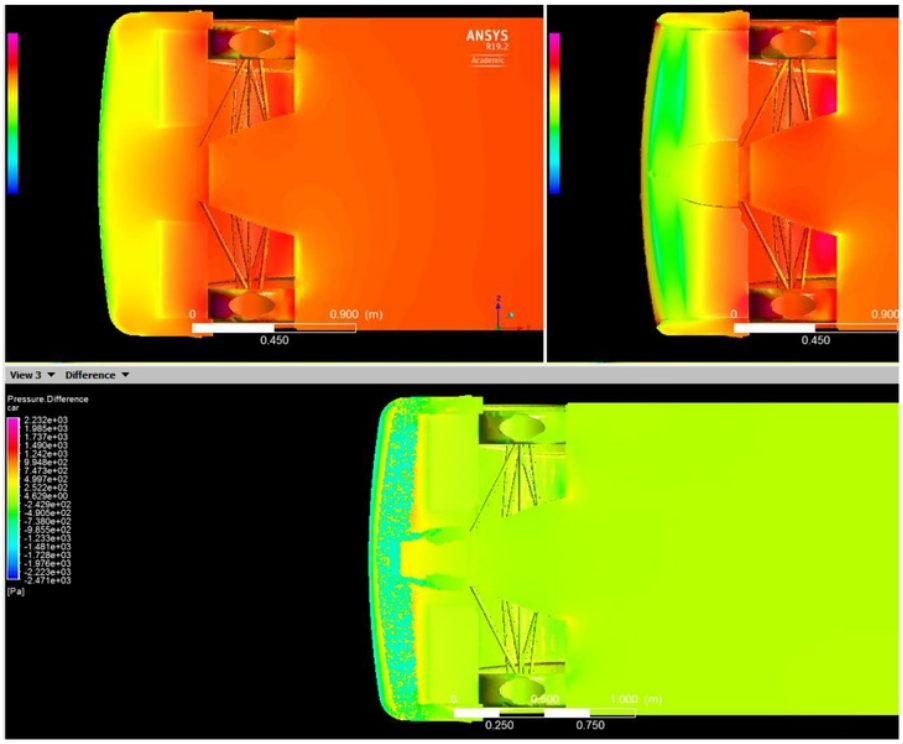


Figure 25 Pressure Contour Lower Surface Case Comparison MK1 and MK2

On the upper surface of the splitter there is also an increase in the pressure seen behind the raised leading edge highlighted in figure twenty-six

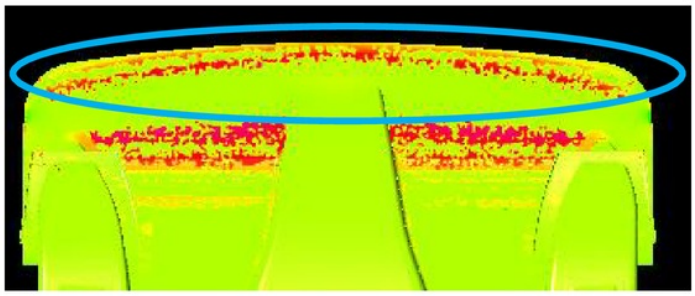


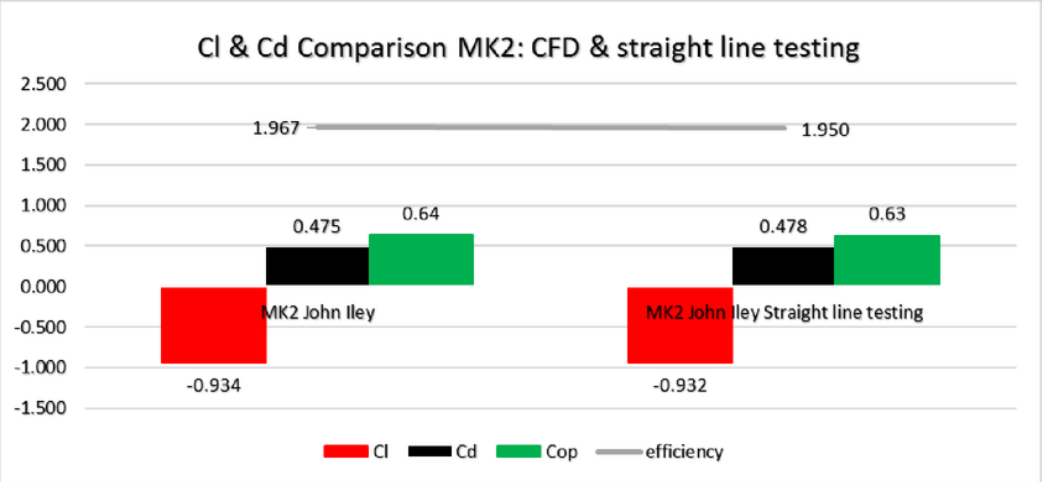
Figure 26 Pressure Contour Upper Surface Case Comparison MK1 and MK2

The pressure differential seen between the upper and lower surfaces has increased, as a result of the geometry changes seen in the expansion zones as well as the radiused leading edge. This pressure differential will yield a greater level of downforce being generated by the splitter (Hucho, 1987).

This change in velocity and pressure proves that this concept works more effectively while static.

3.1.2 Simulator Testing: Aerodynamic Validation

It was decided to program this model in the same manner as previously investigated in section 2.2. Using the total Cl of the vehicle and the CoP to calculate how much of the downforce is produced by the front compared to the rear. Once programmed, the two straight line tests were repeated with the MK2. Graph twenty-nine below, shows a comparison from the CFD and the straight-line testing that the simulator is predicting.



Graph 29 MK2 Aerodynamic Validation Comparison

Looking at the resulting values from the testing, it can be said that the simulation model of this aerodynamic iteration is accurately representing the CFD results.

3.2 MK3 JHTT02 (Concept)

The JHTT02 is a completely different bodywork package that has been designed within the university by John Hughes, supported by Tim Tudor. This bodywork package has been developed over three years, to increase the aerodynamic potential of the current MCR. Figure twenty-seven, below shows a CAD representation of the JHTT02.

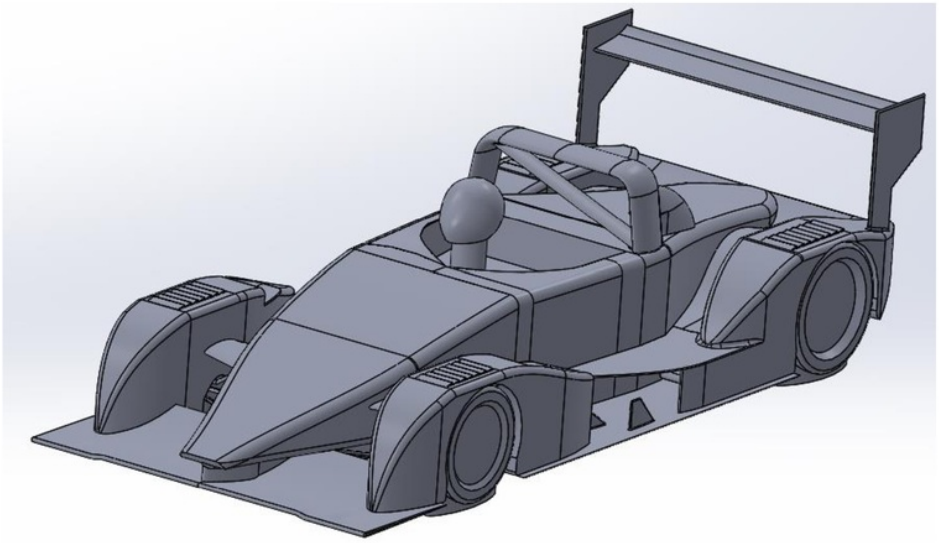
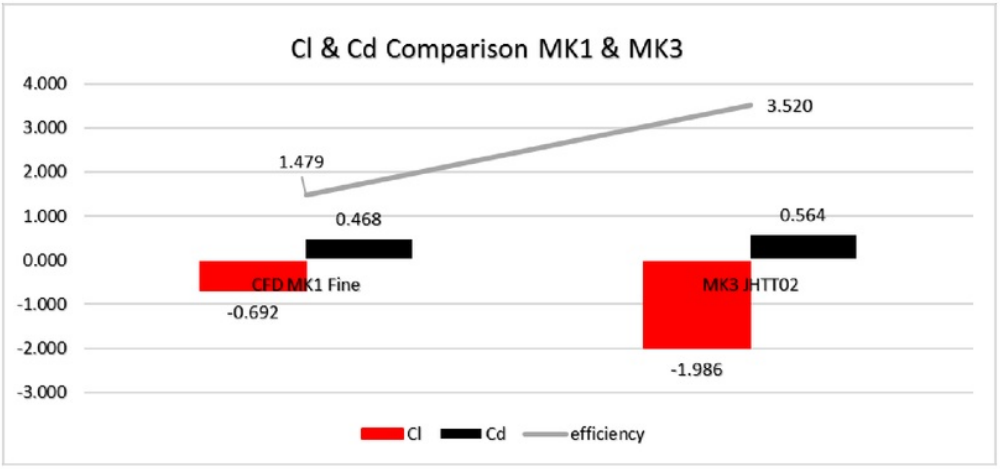


Figure 27 MK3 JHTT02 Concept

When compared to the original bodywork package, significant differences can be seen in the design philosophy implemented. The wheels have their own pontoons, which are separated from the main body of the vehicle. This change in theory should decrease the frontal area of the vehicle, as well as promoting better flow structures around the vehicle.

3.2.1 Aerodynamic Forces

Graph thirty, below shows a comparison from the CFD of the MK1 and the MK3 concepts.



Graph 30 Aerodynamic Comparison Mk1 and MK3

These results clearly show that the MK3 produces notably more downforce, at the expense of a minor increase in drag, which makes the aerodynamic efficiency much higher than

previously. The Cl is over double that of the original, which should give the vehicle more grip through corners, which ought to result in increased minimum cornering speeds. However, with the increase in the Cd, the additional drag force could compromise straight line speeds.

On the upper surface of the MK3, the general pressure distribution is similar to that of the Mk1, this is shown below in Figure twenty-eight. The area at the front, which on the MK1 has a large amount of high pressure, has been reduced due to the decrease in the frontal area, where the detached pontoons prevent the large stagnation zone on the Mk3. There is also a more gradual pressure transition further rearward on the MK3, due to the contoured nature of the rear deck surface.

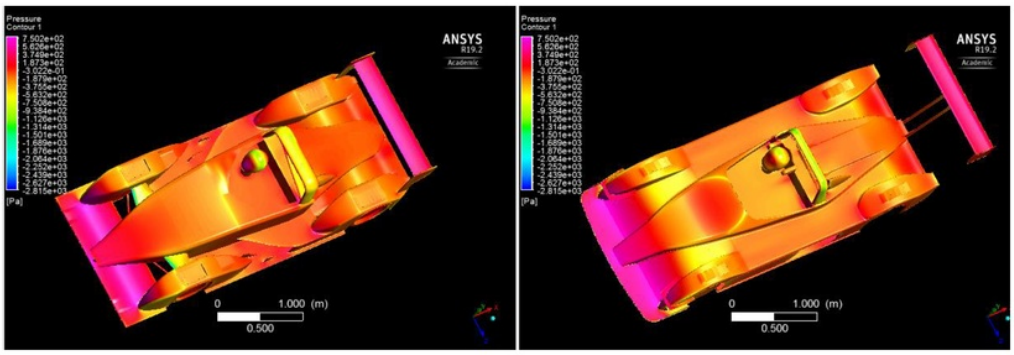


Figure 28 Pressure Contour Comparison Upper Surface MK1 and MK3

The underside seems to be where there is the most geometric difference, where the front splitter difference, linked with the rear end of the vehicle, where there are cut outs in front of the rear wheels, creating somewhat of a Venturi effect. These changes have promoted a significantly higher velocity flow under the vehicle, which has resulted in lower pressure seen on the underside of the Mk3, which is likely to be a major contributing factor to the change in Cl value.

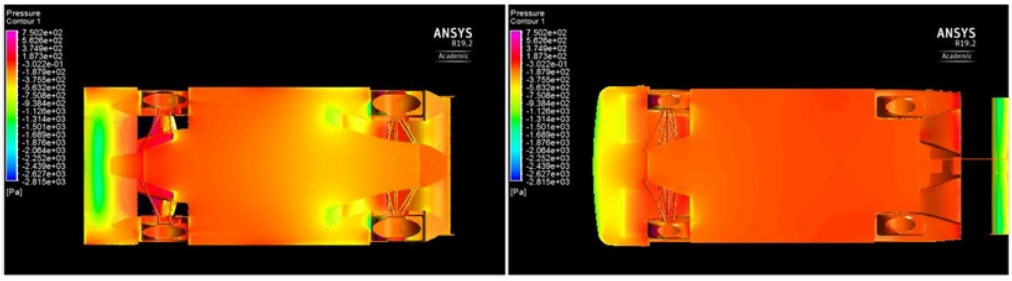
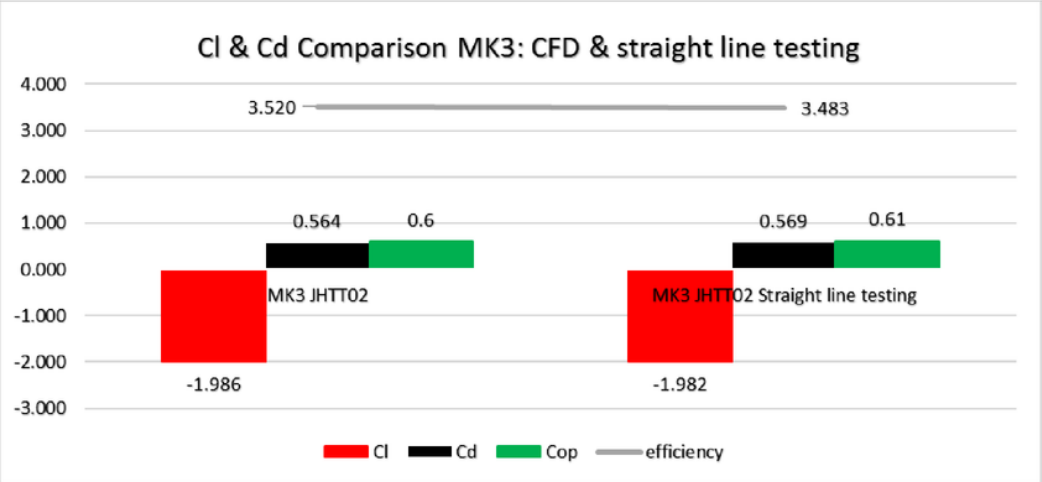


Figure 29 Pressure Contour Comparison Lower Surface MK1 and MK3

3.2.2 Simulator Testing: Aerodynamic Validation

The MK3 concept was tested on the previously detailed straight-line investigations, to validate if the simulator was predicting the Cl and Cd correctly. These results can be seen below in graph thirty-one.



Graph 31 Aerodynamic Validation MK3

Graph thirty-one, shows that the simulator is correctly calculating the aerodynamic forces compared to the CFD results and as such can be considered representative when moving to circuit lap testing.

3.3 MK4 GJ02 (Concept)

The MK4 GJ02 bodywork package has been derived from the MK3 JHTT02. This occurred as inaccuracies were found in the original CAD model that formed the basis of the Mk3, meaning it would not fit the chassis of the actual car, prompting the revisions in the Mk4. This led to the creation of the MK4, which is being prepared for manufacture and test fitting. The MK4 concept is a mixture of the MK2 and the MK3 with the main body being built off the MK3, while incorporating the MK2 splitter. Figure thirty, below shows the MK4 concept.

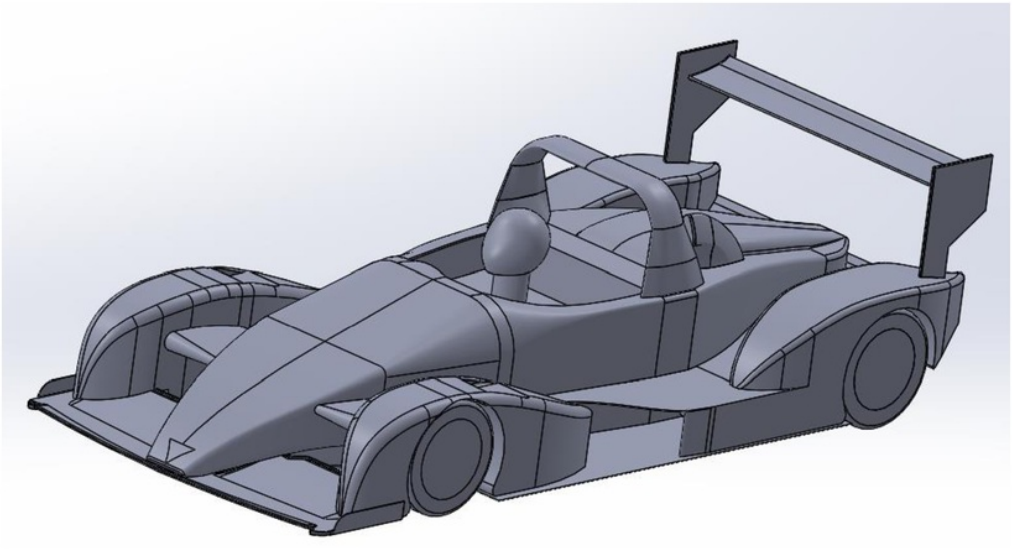
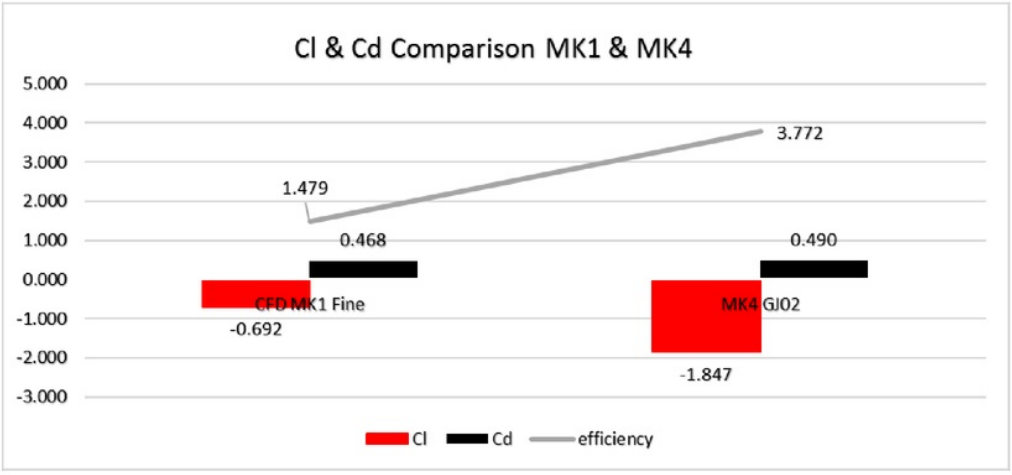


Figure 30 MK4 GJ02

The main design is very similar to the MK3, with some noticeable changes. The front nose has been dropped, to connect to the MK2 splitter and the rear deck has been modified so it fits over the engine and chassis rails. The front pontoons have also been widened slightly to allow for additional clearance of the wheels.

3.3.1 Aerodynamic Forces

Graph thirty-two, below shows the comparison of the aerodynamic forces from the CFD comparing the MK1 and the MK4

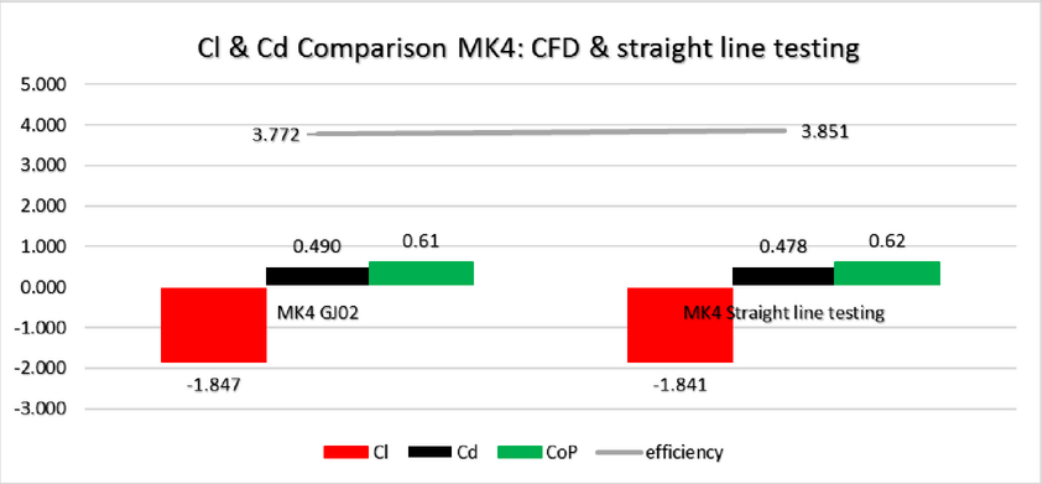


Graph 32 Aerodynamic Comparison MK1 and MK4

From these results there is a clear improvement in the Cl of the vehicle, with a very slight change in the Cd which has given this package a good aerodynamic efficiency value.

3.3.2 Simulator Testing: Aerodynamic Validation

The two straight line tests were again completed, to validate the CFD to the simulation results, these can be seen below in graph thirty-three.

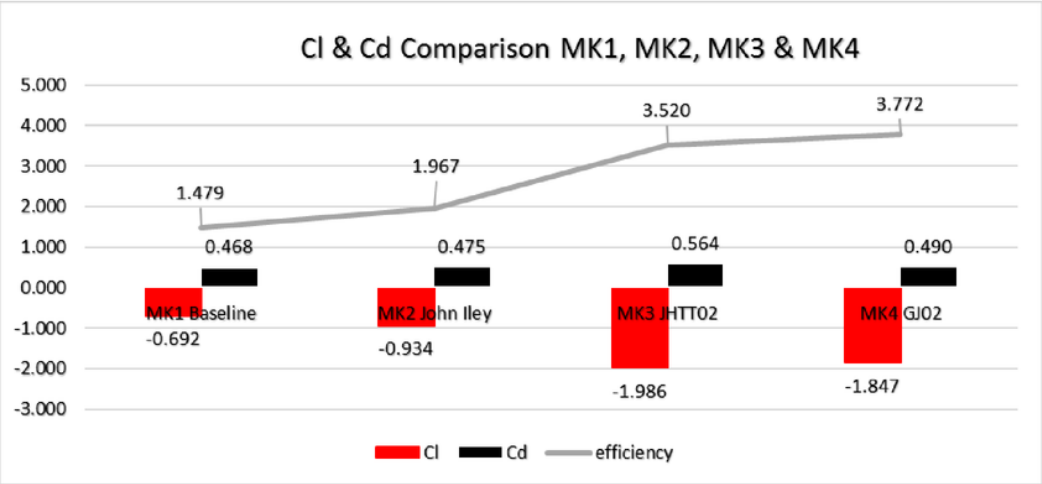


Graph 33 MK4 Aerodynamic Validation

Once again, the results from the simulator can be seen to be accurately calculating the Cl, Cd and CoP when compared to the CFD results.

3.4 Aerodynamic Comparison of all Concepts

Graph thirty-four, below shows all four concepts, comparing the results from the CFD.



Graph 34 Aerodynamic Comparison MK1, MK2, MK3 and MK4

From these results, it is clear that all of the three new design concepts have an increased aerodynamic performance, with the same ride height and angles of rake. This performance change will be expected to influence track results, but they need to be tested under dynamic conditions. The best two concepts are the MK3 and MK4, due to the large amount of extra downforce, with a minimal increase in drag compared to the MK1. Even though the MK3 concept produces the most downforce it also produces a significantly greater amount of drag compared to the MK4, thus resulting in the aerodynamic efficiency to drop below that of the MK4. Due to these contributing factors and the fact that the MK3 concept does not actually fit the vehicle's chassis, investigation into this bodywork concept will not be carried into the next stage of simulation.

4 Simulation Comparison- Lap Testing MK1, MK2 & MK4

This section will investigate how the MK2 and MK4 concepts compare to the MK1 around two different tracks, to analyse how they respond dynamically.

Due to the large increase in downforce produced by the two new concepts, the suspension setup of the vehicle needed to be altered to stop the ride height excessively reducing at maximum speed, to prevent the vehicle contacting on the floor. A setup was found with a raised ride height, stiffer front springs and stiffer damping. Table five, below shows the change in the setup compared to when the MK1 was tested.

Ride height change (Front and Rear)	+10mm
Front springs	+25Lb/Inch
Front dampers	+2 clicks on bump and rebound

Table 5 Setup Changes Required

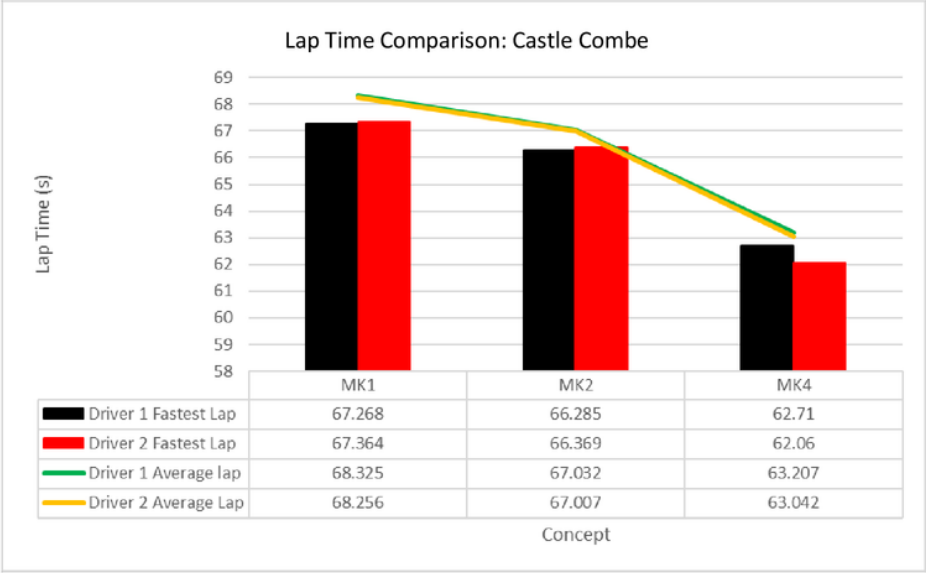
Due to these changes the results will not be directly comparable to the MK1 as the suspension changes will have influenced dynamic behaviour, this needed to be done due to when the vehicle was making contact with the floor there would be no weight transfer and cornering was impossible. Due to the floor contacting the road, the top speeds were hugely affected because of the extra mechanical drag produced by the friction. The lap times were a lot slower than the MK1 as a result of these issues.

Due to one of the largest factors in variation of the data is the driver and how they drive (Kang, et al., 2013), a second driver was tested who has a completely different driving style. Driver one, who has driven for all the testing previously, is fast, smooth and consistent. Driver two is a very aggressive driver who can give fast lap times but can be less consistent, due to pushing the levels of grip and the vehicle to the limit. The difference in driving styles will give two very different samples of cornering techniques, as well as differing driver feedback, which is a good indication of the driver's perception of whether the vehicle can handle well. Also, driver two had never previously driven this simulation model, which eliminated the chance of getting used to the model resulting in faster lap times due to experience, thus giving a more immediate impression of vehicle performance characteristics. Both drivers drove the MK2 and MK4 around Castle Combe and Oulton Park for ten fast laps respectively. This allowed the driver to get the feel for the vehicles handling balance during the out lap, then push the model to the driver's limit for the following ten laps.

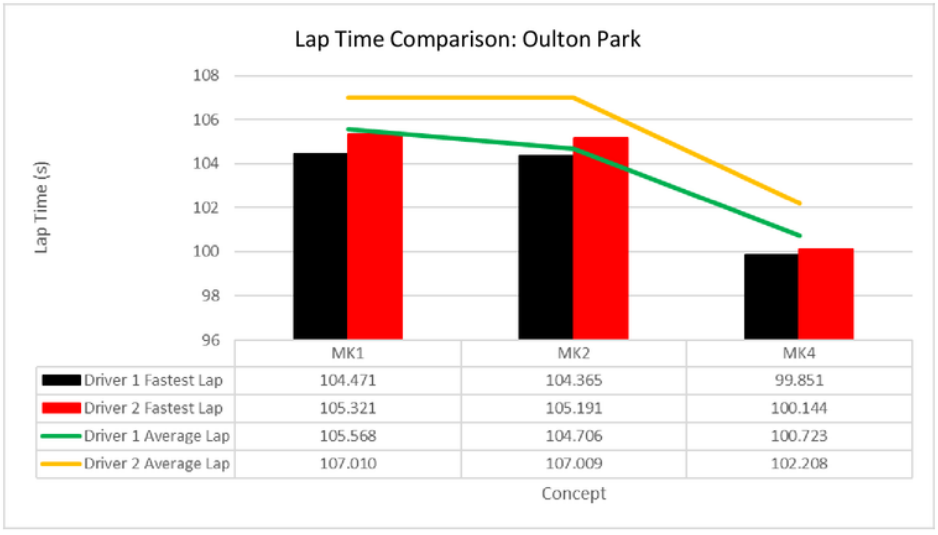
4.1 Lap Time Comparison

Lap times are very important to any race car manufacturer as it shows potential buyers what their vehicle is capable of in relation to other competing vehicle designs. Additionally, the

lower the lap time, the greater the chances the vehicle will succeed in its respective race class. Lap times are a very good and quick indication of how upgrades are performing while on track compared to their original components. Figures thirty-five and thirty-six, below shows two graphs which clearly show the fastest lap times for each driver, and their average lap time over the ten laps completed. It is worth noting that driver two did have a small spin, as a result of driver error, on one of the laps at Oulton Park, which was discounted in these averages. This also highlights the limitations of driver in the loop simulation.



Graph 35 Castle Combe Lap Time Comparison

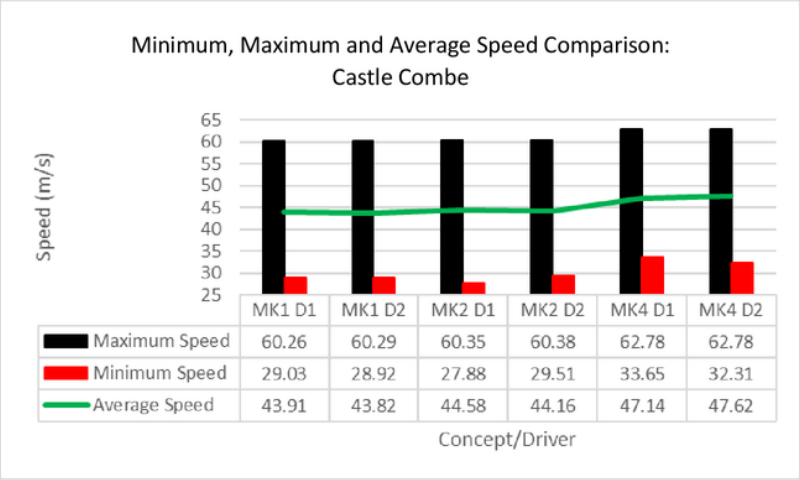


Graph 36 Oulton Park Lap Time Comparison

From these graphs there is a clear improvement for the MK4 concept, with both drivers at each track. At Oulton park there is less of a change between the MK1 and the MK2 for both drivers but there is a minimal improvement for driver two. This could be due to driver two not knowing this track as well as Castle Combe, rather than an inherent limitation of the vehicle's performance characteristics. It is also worth noting that, Oulton Park incorporates several slow speed corners, where the increased downforce levels of the new designs will have little effect due to the slower speeds, potentially explaining why there is less improvement seen at Oulton Park compared to Castle Combe. From these graphs the MK4 is overall the better performing, while the mk2 shows an improvement over the MK1 baseline. The trend seen in the data follows the CFD data, where the Mk4 was proven to generate notably more downforce, with greater efficiency than the Mk2, hence the reduced lap times of the Mk4 compared to other designs.

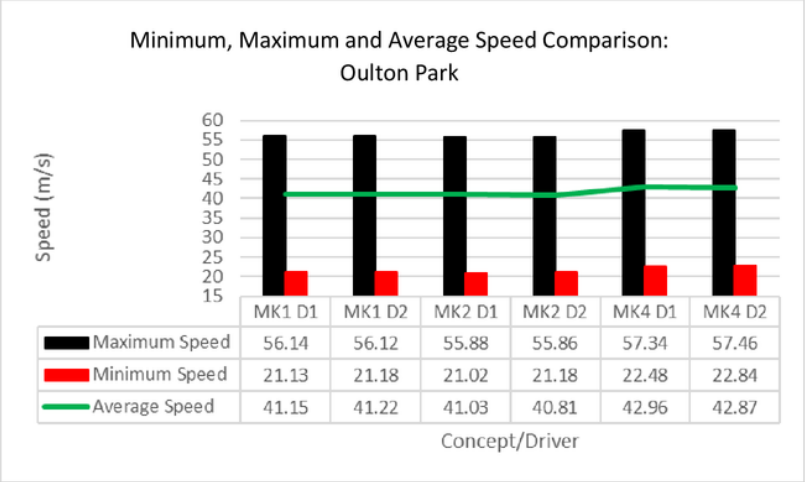
4.2 Speed Comparison

Aerodynamic changes can really influence the speeds around different parts of the track, for example if the drag is high it will reduce the top speed of the vehicle but if the downforce is high it will have more grip around corners increasing the speed during the turn (Metz & Metz, 2000). Due to this, it can be said that different track layouts require different aerodynamic characteristics of a vehicle, which can be seen in the differing levels of performance gain at two very different types of track from the testing previously detailed. It was decided to investigate the minimum, maximum and average speed over the entire lap at both tracks, as this will give an indication as to the performance the driver is being able to extract from each concept, which is shown below in graphs thirty-seven and thirty-eight, where D1 notates driver one and D2 notates driver two.



Graph 37 Castle Combe Speed Comparison

As with the lap time differences shown previously, there is a clear trend where the MK4 achieves a higher maximum speed around Castle Combe than the other two concepts, while there is not much difference between the MK1 and MK2 concepts. The MK4 geometry can also get around the tighter areas of the track at a higher speed due to the minimum speeds being higher than the other two concepts, as will be explained later in this report. This in turn increases the average speed over the whole lap, which would be why the lap times were the lowest in total. There is not much difference between the MK1 and the MK2 for both drivers, indicating consistency of data. For the MK2 the average is higher for both driver which indicates that the change to the vehicle's handling balance has proven beneficial over the course of a lap, despite the lower minimum speeds seen. This will be investigated.



	MK1 D1	MK1 D2	MK2 D1	MK2 D2	MK4 D1	MK4 D2
Maximum Speed	56.14	56.12	55.88	55.86	57.34	57.46
Minimum Speed	21.13	21.18	21.02	21.18	22.48	22.84
Average Speed	41.15	41.22	41.03	40.81	42.96	42.87

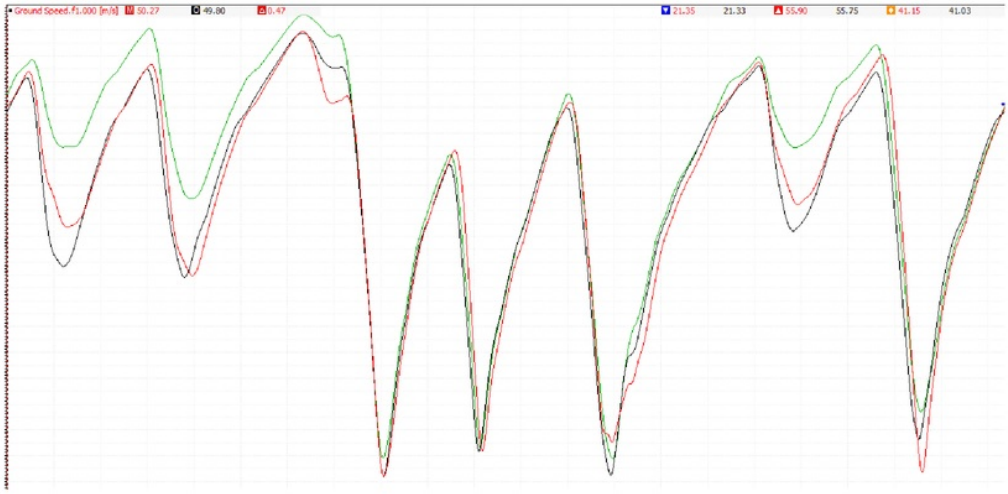
Graph 38 Oulton Park Speed Comparison

The speeds around Oulton Park follow a similar trend to that of Castle Combe, where the MK4 has the highest of all three of the variables and the MK1 and the MK2 are very similar. Once again driver two maintains higher minimum speeds than driver one resulting in higher average speeds.

From these graphs even though the MK4 has the highest value for the Cd it still produces the highest top speed. This is likely due to being able to carry more speed through corners, thus starting a straight at an overall higher speed than the previous concepts.

Looking at the data like this gives a rough estimate of how the vehicle is handling but to see where each concept is better than another the data needed to be investigated further. The main areas which will be looked at will be the high and low speed corners to see how the aerodynamic changes have affected the dynamic performance. Graph thirty-nine, below shows a screenshot from MoTeC from driver one around Oulton Park comparing the speed

against track distance of all three concepts. the red line is the MK1, black line is the MK2 and the green is the MK4. These colours will be used through this section of analysis.



Graph 39 Oulton Park Speed Comparison

From this the MK4 is much faster through the high-speed corners, as expected given that lift force is a factor of velocity, which is also shown below in figure thirty-two, which is a zoomed in section from turn one, a declining gradient, high speed, right handed corner also shown below in figure thirty-one.

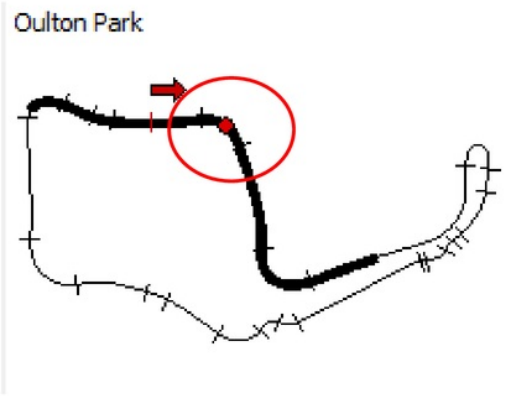


Figure 31 Oulton Park Track Position Turn one

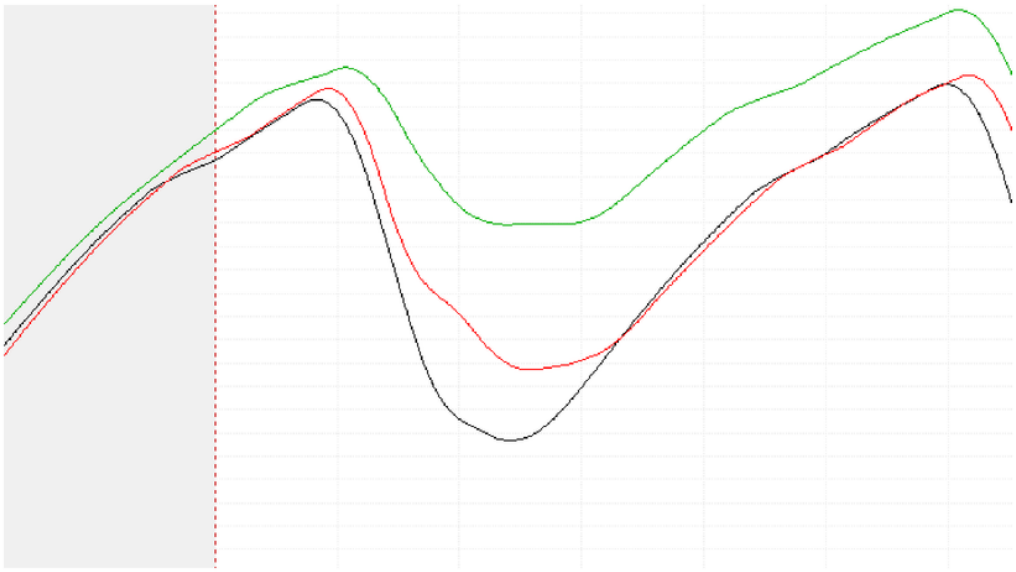


Figure 32 Oulton Park Speed Comparison - Turn One

The above data trace shows that the MK2 is slower mid corner, but there is more speed on the exit which helps carry speed going down the straight. This could be due to the driver feeling more comfortable around this corner in the MK1 configuration, considering that the Mk2 should have increased downforce and theoretically should be able to maintain higher apex speeds. However, this highlights the importance of handling balance, as opposed to simply raw downforce values (Mariani, et al., 2015). This is not the case for every fast corner on the track, for example at turn three, which is a fast sweeping left hand corner shown below in figures thirty-tree and thirty-four.

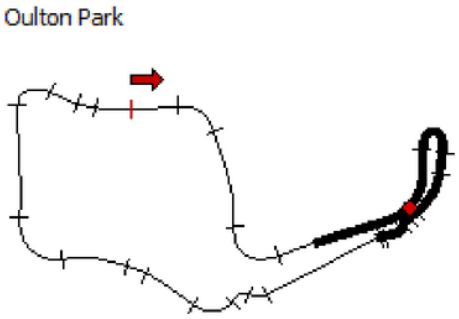


Figure 33 Oulton Park Turn 4

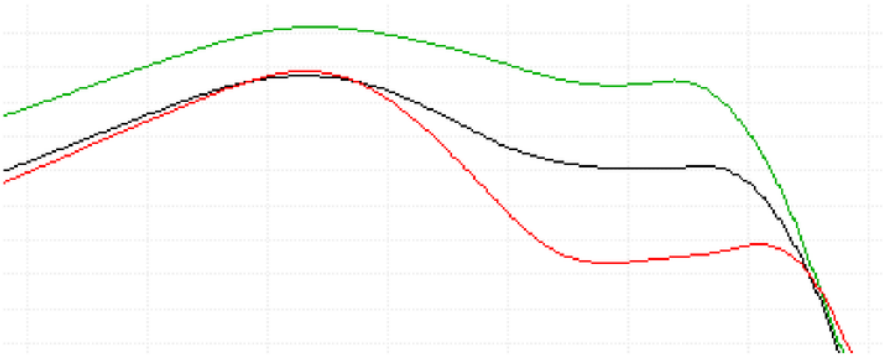


Figure 34 Oulton Park Speed Comparison - Turn Four

This shows that the MK2 achieves higher cornering speeds than the Mk1 through this section, which is the fastest corner on the circuit. This could be due to the extra downforce, and large corner radius meaning that the extra downforce outweighs any handling imbalance, resulting in higher apex speeds. Figure thirty-five, below shows the total wheel loads of the vehicle from the same time period, proving that the MK2 has more total wheel loads, thus more downforce, as the total wheel load minus the static load is the aerodynamic load.



Figure 35 Oulton Park Wheel Load Comparison - Turn Four

A similar trend can be seen in the very low speed corners. This is shown below in figure thirty-six, which shows the speed around the banked hairpin and the first chicane. Highlighted below

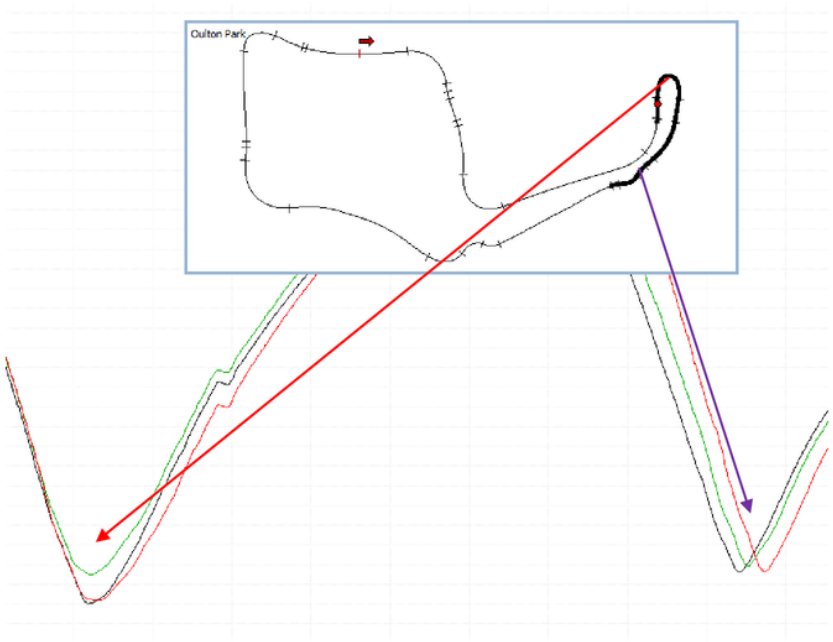


Figure 36 Oulton Park Speed Comparison - Turn Five and Seven

Around the hairpin, the MK4 was able to take the corner at a higher speed than the other two, which are very evenly matched, with the MK2 getting a better exit again and carrying more speed out of it. Given this is a relatively slow speed corner, the data is highlighting the minimal amounts of downforce being generated by the Mk1 and Mk2 configurations, compared to the Mk4 (Plotkin & Katz, 2002).The data traces for the chicane show that all concepts have a near identical speed through the corner. This could be a result of the rapid direction change experienced through the chicane, so the vehicle is primarily relying on its mechanical grip and weight transfer characteristics as the limiting factor, rather than aerodynamic grip as seen in the relatively steady state corner previously.

4.3 G-force Comparison

With extra downforce there is an expectation to produce higher lateral G-forces while cornering at high speed as a result of the additional tyre grip available (Morse, 2016). This section will investigate the lateral and longitudinal G-forces each concept produces

Figures thirty-seven and thirty-eight, below shows a comparison of the longitudinal and lateral G-force of driver one around Castle Combe and Oulton Park respectively for all three of the concepts.

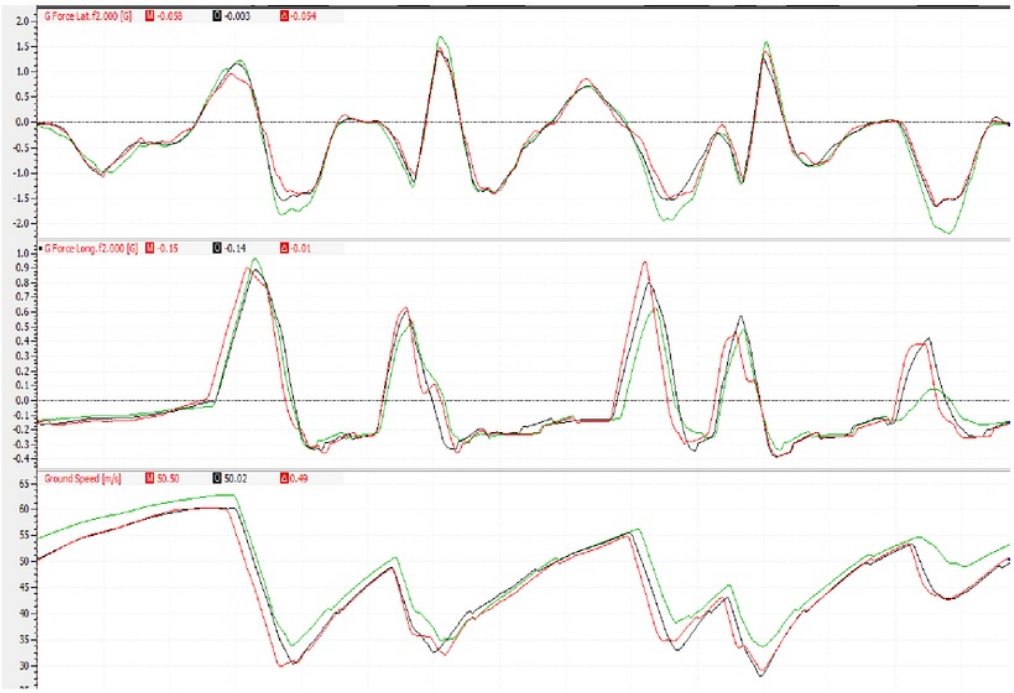


Figure 37 Castle Combe G Force Comparison

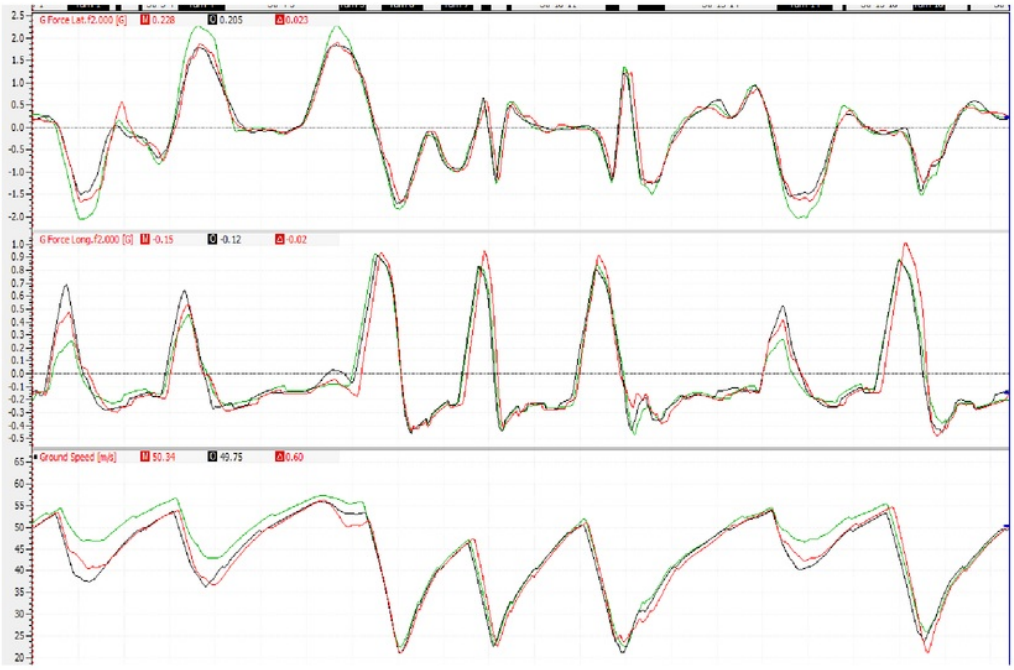


Figure 38 Oulton Park G Force Comparison

At both of the tracks there seems to be similar trends when comparing the different concepts, for example the MK4 reaches a much higher lateral G-force around the fast corners of the track, while the MK1 and MK2 are very similar, as outlined below in figure thirty-nine, which is from turns three and four at Oulton park

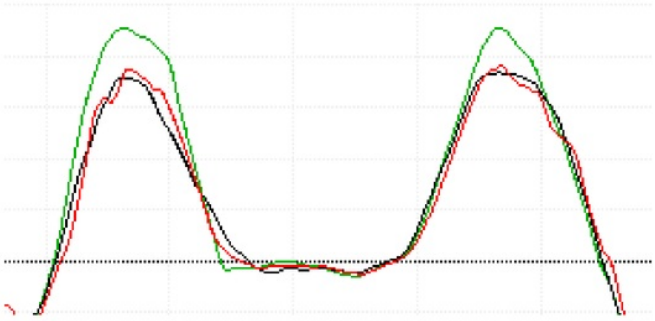


Figure 39 Oulton Park G Force Comparison - Turn Three and Four

The reason the MK4 produced a higher lateral G-force is due to the extra downforce, and resultant increased available tyre grip, allowing the vehicle to negotiate this corner at higher speeds. This is supported by a book called aerodynamics of road vehicles, which states that a vehicle with more negative lift produces a higher maximum lateral acceleration with speed (Hucho, 1987). This also explains why the Mk1 and the MK2 are very similar, as their

downforce levels will be quite even. This is not the case in the very slow speed corners where aerodynamics does not affect this as much, for example the first chicane shown below in figure forty. This again highlights that mechanical grip is the limiting factor in these low speed corners.

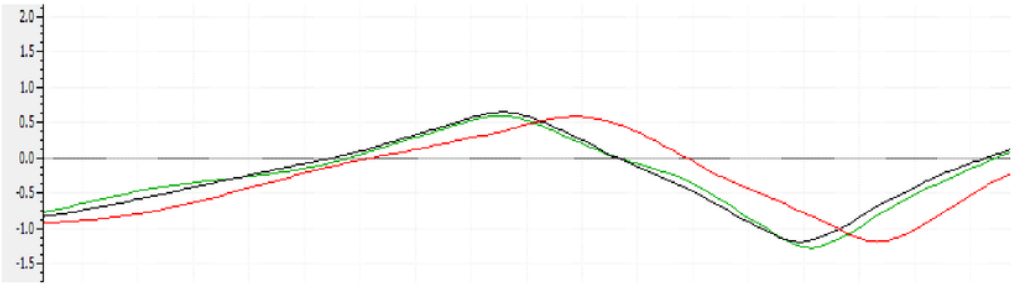


Figure 40 Oulton Park Lateral G Force Comparison - Turn Seven

The longitudinal G-force produced by the three concepts is quite different than the lateral forces. The MK1 seems to produce the highest peak under braking into most of the corners shown below in figure forty-one.

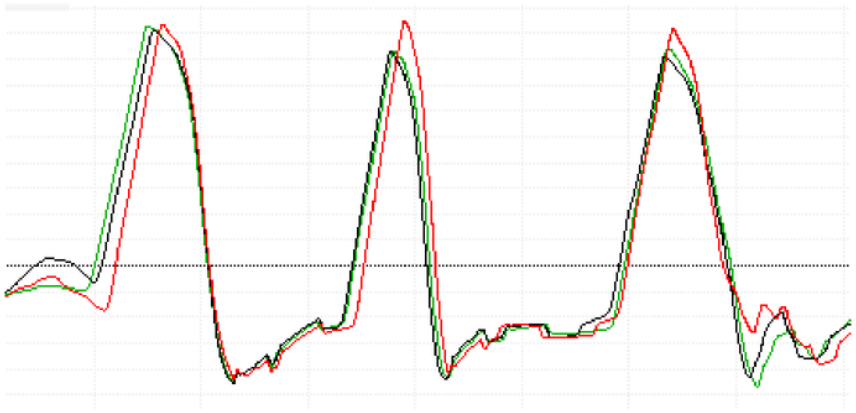


Figure 41 Oulton Park Longitudinal G Force Comparison

Originally it was thought that due to having less downforce the vehicle needed more braking force to slow it down but looking into the braking percentage the MK1 needed less or equal force to the other two concepts, shown below in figure forty-two. This is also surprising, given that the additional downforce the Mk2 and Mk4 concepts produce at the start of the braking zone (high speed), should give increased tyre grip, thus providing greater levels of available grip for braking prior to experiencing brake locking.

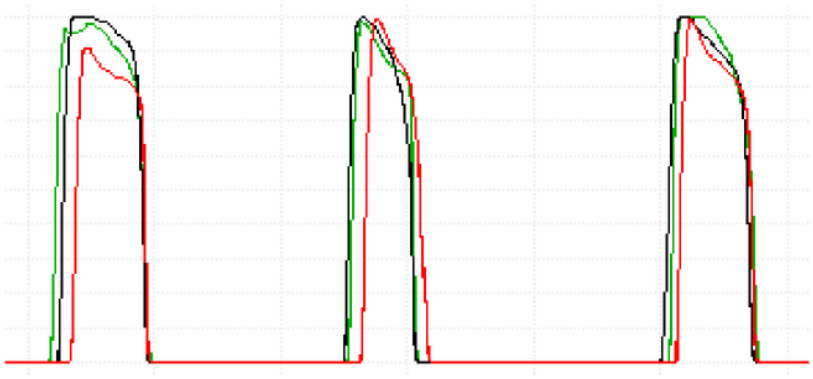


Figure 42 Oulton Park Braking Force Required

Due to these results it was concluded that this change in the braking differences were due to driver evolution and an adaptation of style between the concepts. This was decided due to the driver braking later and not carrying the seed onto the straight, displayed below in Figure forty-three.

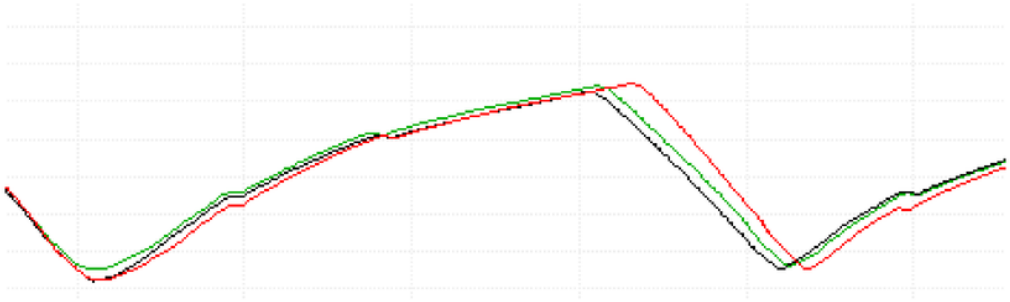


Figure 43 Oulton Park Later Braking Example

4.4 Dynamic Aerodynamic Performance Comparison

Using the aerodynamic force channels that were created for the straight-line tests, it is possible to investigate the change of aerodynamic forces that the vehicle produces while track testing. This can give a good indication of how the concept is performing under dynamic conditions. Due to the degradation factors being set to zero these results will not be absolute, but should be representative. Figure forty-four, below, still demonstrates a significant change in aerodynamic loadings between the different designs, at Castle Combe.

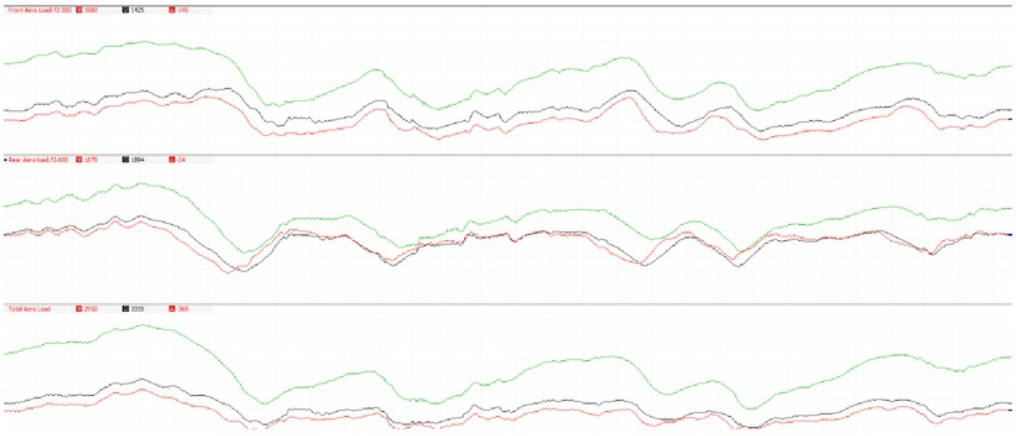


Figure 44 Castle Combe Aerodynamic Load Comparison

The MK4, as predicted, is producing the largest front and rear levels of downforce around Castle Combe, which in turn produces the most overall downforce levels. Although an increase in overall downforce is seen with the Mk2, compared to the Mk1, it is minimal. The main difference is the front-end downforce is higher for the MK2, which is to be expected given the new design of splitter, which the CFD results proved to be more effective than the baseline version. The same trend can be seen while testing them at Oulton Park shown below in figure forty-five.

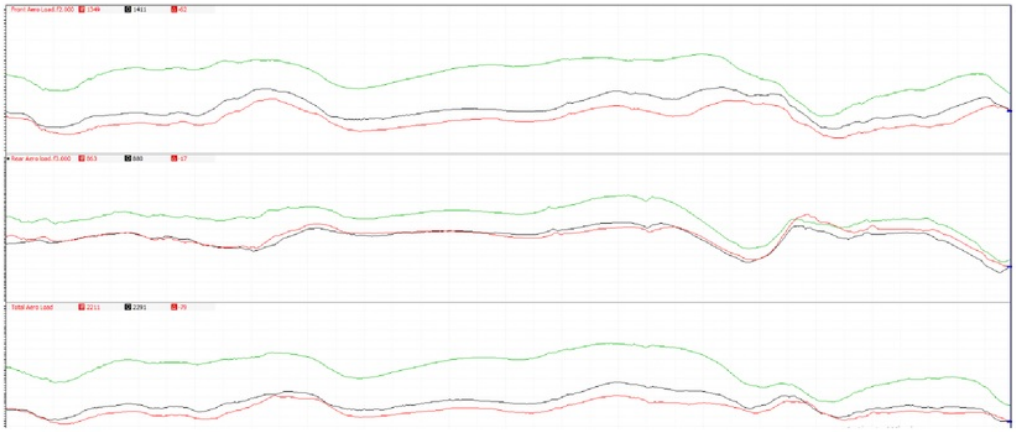


Figure 45 Oulton Park Aerodynamic Load Comparison

This data supports why the MK4 can go corner at a higher speed, due to the extra tyre grip from the higher levels of downforce produced. (Hucho, 1987)

To better analyse the performance of the concepts, data from both drivers is compared, to look more into the handling characteristics of the vehicles that have resulted from the changes in downforce. Figure forty-six, below shows an overlay of both drivers' data.

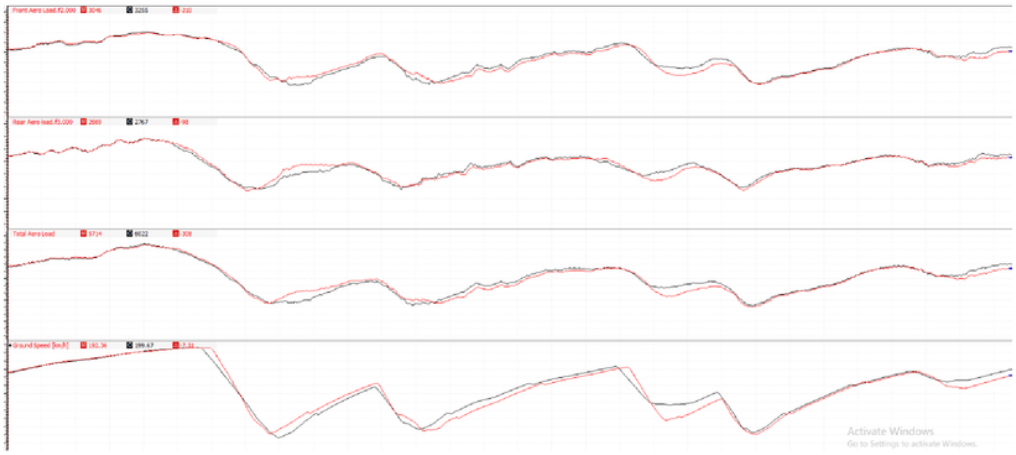


Figure 46 Aerodynamic Load Comparison - Different Drivers

The trend seen in the data is very similar for both drivers, highlighting that the design performs consistently regardless of driver. However, it is worth noting that there are some discrepancies in the aerodynamic loads produced in sections of the lap, which correspond to deviations in vehicle speed, likely due to differences in driving styles rather than any vehicle related parameter.

When the vehicle is in hard braking zones the front and rear aerodynamic loads of all the concepts decrease, which is to be expected due to the decreasing speed resulting in decreasing downforce generation. However, when this happens the centre of pressure seems to move farther forward and then moves back to a more constant state when starting to accelerate again this is shown below in figure forty-seven.

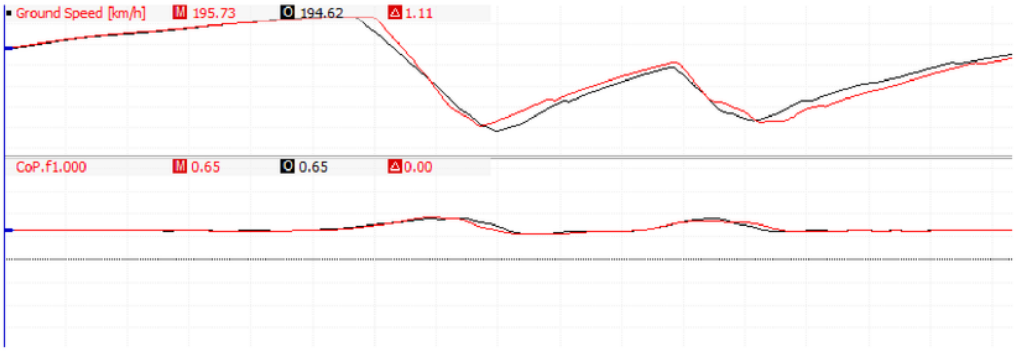


Figure 47 Slight Variation of CoP with Speed

This was not expected to occur due to the degradation factors being set to zero. Due to this it was concluded that something within the coding is still affecting the aerodynamic calculations that could be influencing the results. This could be out of the programmer's control and could be being controlled by the physics engine itself.

4.5 Understeer and Oversteer

Within MoTeC a maths channel was created to show if the vehicle is understeering or oversteering during the course of a lap. To be able to do this the corner radius needed to be calculated in steady state. Using the Skidpad track, a 200m diameter circle is mapped out and this was followed at a speed of 5.56m/s. From the corner radius the theoretical steering angle was calculated using the wheel base of the vehicle and the corner radius. This is shown below in figure forty-eight.

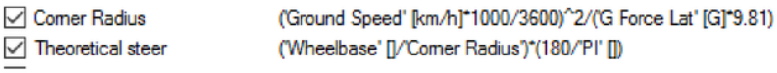


Figure 48 Corner Radius and Theoretical Steer Maths Channels

Due to there being a steering ratio between the steering wheel movement and the actual wheel steer, a correction factor was calculated to adjust the offset that this produces. This is worked out from the theoretical steering angle from the steady state corner and the correction factor which divides the corner radius by the steering wheel percentage shown below in figure forty-nine.

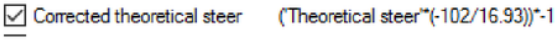


Figure 49 Corrected Theoretical Steer Maths Channel

Using this the understeer channel was created by taking the theoretical steer from the value for the steering angle shown below in figure fifty.

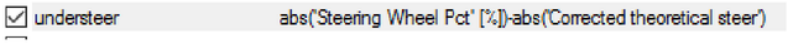


Figure 50 Understeer Channel

Using this channel each concept was compared which can be seen below in figure fifty-one. the way the channel is constructed a positive number is understeer and if it is negative it indicated oversteer.

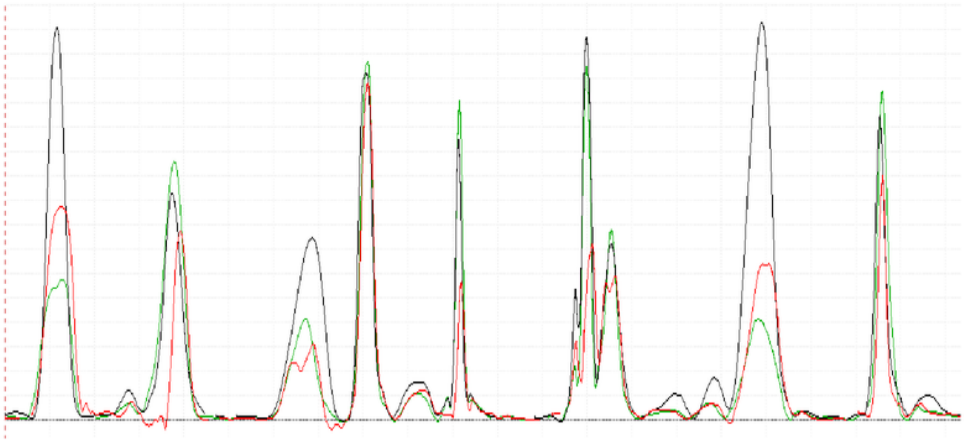


Figure 51 Understeer Comparison

From figure fifty-one, it shows that the MK2 understeers more than the MK1, which is not what was expected given the extra downforce on the front of the vehicle and the CoP being 4% further forward on the Mk2. This is also seen from the MK4 concept in some of the corners. This could be due to the higher velocity of the MK2 and the MK4. This can be seen below in figure fifty-two, which is from turn 4 of Oulton Park.

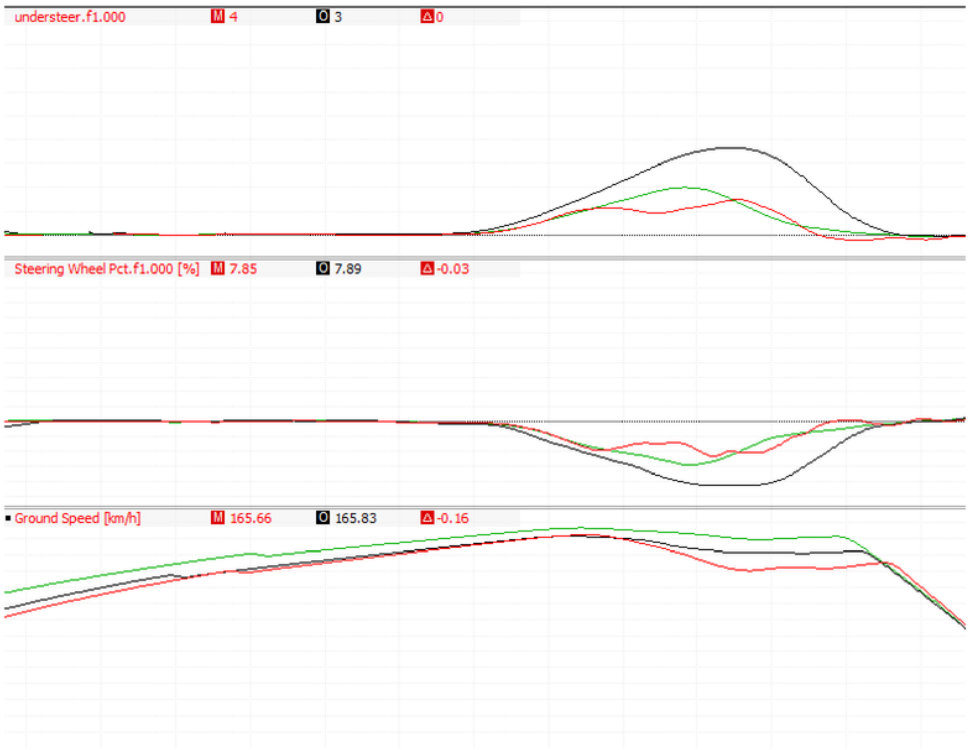


Figure 52 Oulton Park Understeer Comparison - Turn Four

Figure fifty-two clearly shows that both the MK2 and the MK4 need a higher steering angle around this corner due to the higher speed which is inducing understeer. Another indication of understeer is that there is a much higher steering percentage used in figure fifty-two for the MK2. This could be due to the extra downforce produced from the MK4 the driver felt more comfortable with the extra understeer produced. None of the concepts seem to show any signs of real oversteer. Through a few corners the MK4 excels and produces much less understeer than the other two configurations, this is apparent at turn fifteen which is the fastest corner of the track, where aerodynamics should have a vital role. This is shown below in figure fifty-three on the first crest in the screen shot.

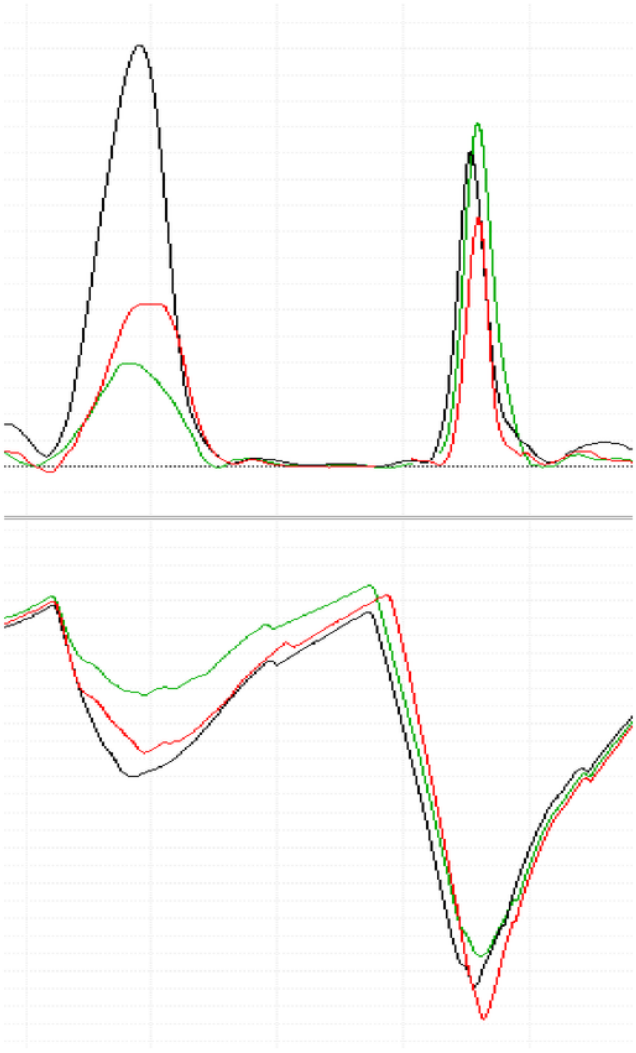


Figure 53 Oulton Par Understeer Comparison - Turn Fifteen

This corner is taken at a much higher speed than the other concepts, but it understeers the least. The second corner shown is a very low speed corner where the aerodynamics do not affect the handling greatly, which shows that the MK4 does in fact understeer more than the other two concepts. This is due to the higher speed the corner was taken at thus making the vehicle understeer as the mechanical grip was not available to achieve the drivers steering request.

Data from both drivers was again compared to see how the MK4 performed with different driving styles. The trace for the understeer channel can be seen below in figure fifty-four, showing the fastest lap around Castle Combe. Driver one is the red trace and driver two is the black trace.

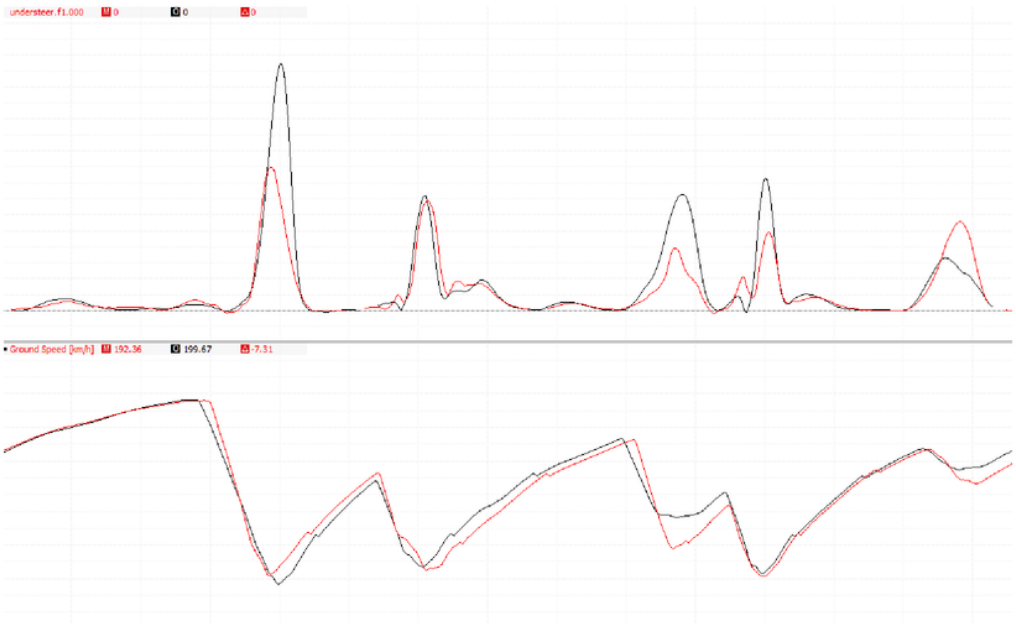


Figure 54 Understeer Comparison Both Drivers

This comparison clearly shows that driver two induces more understeer in nearly every corner, except the final corner. This difference in results could just de down to driver preference and the different lines that they have taken. On these laps, even though driver two is creating more understeer, more speed is carried through the corner making the lap time decrease overall. This proves that even if a vehicle is understeering, it is not always detrimental to lap times. It is possible to go faster if the understeer is controlled properly and does not become excessive. The data also shows how different drivers could influence the results, which is why it has been important to test with the same driver throughout this report, as well as utilising a secondary driver to provide comparative data throughout.

4.6 Driver Feedback

Each driver was required to fill out a driver feedback sheet for the MK1, MK2 and MK4 concepts these can be seen below. The 'feel' experienced by the driver is critical to their ability to extract performance from a vehicle (Segers, 2008), and as such was deemed critical to capture. The driver did not know which concept they were testing when they were driving, leading to a blind test scenario where the driver's performance would be without bias. Immediately on completion of the driving session the drivers were required to complete the feedback form, so that the handling characteristics of the vehicle were fresh in their mind.

Driver One

MK1	Generally good balance, although rear end goes light under heavy braking and in high speed direction changes meaning lift and coast into heavy braking zones is necessary and throttle feathering through high speed corners also necessary. Front turns in well, but then suffers from some mild understeer as the front 'settles' before gripping up again.
MK2	Has a very compliant rear end, does not try to break away in any speed corner, or under traction. Braking stability good, relatively neutral front/rear. Front turns in well, can be aggressive on initial turn in, however mid-corner understeer is still an issue. Car washes out after settling following turn in, is hampering lap times somewhat as have to wait for the front end to bite again.
MK4	Considerably more downforce. Turn in is much better, mid corner understeer is reduced, to the point where it is basically not an issue now. Rear end feels light during high speed turns, must be careful not to be too aggressive on turn in as the

	rear wants to wander. Generally, very good balance apart from slight high-speed issue. The oversteering tendency suits my preference though, and it's still very progressive, you can balance the car with the throttle easily even when the rear drifts at high speed. Very drivable, much faster.

Table 6 Driver One Feedback

Driver Two

MK1	Vehicle seems to handle well at low and high speeds. In both types of corners the vehicle tends to understeer on initial turn in and then also mid corner if the speed is too high. The rear feels a little unstable around fast corners corrected with a slight lift of the throttle which is costing overall speed on the straights due to not getting good exits to the corners
MK2	The turn in response of this model is very good which works well for my aggressive driving style but still suffers this mid corner understeer it does feel that the balance is more forward making the rear a little unpredictable but is easily corrected. Stable at high speeds and it seems that the rear end has good grip mid corner even if the front is understeering slightly once settled.

MK3	Very responsive turn in and very “grippy” around fast speed corners this model clearly has a lot of downforce. In the slow speed corners there is a hint of understeer but much less than the other two models. This model can be driven very aggressively which suits my driving style. The aero balance of the vehicle feels very neutral and stable which makes this model predictable and fast. This model seems to oversteer more than the others which helps reduce the understeer in the high speed corners but this can make it slightly unpredictable, which I prefer over a vehicle which is understeering. This model is by far the fastest and the easiest to drive fast and smooth.

Table 7 Driver Two Feedback

Simulating with driver feedback can influence some design ideas and modifications which could reduce the number of porotypes that would need to be made. The feedback from both drivers stated that the MK4 felt the most stable around the corners which confirms why the MK4 felt like it was not understeering as much but from the data it shows that it is, which must be from the added downforce that this concept produces. This feedback also confirms that the MK4 is the nicest to drive due to the added downforce of that concept.

4.7 Industry Standard Testing

Every vehicle that is designed for public use must be tested to given industry standard procedures, which benchmark the handling characteristics of the vehicle. It was decided to test each concept on two of these industry standard tests. The two that were chosen was the lane change manoeuvre and a one-hundred metre radius corner in steady state (SAE Interantional, 2012).

4.7.1 Lane Change Manoeuvre

The lane change manoeuvre is to mimic a swerve manoeuvre at high speeds, from one lane into another and back into the original lane. This is usually setup with cones which is outlined below in figure fifty-five.

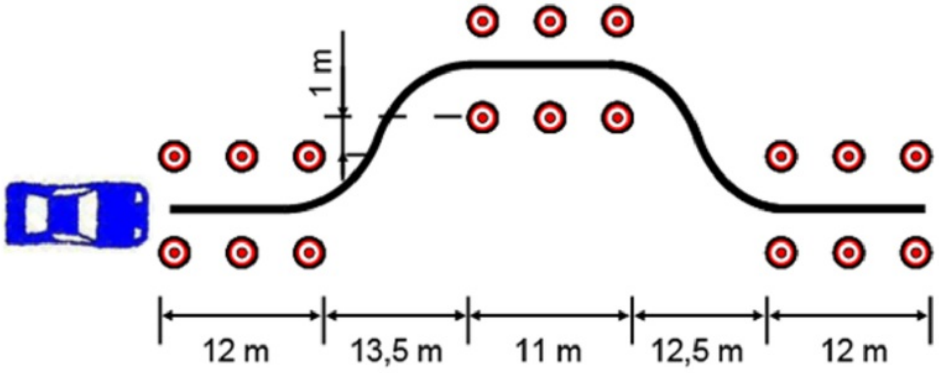


Figure 55 Lane Change Manoeuvre Layout

(FKFS, 2018)

This layout had been previously produced using Bobs track builder for another project. A screen shot from Bobs track builder can be seen below in figure fifty-six.

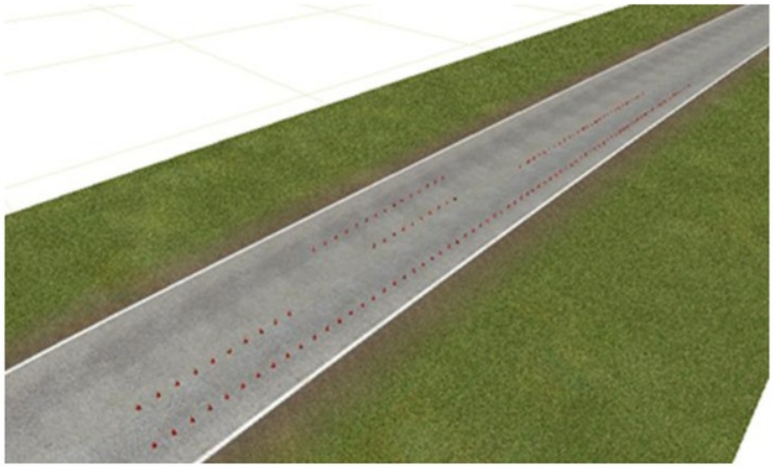
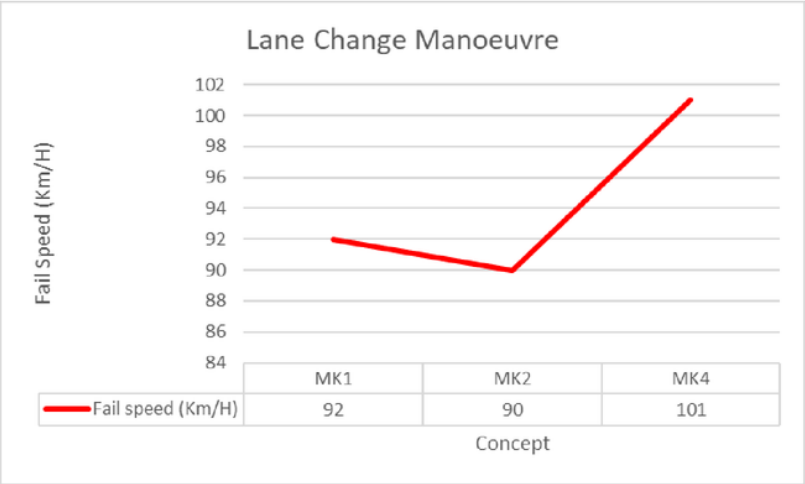


Figure 56 Lane Change Within the Simulator (Bridgeland & Noble, 2018)

All three of the concepts were tested on this track, the results can be seen below in graph forty, with the speed at which the vehicle was no longer able to complete the manoeuvre, the fail speed, being recorded.

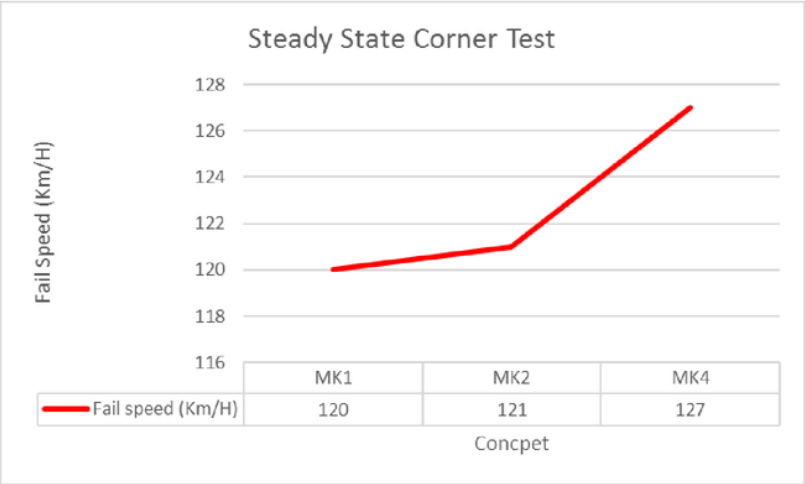


Graph 40 Lane Change Manoeuvre Results

These results show that, as predicted the Mk4 failed at a higher speed than the other two concepts, in keeping with the CFD and track testing data, but interestingly the MK2 failed before the MK1. The driver said that "even though the MK2 turns in very quickly and sharply this seems to unsettle the rear after the first change and the vehicle does not have time to settle before having to turn back" this could explain why the speed was actually lower thank the MK1. Again, this issue demonstrates how the overall balance of the vehicle is often more important than a single parameter such as downforce, given that the higher downforce levels have not yielded better results.

4.7.2 Steady State Corner Test

Using the circles that are marked out on the Skidpad track, each concept was tested at 1KM/H increments around a radius of 100m. The speed was increased until the line could not be followed, with minimal steering input angle change due to understeer or oversteer. Graph forty-one, below shows the results from this test.



Graph 41 Steady State Corner Results

As with the lane change manoeuvre the MK4 failed the test at the highest speed, again expected given the increased downforce and relatively neutral handling balance reported by the drivers. The MK2 was better in this test than the Mk1, due to the steadier state nature of the test not upsetting the vehicle balance, unlike the lane change manoeuvre.

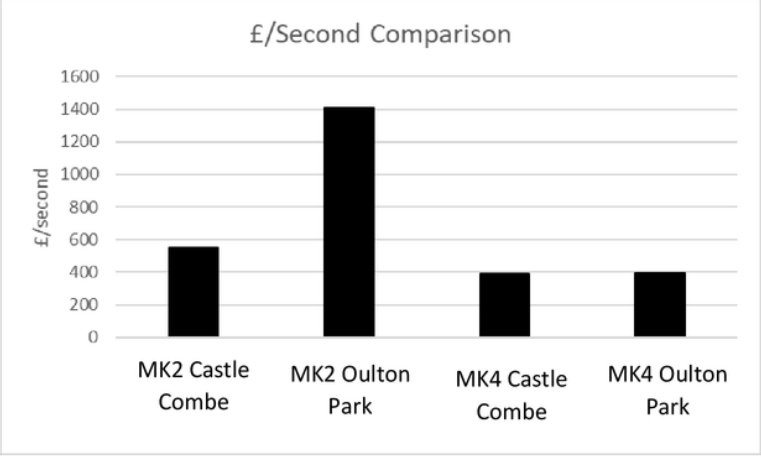
5 Conclusions

Within this report many different validation techniques have taken place which have worked very well. CFD validation worked, gave good results close to published data and is a valid method of preparing CFD software for accurate and repeatable results.

CFD testing of the concepts, again correlated well to the MIRA and Total Sim data, so was proven accurate and valid methods. This computational method of testing design concepts can be much quicker than real world or wind tunnel testing and can give relatively fast outputs of data as to the performance of a concept.

Sim testing, again with the correlation to the real car data has proven the driver in the loop simulator can be used effectively as a tool to computationally model a vehicles dynamic performance, and that the circuit testing has demonstrated changes in vehicle handling balance so it can be used confidently as a testing method for vehicle designs and upgrades.

In conclusion to this report there is a clear advantage of the MK4 GJ02 bodywork concept over the MK2 and the MK1. There would be some complications with this design, that would need to be addressed. The largest would be the cost to produce the whole bodywork package. The same could be said for the MK2 Iley design, but this has already been made and test fitted on the vehicle at just a cost of £450 and an additional updated design for £250, for a total of £700 (Iley, 2019). It is predicted that the MK4 bodywork could cost in excess of £2000, including tooling for manufacture, materials and manufacturing the concept (Jones, et al., 2019). Using these figures, a £/second graph was produced for the MK2 and the MK4 for both tracks using the average between both drivers to calculate the lap time improvement. This is shown below in Graph forty-two.



Graph 42 £/Second Comparison MK2 and MK4

The MK4 costs a lot more than the MK2 but with the gains within the lap times produced there is a clear advantage of spending the time and money on the MK4 bodywork. This is also backed up by the overall performance and the driver feedback, showing the MK4 is far superior to the MK1 and the MK2 and would be a worthy investment in the future of the race team.

As highlighted earlier in this report, the MK4 concept would take a lot more work to optimise the vehicle to the added downforce. Proven by having to stiffen the front springs and dampers in earlier testing, to make the model driveable. This would result in an entire setup change of the vehicle which can also be very costly and time consuming taking it to track and testing. These unknown costs have not been factored into the above cost/benefit analysis.

The MK2 is an easy bolt on modification, which as stated in this report, has its advantages but would also require a setup change of the vehicle. Whilst being easy to implement, consideration should also be given to the impact on handling balance found in the testing, where the vehicle became slightly less predictable.

Due this report is all theoretical and some further validation could be done to improve the accuracy of the model. And some further track testing could be done to help make the model more accurate.

6 Evaluation & Further Works

Simulation is a never-ending cycle of changes and improvements that could be made to the model to increase the accuracy of the model. Within this report some parts of the programming were changed to make the model as accurate as possible, within the time frame provided. The main part of the model that was ignored were the degradation factors within the aerodynamics section of the HDV file. It was decided to not program these due to the amount of computing time that would have been necessary. To work out the degradation factors, full attitude studies for all concepts would need to be conducted in CFD to determine the impact of roll, pitch and yaw on the aerodynamic performance. Due to each CFD run taking an average of 12 hours, this was deemed not possible within this time frame. The use of design of experiment software's could reduce the amount of CFD runs that would have been needed due to its prediction and interpolation capabilities. These degradation factors would increase the validity of the models, as they would accurately model the vehicles aerodynamic sensitivity to attitude change.

All the CFD runs that were produced during this report were done statically. This was done due to the wind tunnel data from the vehicle was also static. In the real world the wheels and the road would be moving which can have a massive impact on the results obtained. A case could be made that CFD with moving road and wheels is actually more representative than that of a static case, as found by the investigation of (Axereo-Cilies & Iaccarino, 2012) which found significant change when modelling wheels as rotating bodies in CFD. Due to this, for further work it could be investigated for each of the concepts, to conduct moving road, rotating wheel CFD runs to give more representative dynamic values. To highlight this, a rough CFD run with rotating wheels and moving road was completed on the MK4 concept, to see the difference between the results. It should be noted that the mesh used was not representative of those used previously, this run was conducted simply to gain a representative comparison. The CL and CD values can be seen below in table eight.

configuration	Cl	Cd	efficiency	CoP
MK4 GJ02	-1.847	0.490	3.772	0.61
MK4 moving road	-2.142	0.510	4.197	0.59

Table 8 Moving Road and Rotating Wheels Comparison MK4

The difference in the wake region can also be seen below in figure fifty-seven, Where the first picture is the static test and the bottom has rotating wheels and the moving road.

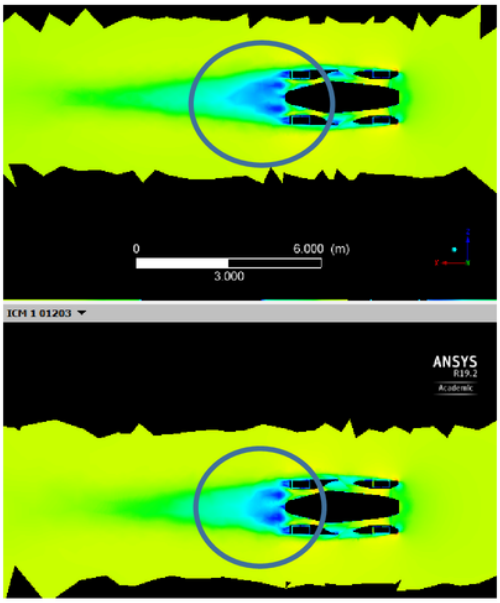


Figure 57 Moving Road and Rotating Wheels comparison MK4

There is quite a difference with these results which would confirm that this further work would be a valid investigation which could affect the simulation results.

Other real vehicle data could also be collected with the real vehicle with the MK2 Iley splitter attached to the vehicle due to it already being constructed and test fitted. The straight-line testing could be repeated using the real vehicle which would give another point of validation to the simulation model and CFD data collect within this report. This was not possible within this report due to the vehicle being in its off-season period and was being rebuilt ready for the next season. Further work could also be conducted on track where the simulation model could be compared to real track data to confirm the validity of the model.

The simulation model could be further optimised for each of the bodywork concepts to find an exact setup for each concept. While some setup optimisation was conducted during this investigation, time limitations meant that it was not as rigorous as would have been liked and as such it would have been preferred to expand this area of focus. This would include parameter sweeps to see the effect of different ride heights and damper settings. This investigation could yield results that increase the effectiveness of each concept. This would also decrease the track testing that would be needed to optimise the new concepts without the added cost and time of going to track (Segers, 2008) and risking damage to new components.

Within this report two drivers were used that have experience simulator driving but not real-world racing experience. Testing more drivers would create broader data pool, that could produce different results with different driving styles. Further work could be carried out to investigate the effect of testing additional drivers who don't have experience in the simulator but do race. This would hopefully generate a wider spread of data, allowing deeper analysis, whilst further eliminating the influence of driving style and 'fear factor' on the results.

7 References

ansible Motion, 2016. *Boosting Race Track Performance With Simulation,* s.l.: Ansible motion LTD.

Ansys, 2016. *Handbook.* s.l.:s.n.

Axereo-Cilies, J. & Iaccarino, G., 2012. An Aerodynamic Investigation of an Isolated Rotating F1 Wheel Assembly. *Journal of Fluids Engineering,* 134(12), pp. 101-121.

Base Performance Simulators, 2009. *Simulator Manual,* s.l.: Base Performance Simulators.

Bernard, J. E. & Clover, C. L., 1994. Validation of Computer Simulations of Vehicle Dynamics. In: *Vehicle Dynamics and Simulation.* Iowa: SAE international, pp. 159-168.

Blais, B. & Bertland, F., 2015. On the use of the method of manufactured solutions for the varification of CFD codes for the volume-aveaged Navier-Stoke equations. *Computers and Fluids,* Volume 114, pp. 121-129.

Brayshaw, D. & Harrison, M., 2005. *A quasi steady state approach to race car lap simulation in order to understand the effects of racing line and centre of gravity location ,* s.l.: Cranfield University.

Bridgeland, J. B. & Noble, A., 2018. *Group Project Report - Simulation,* s.l.: s.n.

Castillo, J., Cabrera, J., Guerra, A. & Simon, A., 2016. A nove; e;ectrohydraulic brake system with tire-road friction eastimation and continuous brake pressure control. *IEEE transactions on industrial electronics,* Volume 63, pp. 1863-1875.

CFD, 2019. *CFD intro.* [Online]
Available at: http://www.cham.co.uk/phoenics/d_polis/d_info/cfdintro.htm

Chang, F. & Lu, Z. H., 2008. Dynamic model of an air spring and integration into a vehicle dynamics model. *Proceedings of the Institute of Mechanical Engineers, Part D,* Volume 222, pp. 1813-1825.

Colunga, I. & Bradley, A., 2014. *Modelling of transient cornering and suspension dynamics, and investigation into the control strategies for an ideal driver in a lap time simulator,* s.l.: s.n.

Dominy, R. G., Ryan, A. & Sims-Williams, D. B., 2000. The influence of slipstreaming on sports prototype race car performance. *Proceedings of the Institution of Mechanical Engineers,* 214(8), p. 887.

FKFS, 2018. *Driving Dynamics Road test.* [Online]
Available at: http://www.fkfs.de/en/automotive-engineering/leistungen/driving-dynamics/road-

test/
[Accessed 1 2 2019].

Gartman, A., Fister, W., Schwanghart, W. & Muller, M. D., 2011. CFD modeling and validation of measured wind field data in a portable wind tunnel. *Aeolian research,* Volume 3, pp. 315-325.

Gilani, R., 2012. *Engine simulation model for a formula SA race car: applied design, development, corelation and optimisation,* s.l.: s.n.

Haaland, J. M., 2017. *Vehicle Dynamics Simulation for setting up a Four-Wheel Independent Drive Electric Race Car,* s.l.: NTNU.

Hoyle, C. & Hurdwell, R., 2016. *Investing in CarMaker for Driver-In-The-Loop Simulation,* s.l.: rFpro.

Hucho, W.-H., 1987. *Aerodynamics of Road Vehicles.* london: Butterworths.

Iley, J., 2019. *UWTSD Sports 2000 Front Splitter Project.* s.l.:s.n.

Image Space Incorporated, 2016. *About ISI.* [Online]
Available at: www.imagespaceinc.coom
[Accessed 10 03 2019].

Jones, G. et al., 2019. *Year Two Group Project,* s.l.: s.n.

Kang, Y. et al., 2013. Design of Driver-in-the-Loop Simulator. In: *Sensors & Transducers.* Beijing: IFSA, pp. 401-407.

Katz, A. & Venkateswaran, S., 2011. Mesh quality effects on the accuracy of CFD colutions on unstructred meshes. *Journal of computational physics,* Volume 230, pp. 7670-3686.

Katz, J., 1995. *Race Car Aerodynamics: Designing for speed.* Cambridge: Bentley.

Lanfrit, M., 2005. Best practice guidelines for handling Automotive External Aerodynamics with FLUENT.

Maha, 2018. *Maha Group.* [Online]
Available at: https://www.maha.co.uk/maha-group.htm
[Accessed 03 2019].

Mariani, F., Poggiani, C., Risi, F. & Scappaticci, L., 2015. Formula-SAE Racing Car: Experimental and Numerical Analysis of the External Aerodynamics. *Formula-SAE Racing Car: Experimental and Numerical Analysis of the External Aerodynamics,* Volume 81.

Mariani, F., Poggiani, C., Risi, F. & Scappaticci, L., 2015. Formula-SAE Racing Car: Experimental and Numerical Analysis of the External Aerodynamics. *69th Conference of the Italian Thermal Engineering Association, ATI 2014,* Volume 81, pp. 1013-1029.

MCR race cars, 2019. *MCR race cars.* [Online]
Available at: https://mcrracecars.co.uk/
[Accessed 2019].

Metz, D. & Metz, G., 2000. *Sensitivity of cornering speeds to banking and aerodynamics.* s.l., s.n.

Morse, P., 2016. *Race car tuning with driver in the loop simulators.* [Online]
Available at: https://www.ansiblemotion.com/automotive-driver-in-the-loop-simulation-articles/race-car-tuning-with-driver-in-the-loop-simulators
[Accessed 01 04 2019].

Nasa, 2012. *Determining Centre Of Pressure.* [Online]
Available at: https://www.grc.nasa.gov/www/k-12/rocket/rktcp.html
[Accessed 05 03 2019].

NASA, 2017. *what is aerodynamics.* [Online]
Available at: https://www.nasa.gov/audience/forstudents/5-8/features/nasa-knows/what-is-aerodynamics-58.html
[Accessed 02 03 2019].

Photgraphy, K., 2017. *SRCC Sports 2000 photos.* s.l.:s.n.

Plotkin, A. & Katz, J., 2002. Low Speed aerodynamics. p. 64.

rFactor.net, 2013. *History of rFactor.* [Online]
Available at: www.rfactor.net
[Accessed 10 12 2018].

rFpro, 2017. *Motorsport Simulation.* [Online]
Available at: http://www.rfpro.com/motorsport/
[Accessed 17 03 2019].

Rumerman, J., 2019. *evolution of technology.* [Online]
Available at: https://www.centennialofflight.net/essay/Evolution_of_Technology/first_wind_tunnels/Tech34.htm
[Accessed 12 1 2019].

SAE Interantional, 2012. *Vehicle Industry Standard.* [Online]
Available at: https://www.sae.org/news/2019/04/sae-government-industry
[Accessed 2019].

SAE International, 2014. Ferarri Changes Course on Track Simulation Software. *SAE International Online.*

SAHIN, D., 2004. WIND TUNNEL BLOCKAGE CORRECTIONS:. *WIND TUNNEL BLOCKAGE CORRECTIONS: .*

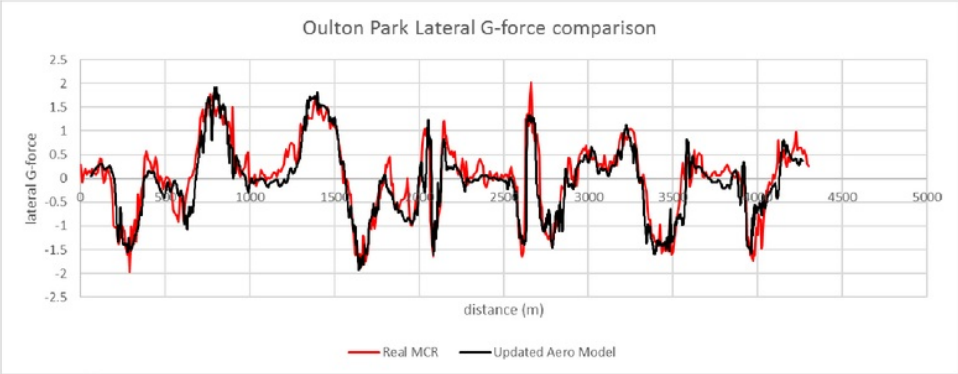
sas Ip, n.d. *mesh quality.* [Online]
Available at: https://www.sharcnet.ca/Software/Ansys/17.0/en-us/help/flu_ug/flu_ug_mesh_quality.html

Segers, J., 2008. *Analysis Techniques for Race Car Aquisition.* USA: SAE International.

Toyota Motorsport, 2011. Formula One race cars get faster thanks to particle-image velocimetry and CFD. *Formula One race cars get faster thanks to particle-image velocimetry and CFD ,* 83(11).

8 Appendix

Appendix 1



Appendix 2

